Transfer Matrices and Partition-Function Zeros for Antiferromagnetic Potts Models

I. General Theory and Square-Lattice Chromatic Polynomial

Jesús Salas
Departamento de Física Teórica
Facultad de Ciencias, Universidad de Zaragoza
Zaragoza 50009, SPAIN
JESUS@MELKWEG.UNIZAR.ES

Alan D. Sokal
Department of Physics
New York University
4 Washington Place
New York, NY 10003 USA
SOKAL@NYU.EDU

April 19, 2000
revised December 13, 2000

Abstract

We study the chromatic polynomials (= zero-temperature antiferromagnetic Potts-model partition functions) $P_G(q)$ for $m \times n$ rectangular subsets of the square lattice, with $m \leq 8$ (free or periodic transverse boundary conditions) and n arbitrary (free longitudinal boundary conditions), using a transfer matrix in the Fortuin-Kasteleyn representation. In particular, we extract the limiting curves of partition-function zeros when $n \to \infty$, which arise from the crossing in modulus of dominant eigenvalues (Beraha–Kahane–Weiss theorem). We also provide evidence that the Beraha numbers B_2, B_3, B_4, B_5 are limiting points of partition-function zeros as $n \to \infty$ whenever the strip width m is ≥ 7 (periodic transverse b.c.) or ≥ 8 (free transverse b.c.). Along the way, we prove that a noninteger Beraha number (except perhaps B_{10}) cannot be a chromatic root of any graph.

Key Words: Chromatic polynomial; chromatic root; antiferromagnetic Potts model; square lattice; transfer matrix; Fortuin-Kasteleyn representation; Temperley-Lieb algebra; Beraha–Kahane–Weiss theorem; Beraha numbers.

1 Introduction

The Potts model [1, 2, 3] plays an important role in the general theory of critical phenomena, especially in two dimensions [4, 5, 6], and has applications to various condensed-matter systems [2]. Ferromagnetic Potts models have been extensively studied over the last two decades, and much is known about their phase diagrams [2, 3] and critical exponents [5, 6, 7]. But for antiferromagnetic Potts models, many basic questions remain open: Is there a phase transition at finite temperature, and if so, of what order? What is the nature of the low-temperature phase(s)? If there is a critical point, what are the critical exponents and the universality classes? The answers to these questions are expected to be highly lattice-dependent, in sharp contrast to the universality typically enjoyed by ferromagnets.

According to the Yang-Lee picture of phase transitions [8], information about the possible loci of phase transitions can be obtained by investigating the zeros of the partition function when one or more physical parameters (e.g. temperature or magnetic field) are allowed to take *complex* values. For the Potts model on a finite graph G, the partition function $Z_G(q,v)$ depends on the number q of Potts states and on the temperature-like variable $v = e^{\beta J} - 1$. The Fortuin-Kasteleyn representation [9, 10] shows that $Z_G(q,v)$ is a polynomial in q and v (see Section 2.1), so it makes sense for either or both of these variables to be made complex. In particular, the chromatic polynomial $P_G(q) = Z_G(q,-1)$ corresponds to the zero-temperature limit of the antiferromagnetic Potts model ($J = -\infty$, $v = -1$).

Many investigations of the zeros of Potts partition functions in the complex q- and/or v-plane have been performed in the last few years, notably by Shrock and collaborators [11, 12, 13, 14, 15, 16, 17, 18, 19, 20, 21, 22, 23, 24, 25, 26, 27, 28, 29, 30, 31, 32, 33, 34, 35]. The best results concern families G_n of graphs for which the partition function can be expressed via a transfer matrix T of fixed size $M \times M$:

$$Z_{G_n}(q,v) = \mathrm{tr}[A(q,v)\, T(q,v)^n] \tag{1.1a}$$

$$= \sum_{k=1}^{M} \alpha_k(q,v)\, \lambda_k(q,v)^n \,, \tag{1.1b}$$

where the transfer matrix $T(q,v)$ and the boundary-condition matrix $A(q,v)$ are polynomials in q and v, so that the eigenvalues $\{\lambda_k\}$ of T and the amplitudes $\{\alpha_k\}$ are algebraic functions of q and v. It then follows, using a theorem of Beraha–Kahane–Weiss [36, 37, 38, 39, 40], that the zeros of $Z_{G_n}(q,v)$ accumulate along the curves $\mathcal{B}$ where T has two or more dominant eigenvalues (i.e. eigenvalues of maximum modulus), as well as at the isolated points where T has a single dominant eigenvalue λ_k whose corresponding amplitude α_k vanishes. See Section 2.2 for more details.

For ferromagnetic Potts models on the square, triangular and hexagonal lattices, the exact critical curves $v_c(q)$ in the *real* (q,v)-plane have long been known [4]. For antiferromagnetic Potts models, by contrast, there are some tantalizing conjectures concerning the critical loci, but many aspects remain obscure.[1] The two best-understood

[1] For a more detailed review, see [41, Section 1].

cases appear to be the square and triangular lattices:

Square lattice. Baxter [4, 42] has determined the exact free energy (among other quantities) for the square-lattice Potts model on two special curves in the (q, v)-plane:

$$v = \pm\sqrt{q} \tag{1.2}$$

$$v = -2 \pm \sqrt{4-q} \tag{1.3}$$

Curve (1.2_+) is known to correspond to the ferromagnetic critical point, and Baxter [42] conjectured that curve (1.3_+) corresponds to the antiferromagnetic critical point. For $q = 2$ this gives the known exact value [43]; for $q = 3$ it predicts a zero-temperature critical point ($v_c = -1$), in accordance with strong analytical and numerical evidence [44, 45, 46, 47, 48, 49, 50]; and for $q > 3$ it predicts that the putative critical point lies in the unphysical region ($v < -1$ or v complex), so that the entire physical region $-1 \le v \le 0$ lies in the disordered phase, in agreement with numerical evidence for $q = 4$ [50]. For some interesting further speculations, see Saleur [51, 52].

Triangular lattice. Baxter and collaborators [53, 54, 55] have determined the exact free energy (among other quantities) for the triangular-lattice Potts model on two special curves in the (q, v)-plane:

$$v^3 + 3v^2 - q = 0 \tag{1.4}$$

$$v = -1 \tag{1.5}$$

The uppermost branch ($v \ge 0$) of curve (1.4) is known to correspond to the ferromagnetic critical point [53, 4]; and Baxter [54] initially conjectured (following a hint of Nienhuis [56]) that (1.5) — which is the zero-temperature antiferromagnetic model, hence the chromatic polynomial — corresponds in the interval $0 \le q \le 4$ to the antiferromagnetic critical point. This prediction of a zero-temperature critical point is known to be correct for $q = 2$ [57, 58, 59] and is believed to be correct also for $q = 4$ [60, 61, 62]. On the other hand, for $q = 3$ this prediction contradicts the rigorous result [63], based on Pirogov-Sinai theory, that there is a low-temperature phase with long-range order and small correlation length.[2] For the model (1.5), Baxter [54] computed three different expressions $\lambda_i(q)$ $[i = 1, 2, 3]$ that he argued correspond to the dominant eigenvalues of the transfer matrix in different regions $\mathcal{D}_i$ of the complex q-plane; in a second paper [55] he provided corrected estimates for the precise locations of $\mathcal{D}_1, \mathcal{D}_2, \mathcal{D}_3$. Unfortunately, no analogous analytic prediction is available for the chromatic polynomials of other two-dimensional lattices.

One way to test the conjecture that (1.3_+) is a critical curve for the square-lattice Potts model is to compute the partition function $Z_{m\times n}(q, v)$ for $m \times n$ strips of the square lattice, investigate its zero variety in the complex (q, v)-space, and test whether the zeros of $Z_{m\times n}(q, v)$ appear to be converging to (1.3_+) as $m, n \to \infty$. Here we shall carry out this program for the zero-temperature antiferromagnetic model

[2] A Monte Carlo study of the $q = 3$ model found strong evidence for a first-order transition to an ordered phase at $\beta J \approx -1.594$ [64].

($v = -1$).[3] Using a transfer matrix in the Fortuin-Kasteleyn representation [66], we shall compute the chromatic polynomials $P_{m\times n}(q)$ for $m \times n$ square-lattice strips of width $m \leq 8$ (free or periodic transverse boundary conditions) and arbitrary length n (free longitudinal boundary conditions). In particular, we shall extract the limiting curves $\mathcal{B}$ of partition-function zeros when $n \to \infty$, which arise from the crossing in modulus of dominant eigenvalues in accordance with the Beraha–Kahane–Weiss theorem.[4] Finally, we shall attempt to understand the behavior of these limiting curves as $m \to \infty$. Of course, there is little doubt in this case that they will converge to the critical point of the zero-temperature model, $q_c = 3$; but it is illuminating to see this convergence explicitly and to view the critical *point* $q_c = 3$ as simply one (real) point on a complex critical *curve*. Not surprisingly, we find for this critical curve a shape that is qualitatively similar to that found by Baxter [55] for the triangular lattice, with the zero-temperature critical point lying now at $q_c = 3$ rather than $q_c = 4$.

A special role in the theory of chromatic polynomials appears to be played by the *Beraha numbers* $B_n = 4\cos^2(\pi/n)$ [see Table 1 for the first few B_n]. As we shall show in Section 2.3, a noninteger Beraha number (except possibly B_{10}) cannot be a chromatic root of any graph. Nevertheless, Beraha [67] observed that planar graphs frequently have chromatic roots very *near* one or more of the B_n.[5] Indeed, Beraha, Kahane and Weiss [38, 39] found families of planar graphs that have chromatic roots *converging* to B_5, B_7 or B_{10}.[6]

Here we shall provide additional curious evidence in favor of the idea that chromatic roots tend to accumulate at the Beraha numbers. We find empirically (at least for $m \leq 8$) that on a square-lattice strip of width m with either free or periodic transverse b.c., there is at least one vanishing amplitude $\alpha_i(q)$ at each of the first m Beraha numbers $B_2, \ldots, B_{m+1}$ (but not higher ones). Assuming that this behavior persists for all m, in the limit $m \to \infty$ all the Beraha numbers will be zeros of some amplitude. Moreover, in all the cases except $m = 7, 8$ with free transverse b.c. (where our computer power gave out) and $m = 8$ with periodic transverse b.c. (see

[3] In future work [65] we plan to extend this analysis to the antiferromagnetic model at nonzero temperature ($-1 < v < 0$). See also [30].

[4] Here we follow in the footsteps of Shrock and collaborators [17, 19, 32], who have been carrying out this program using a generating-function approach that is equivalent to transfer matrices; they determine the recurrence relations by repeated use of the deletion-contraction identity. In particular, Shrock *et al.* have computed the transfer matrices for square-lattice strips of width $m \leq 5_{\rm F}$ and $m \leq 6_{\rm P}$ (leading to matrices of size up to 7×7), and have computed the limiting curves $\mathcal{B}$ of partition-function zeros for $m \leq 4_{\rm F}$ and $m \leq 5_{\rm P}$. [Here the subscript F (resp. P) denotes free (resp. periodic) boundary conditions.] By explicit use of transfer matrices, we are able to automate the former calculation and handle much larger transfer matrices (here up to 127×127); and using the resultant method (Section 4.1.1) we are able to detect small gaps and other fine details in the limiting curves.

[5] For B_5 this was observed earlier by Berman and Tutte [68].

[6] The graphs in question are $4_{\rm P} \times n_{\rm F}$, $5_{\rm P} \times n_{\rm F}$ and $2_{\rm F} \times n_{\rm P}$ strips of the triangular lattice (with an extra vertex adjoined at top and bottom in the first two cases). In the case of B_5 and B_7, Beraha, Kahane and Weiss [39] proved that there are even *real* chromatic roots converging to them.

Section 7.2 for a discussion on this point), we verified that the vanishing amplitude corresponds to the eigenvalue obtained by analytic continuation in q from the one that is dominant at small real q (e.g. at $q = 1$), in agreement with a conjecture of Baxter [55, p. 5255]. Thus, the first few Beraha numbers — namely, those (up to at most B_{m+1}) that lie below the point $q_0(m)$ where the dominant-eigenvalue-crossing locus $\mathcal{B}$ intersects the real axis — correspond to the vanishing of a dominant amplitude and hence (via the Beraha–Kahane–Weiss theorem) to a limit point of chromatic roots, while the remaining Beraha numbers do not. As the strip width m grows, this crossing point $q_0(m)$ increases and presumably tends to a limiting value $q_0(\infty)$; for the square lattice, we expect $q_0(\infty)$ to lie somewhere around 2.9, i.e. strictly between B_5 and B_6. Therefore, for all sufficiently large strip widths, we expect the Beraha numbers B_2, B_3, B_4, B_5 — but not higher ones — to be limiting points of chromatic roots. Our data confirm (at least up to $m = 8$) that B_2, B_3, B_4 are limiting points of zeros for all widths $m \geq 4$, and that B_5 is a limiting point of zeros for all widths $m \geq 7$ (cylindrical b.c.) or $m \geq 8$ (free b.c.). This scenario for the accumulation of chromatic roots at *some* of the Beraha numbers was set forth by Baxter [55] and elaborated by Saleur [51]. For further speculations on the special role of the Beraha numbers in the Potts model, and especially for the chromatic polynomials of planar graphs, see [68, 69, 70, 71, 72, 73, 74, 55, 75, 76, 77, 51, 52, 78, 79, 80, 81, 82, 83, 84, 85].

The plan of this paper is as follows: In Section 2 we review the Fortuin-Kasteleyn representation, the Beraha–Kahane–Weiss theorem, and some algebraic number theory related to the Beraha numbers. In Section 3 we explain how to construct transfer matrices for the Potts model in the spin representation and in the Fortuin-Kasteleyn representation, and we compute the dimensions of these transfer matrices. In Section 4 we discuss the general properties of the dominant-eigenvalue-crossing curves $\mathcal{B}$ and the isolated limiting points of zeros. In Sections 5 and 6 we present our numerical results for square-lattice strips with free and cylindrical boundary conditions. In Section 7 we analyze the theoretical import of our calculations, and discuss prospects for future work [86, 87, 88, 65].

2 Preliminaries

In Sections 2.1 and 2.2 we review some well-known facts about the Fortuin-Kasteleyn representation and the Beraha–Kahane–Weiss theorem, which will play a fundamental role in the remainder of the paper. We also use these sections to set the notation. In Section 2.3 we discuss some algebraic number theory related to the Beraha numbers; this section contains a few new results, notably Corollary 2.4.

2.1 Fortuin-Kasteleyn representation of the Potts model

Let $G = (V, E)$ be a finite undirected graph with vertex set V and edge set E, let $\{J_e\}_{e \in E}$ be a set of couplings, and let q be a positive integer. Then the *q-state Potts model* on G with couplings $\{J_e\}$ is, by definition, the canonical ensemble at inverse temperature β for a model of spins $\{\sigma_x\}_{x \in V}$ taking values in the set $\{1, 2, \ldots, q\}$,

interacting via a Hamiltonian

$$H(\{\sigma\}) \;=\; -\sum_{e=\langle xy\rangle\in E} J_e \delta(\sigma_x,\sigma_y) \tag{2.1}$$

where δ is the Kronecker delta. The partition function is thus

$$Z_G(q,\{v_e\}) \;=\; \sum_{\{\sigma\}} \prod_{e=\langle xy\rangle\in E} [1+v_e\delta(\sigma_x,\sigma_y)] \;, \tag{2.2}$$

where we have written

$$v_e \;=\; e^{\beta J_e} - 1 \;. \tag{2.3}$$

A coupling J_e (or v_e) is called ferromagnetic if $J_e \geq 0$ ($v_e \geq 0$) and antiferromagnetic if $-\infty \leq J_e \leq 0$ ($-1 \leq v_e \leq 0$). The q-coloring problem, in which adjacent spins are required to take different values, corresponds to the zero-temperature limit of the antiferromagnetic Potts model (namely $J_e = -\infty$, $v_e = -1$).

In fact, $Z_G(q,\{v_e\})$ is the restriction to positive integers q of a *polynomial* in q and $\{v_e\}$ (with coefficients that are in fact 0 or 1). To see this, expand out the product over $e \in E$ in (2.2), and let $E' \subseteq E$ be the set of edges for which the term $v_e\delta(\sigma_x,\sigma_y)$ is taken. Now perform the sum over configurations $\{\sigma\}$: in each connected component of the subgraph (V,E') the spin value σ_x must be constant, and there are no other constraints. Therefore,

$$Z_G(q,\{v_e\}) \;=\; \sum_{E'\subseteq E} q^{k(E')} \prod_{e\in E'} v_e \;, \tag{2.4}$$

where $k(E')$ is the number of connected components (including isolated vertices) in the subgraph (V,E'). The expansion (2.4) was discovered by Birkhoff [89] and Whitney [90] for the special case $v_e = -1$ (see also Tutte [91, 92]); in its general form it is due to Fortuin and Kasteleyn [9, 10] (see also [93]). We shall henceforth take (2.4) as the *definition* of $Z_G(q,\{v_e\})$ for arbitrary complex numbers q and $\{v_e\}$. When v_e takes the same value v for all edges e, we write $Z_G(q,v)$. When $v_e = -1$ for all edges e, this defines the chromatic polynomial $P_G(q)$. Note that the chromatic polynomial $P_G(q)$ of any loopless graph G is a monic polynomial in q with integer coefficients.[7] See [94, 95] for excellent reviews on chromatic polynomials, and [96] for an extensive bibliography.

2.2 Beraha–Kahane–Weiss theorem

A central role in our work is played by a theorem on analytic functions due to Beraha, Kahane and Weiss [36, 37, 38, 39] and generalized slightly by one of us [40]. The situation is as follows: Let D be a domain (connected open set) in the complex

[7] A *loop*, in graph-theoretic terminology, is an edge connecting a vertex to itself. Obviously, if G has a loop, then its chromatic polynomial is identically zero.

plane, and let $\alpha_1, \ldots, \alpha_M, \lambda_1, \ldots, \lambda_M$ ($M \ge 2$) be analytic functions on D, none of which is identically zero. For each integer $n \ge 0$, define

$$f_n(z) \;=\; \sum_{k=1}^{M} \alpha_k(z)\, \lambda_k(z)^n \;. \tag{2.5}$$

We are interested in the zero sets

$$\mathcal{Z}(f_n) \;=\; \{z \in D\colon\; f_n(z) = 0\} \tag{2.6}$$

and in particular in their limit sets as $n \to \infty$:

$$\begin{aligned} \liminf \mathcal{Z}(f_n) \;&=\; \{z \in D\colon \text{every neighborhood } U \ni z \text{ has a nonempty intersection} \\ &\qquad \text{with all but finitely many of the sets } \mathcal{Z}(f_n)\} \end{aligned} \tag{2.7}$$

$$\begin{aligned} \limsup \mathcal{Z}(f_n) \;&=\; \{z \in D\colon \text{every neighborhood } U \ni z \text{ has a nonempty intersection} \\ &\qquad \text{with infinitely many of the sets } \mathcal{Z}(f_n)\} \end{aligned} \tag{2.8}$$

Let us call an index k *dominant at* z if $|\lambda_k(z)| \ge |\lambda_l(z)|$ for all l ($1 \le l \le M$); and let us write

$$D_k \;=\; \{z \in D\colon\; k \text{ is dominant at } z\} \;. \tag{2.9}$$

Then the limiting zero sets can be completely characterized as follows:

Theorem 2.1 [36, 37, 38, 39, 40] *Let D be a domain in $\mathbb{C}$, and let $\alpha_1, \ldots, \alpha_M, \lambda_1, \ldots, \lambda_M$ ($M \ge 2$) be analytic functions on D, none of which is identically zero. Let us further assume a "no-degenerate-dominance" condition: there do not exist indices $k \ne k'$ such that $\lambda_k \equiv \omega\lambda_{k'}$ for some constant ω with $|\omega| = 1$ and such that D_k ($= D_{k'}$) has nonempty interior. For each integer $n \ge 0$, define f_n by*

$$f_n(z) \;=\; \sum_{k=1}^{M} \alpha_k(z)\, \lambda_k(z)^n \;.$$

Then $\liminf \mathcal{Z}(f_n) = \limsup \mathcal{Z}(f_n)$, and a point z lies in this set if and only if either

(a) There is a unique dominant index k at z, and $\alpha_k(z) = 0$; or

(b) There are two or more dominant indices at z.

Note that case (a) consists of isolated points in D, while case (b) consists of curves (plus possibly isolated points where all the λ_k vanish simultaneously). Beraha–Kahane–Weiss considered the special case of Theorem 2.1 in which the f_n are polynomials satisfying a linear finite-order recurrence relation, and they assumed a slightly stronger nondegeneracy condition. (This is all we really need in this paper.) Henceforth we shall denote by $\mathcal{B}$ the locus of points satisfying condition (b).

In the applications considered in this paper, the functions f_n will be of the form $f_n(z) = \mathrm{tr}[A(z)T(z)^n]$ where the $M \times M$ matrices $T(z)$ and $A(z)$ are polynomials in

z; therefore, the functions $\lambda_k(z)$ [which are the eigenvalues of $T(z)$] and $\alpha_k(z)$ will be algebraic functions of z, i.e. locally analytic except at isolated branch points. So one can cover the complex plane minus branch points by a family of simply connected domains D, and then apply Theorem 2.1 separately to each such domain D. The branch points are not covered by this analysis, but they will always be endpoints of curves of type (b), hence also limit points of zeros.

It is interesting to ask about the rate at which the zeros of f_n converge to the limit set. In case (a), it is easy to see that the convergence is exponentially fast. In case (b), simple expansions suggest that the rate is $1/n$ near regular points of the curve $\mathcal{B}$, and $1/n^2$ at branch points (see Sections 4.2.1 and 4.2.2).

In checking for isolated limiting points of zeros [case (a)], the following result will be useful (see Section 4.3):

Lemma 2.2 [39] *Suppose that* $f_n = \sum_{k=1}^{M} \alpha_k \lambda_k^n$, *and define*

$$D \;=\; \begin{pmatrix} f_0 & f_1 & \cdots & f_{M-1} \\ f_1 & f_2 & \cdots & f_M \\ \vdots & \vdots & & \vdots \\ f_{M-1} & f_M & \cdots & f_{2M-2} \end{pmatrix} . \tag{2.10}$$

Then

$$\det D \;=\; \prod_{k=1}^{M} \alpha_k \prod_{1 \le i < j \le M} (\lambda_j - \lambda_i)^2 \; . \tag{2.11}$$

PROOF. It is not difficult to see that $D = \Lambda^{\mathrm{T}} \operatorname{diag}(\alpha_1, \ldots, \alpha_M) \Lambda$ where Λ is the $M \times M$ Vandermonde matrix $\Lambda_{ij} = \lambda_i^{j-1}$. Lemma 2.2 then follows from the well-known formula

$$\det \Lambda \;=\; \prod_{1 \le i < j \le M} (\lambda_j - \lambda_i) \tag{2.12}$$

for the Vandermonde determinant. ∎

We remark that the product $\prod_{i<j} (\lambda_j - \lambda_i)^2$ is the discriminant of the characteristic polynomial of the transfer matrix: see (4.2) below.

2.3 Beraha numbers

We recall [97] that a complex number ζ is called an *algebraic number* (resp. an *algebraic integer*) if it is a root of some monic polynomial with rational (resp. integer) coefficients. Corresponding to any algebraic number ζ, there is a unique monic polynomial p with rational coefficients, called the *minimal polynomial of* ζ (over the rationals), with the property that p divides every polynomial with rational coefficients having ζ as a root. (The minimal polynomial of ζ has integer coefficients if and only if ζ is an algebraic integer.) Two algebraic numbers ζ and ζ' are called *conjugate*

if they have the same minimal polynomial. Conjugacy is obviously an equivalence relation, and so divides the set of algebraic numbers into equivalence classes.

Examples. 1. The numbers $B_5 = (3+\sqrt{5})/2$ and $B_5^* = (3-\sqrt{5})/2$ are conjugates, as they have the same minimal polynomial $p(x) = x^2 - 3x + 1$.

2. The numbers $2^{1/3}$, $2^{1/3}e^{2\pi i/3}$ and $2^{1/3}e^{4\pi i/3}$ are all conjugates, as they have the same minimal polynomial $p(x) = x^3 - 2$.

3. If ζ is a primitive n^{th} root of unity, the minimal polynomial of ζ is the *cyclotomic polynomial*

$$\Phi_n(x) \;=\; \prod_{\substack{1 \le k \le n \\ \gcd(k,n) = 1}} (x \,-\, e^{2\pi k i/n}) \;, \tag{2.13}$$

where the product runs over all positive integers $k \le n$ that are relatively prime to n (see e.g. [98, Section 3.7] for a proof). In particular, Φ_n is a monic polynomial with integer coefficients, irreducible over the field of rational numbers, of degree

$$\deg \Phi_n \;=\; \varphi(n) \tag{2.14}$$

where $\varphi(n)$ is the Euler totient function (i.e. the number of positive integers $k \le n$ that are relatively prime to n). Thus, all the primitive n^{th} roots of unity are mutually conjugate.

4. For $n \ge 2$, let us define the generalized Beraha numbers

$$B_n^{(k)} \;=\; 4\cos^2 \frac{k\pi}{n} \;=\; 2 \,+\, 2\cos \frac{2\pi k}{n} \;, \tag{2.15}$$

and let us call $B_n^{(k)}$ a primitive n^{th} generalized Beraha number in case k is relatively prime to n. Then the minimal polynomial of B_n (or of any primitive $B_n^{(k)}$) is[8]

$$p_n(x) \;=\; \prod_{\substack{1 \le k \le n/2 \\ \gcd(k,n) = 1}} (x \,-\, B_n^{(k)}) \;. \tag{2.16}$$

In Table 1 we show the p_n for $2 \le n \le 16$. p_n is a monic polynomial with integer coefficients, irreducible over the field of rational numbers, of degree

$$\deg p_n \;=\; \begin{cases} 1 & \text{for } n = 2 \\ \varphi(n)/2 & \text{for } n \ge 3 \end{cases} \tag{2.17}$$

[8] The proof of (2.16) requires some elementary Galois theory [98, Chapter 3] [99]: Fix $n \ge 3$ and $\zeta = e^{2\pi i/n}$, and let F be the extension field $\mathbb{Q}(\zeta)$. The irreducibility of the cyclotomic polynomial Φ_n implies that F has dimension $\varphi(n)$ over $\mathbb{Q}$, and that its Galois group $G = \mathrm{Gal}(F/\mathbb{Q})$ is the abelian group $\{\sigma_k\}_{1 \le k \le n,\, \gcd(k,n)=1}$ where $\sigma_k(r) = r$ for $r \in \mathbb{Q}$ and $\sigma_k(\zeta) = \zeta^k$. Now define $c \equiv 2\cos(2\pi/n) = \zeta + \bar{\zeta} \in \mathbb{R}$. By repeated application of the equation $\zeta^2 - c\zeta + 1 = 0$ it follows that $\mathbb{Q}(\zeta) = \mathbb{Q}(c) \oplus \zeta\mathbb{Q}(c)$, so that F has dimension 2 over $\mathbb{Q}(c)$. Therefore, $\mathbb{Q}(c)$ has dimension $\varphi(n)/2$ over $\mathbb{Q}$, so that the minimal polynomial $P(x)$ of c over $\mathbb{Q}$ has degree $\varphi(n)/2$. Now, for every k that is relatively prime to n, let us define $c_k = \sigma_k(c) = \zeta^k + \bar{\zeta}^k$; there are clearly $\varphi(n)/2$ distinct such numbers c_k (note that $c_{n-k} = c_k$). And we have $P(c_k) = P(\sigma_k(c)) = \sigma_k(P(c)) = 0$ since σ_k is a field automorphism and P has rational coefficients. It follows that $P(x) = \prod_{1 \le k \le n/2,\, \gcd(k,n)=1} (x - c_k)$. A trivial shift $x \to x - 2$ gives the same result for the $B_n^{(k)} = 2 + c_k$. We thank Dan Segal for explaining this proof to us.

Thus, all the primitive n^{th} generalized Beraha numbers are mutually conjugate.

The point of this digression into algebraic number theory is, of course, that the chromatic polynomial $P_G(q)$ of any loopless graph G is a monic polynomial with integer coefficients. Therefore, all the chromatic roots of G are algebraic integers; and if ζ is a chromatic root of G, then so are all its conjugates. We therefore have:

Proposition 2.3 *(a) Suppose that ζ has a conjugate lying in one of the intervals $(-\infty, 0)$, $(0, 1)$ or $(1, 32/27]$. Then ζ is not a chromatic root of any loopless graph.*

(b) Suppose that ζ has a conjugate lying in the interval $[5, \infty)$. Then ζ is not a chromatic root of any loopless planar *graph.*

(c) Suppose that ζ has a conjugate lying in the interval $(1, 2)$. Then ζ is not a chromatic root of any plane near-triangulation.

(d) Suppose that ζ has a conjugate lying in the interval $(2, 2.546602\ldots)$, where $2.546602\ldots$ is shorthand for the unique real solution of $q^3 - 9q^2 + 29q - 32 = 0$ (which is the nontrivial chromatic root of the octahedron). Then ζ is not a chromatic root of any plane triangulation.

PROOF. This follows immediately from the facts that there are no chromatic roots in the relevant intervals: see ref. [95] for $(-\infty, 0)$ and $(0, 1)$, ref. [100] for $(1, 32/27]$, refs. [101, 102, 103] for $[5, \infty)$, refs. [101, 104, 105] for $(1, 2)$, and refs. [104, 106] for $(2, 2.546602\ldots)$.[9] ∎

Examples. 1. A special case of Proposition 2.3(a) is the well-known fact [95, p. 23] that $B_5 = (3 + \sqrt{5})/2$ is not a chromatic root of any (loopless) graph, since its conjugate $B_5^* = (3 - \sqrt{5})/2$ lies in $(0, 1)$ [their minimal polynomial is $q^2 - 3q + 1$]. We shall prove a vastly stronger result in Corollary 2.4 below.

2. The number $1 + \sqrt{2}$ is not a chromatic root of any (loopless) graph, since its conjugate $1 - \sqrt{2}$ lies in $(-\infty, 0)$ [their minimal polynomial is $q^2 - 2q - 1$].

3. For $n \geq 5$, none of the numbers $2^{1/n} e^{2\pi k i/n}$ (k integer) is a chromatic root of any (loopless) graph, since their conjugate $2^{1/n}$ lies in $(1, 32/27]$ (their minimal polynomial is $q^n - 2$).[10]

4. The numbers $2 + \sqrt{2\sqrt{2} - 2}$ and $2 \pm i\sqrt{2\sqrt{2} + 2}$ are not chromatic roots of any (loopless) graph, since their conjugate $2 - \sqrt{2\sqrt{2} - 2}$ lies in $(1, 32/27]$ (their minimal polynomial is $q^4 - 8q^3 + 28q^2 - 48q + 28$).

We now state and prove the promised generalization of the fact that B_5 is not a chromatic root:

[9] See also [102, 103] for related results on zero-free intervals.

[10] This barely fails for $n = 4$. It is amusing to note that $32/27 \approx 2^{1/4}$ is equivalent to $(3/2)^{12} \approx 2^7$, which underlies the construction of the well-tempered scale.

Corollary 2.4 *A noninteger primitive n^{th} generalized Beraha number $B_n^{(k)}$ is not a chromatic root of any graph, except possibly when $n = 10$.*

This is an immediate consequence of the case $(0, 1)$ of Proposition 2.3(a) together with the following number-theoretic lemma:

Lemma 2.5 *Let $n = 5, 7, 8, 9$ or $n \geq 11$. Then there exists an integer k, relatively prime to n, in the interval $n/3 < k < n/2$.*

PROOF. If n is a prime ≥ 5, the result is trivial (take $k = \lfloor n/2 \rfloor$). The cases $n = 8, 12$ can be verified by hand (take $k = 3, 5$, respectively). Otherwise, note first that it suffices to find k in the interval $n/3 < k < 2n/3$ (if $k > n/2$, then replace k by $n - k$). So let p be the least prime divisor of n; define $r = \lceil p/3 \rceil \geq 1$, so that $rn/p \geq n/3 > (r-1)n/p$; and let k be either $rn/p + 1$ or $rn/p + 2$. Now the only possible common prime factor of k and n is p: for if $p' \neq p$ were to divide n, then it would also divide n/p; but if p' also divided k, then it would divide $k - rn/p = 1$ or 2, which is impossible since $p' \geq 3$. But p cannot divide *both* choices of k. Therefore, this construction allows k to be chosen relatively prime to n; and k lies in the interval $(n/3, 2n/3)$ provided that $n > 12$ (when $p = 2$), $n > 6$ (when $p = 3$) or $n \geq 15$ (when $p \geq 5$). ∎

Remarks. 1. As mentioned earlier, the case $n = 5$ of Corollary 2.4 is ancient folklore; the case $n = 7$ was stated by Tutte [72, p. 372]. Beraha, Kahane and Weiss [39, p. 53] asserted that the argument for B_5 "can be extended without much difficulty to the case of arbitrary nonintegral B_n", apparently overlooking the problem with B_{10}.

2. The exceptional case $n = 10$ is very curious. We do not know whether $B_{10} = (5 + \sqrt{5})/2 \approx 3.6180339887$ and $B_{10}^* = (5 - \sqrt{5})/2 \approx 1.3819660113$ can be chromatic roots. But Proposition 2.3(c) shows that B_{10} is not a chromatic root of any *plane near-triangulation*. Note also that when G is a *plane triangulation* having n vertices, Tutte's "golden identity" [70] [95, pp. 26–27]

$$P_G(B_{10}) \;=\; (\tau + 2)\tau^{3n-10} P_G(B_5)^2 \tag{2.18}$$

where $\tau = B_5 - 1$ is the golden ratio, together with the fact that $P_G(B_5) \neq 0$, yields the slightly stronger result $P_G(B_{10}) > 0$.

3 Transfer-Matrix Theory

In this section we briefly review the transfer-matrix formalism for the Potts model, both in the spin representation (Section 3.1) and in the Fortuin-Kasteleyn representation (Section 3.2). Thereafter we use only the Fortuin-Kasteleyn representation, which allows us to perform computations for noninteger q. We conclude by computing the size of the FK-representation transfer matrix for the square and triangular lattices with free longitudinal boundary conditions and either free or periodic transverse boundary conditions (Section 3.3).

3.1 Transfer matrix in the spin representation

Consider a graph $G_n = (V_n, E_n)$ consisting of n identical "layers", with connections between adjacent layers repeated in a regular fashion. Then the partition function of the Potts model on G can be written in terms of a transfer matrix.

To make this precise, let V^0 be the set of vertices in a single layer, let E^0 be the set of edges within a single layer (we call these *horizontal* edges), and let E^* be the set of edges connecting each layer to the next one (we call these *vertical* edges). Note that E^0 is a set of unordered pairs of elements of V^0, while E^* is a set of ordered pairs of elements of V^0. The vertex set of the graph G_n is then

$$V_n \;=\; V^0 \times \{1, \ldots, n\} \;=\; \{(x,i)\colon\, x \in V^0 \text{ and } 1 \le i \le n\}\;, \tag{3.1}$$

while the edge set is either

$$E_n^{\text{free}} \;=\; \bigcup_{i=1}^{n} E_i^{\text{horiz}} \bigcup \bigcup_{i=1}^{n-1} E_i^{\text{vert}} \tag{3.2}$$

for free longitudinal boundary conditions or

$$E_n^{\text{per}} \;=\; \bigcup_{i=1}^{n} E_i^{\text{horiz}} \bigcup \bigcup_{i=1}^{n} E_i^{\text{vert}} \tag{3.3}$$

for periodic longitudinal boundary conditions, where

$$E_i^{\text{horiz}} \;=\; \{\langle (x,i), (x',i)\rangle\colon\, \langle xx'\rangle \in E^0\} \tag{3.4}$$

and

$$E_i^{\text{vert}} \;=\; \{\langle (x,i), (x',i+1)\rangle\colon\, (x,x') \in E^*\} \tag{3.5}$$

and of course layer $n+1$ is identified with layer 1. We also assume that the couplings are identical from layer to layer: that is, we are given weights $\{v_e\}_{e \in E^0 \cup E^*}$, and we define the edge weights for G_n by

$$v_{\langle (x,i),(x',i)\rangle} \;=\; v_{\langle xx'\rangle} \qquad \text{for } \langle xx'\rangle \in E^0 \tag{3.6a}$$

$$v_{\langle (x,i),(x',i+1)\rangle} \;=\; v_{(x,x)} \qquad \text{for } (x,x') \in E^* \tag{3.6b}$$

We now fix an integer $q \ge 1$, and let $\Sigma = \{1, \ldots, q\}^{V^0}$ be the space of spin configurations on a single layer; we denote a generic such configuration by $\boldsymbol{\sigma} = \{\sigma_x\}_{x \in V^0}$. We then define the matrices H and V, which encode the Boltzmann factors corresponding to horizontal and vertical edges, respectively:

$$\mathsf{H}(\boldsymbol{\sigma}', \boldsymbol{\sigma}) \;=\; \delta(\boldsymbol{\sigma}, \boldsymbol{\sigma}') \prod_{\langle xx'\rangle \in E^0} [1 + v_{\langle xx'\rangle} \delta(\sigma_x, \sigma_{x'})] \tag{3.7}$$

$$\mathsf{V}(\boldsymbol{\sigma}', \boldsymbol{\sigma}) \;=\; \prod_{(x,x') \in E^*} [1 + v_{(x,x')} \delta(\sigma_x, \sigma'_{x'})] \tag{3.8}$$

The partition function of the Potts model on G_n is then

$$Z_{G_n^{\rm free}}(q, \{v_e\}) \;=\; \mathbf{1}^{\rm T} \mathsf{H} (\mathsf{V}\mathsf{H})^{n-1} \mathbf{1} \tag{3.9}$$

$$Z_{G_n^{\rm per}}(q, \{v_e\}) \;=\; {\rm tr}[(\mathsf{V}\mathsf{H})^n] \tag{3.10}$$

where $\mathbf{1}$ is the vector whose entries all equal 1, and ${}^{\rm T}$ denotes transpose. The transfer matrix is thus

$$\mathsf{T} \;=\; \mathsf{V}\mathsf{H} \,. \tag{3.11}$$

It has size $q^m \times q^m$, where $m = |V^0|$ is the number of sites in each layer.

The horizontal matrix H is diagonal in the spin basis, hence sparse; its computation takes a time of order $|E^0| q^m \lesssim m^2 q^m$. But since the vertical matrix V is dense, its computation takes in general a time of order $|E^*| q^{2m}$. This is a severe constraint on the practical applicability of the transfer-matrix method. However, when the graphs G_n are *planar*, V can be written as a product of sparse matrices that correspond to the replacement of *one* site on layer i by the corresponding site on layer $i+1$, so that its computation takes only a time of order mq^m. (Indeed, this can be done for an arbitrary planar graph, whether or not it consists of repeated layers [79].) This factorization of V can also be performed for some non-planar graphs, including all those in which the single-layer vertex set V^0 can be ordered in such a way that $(x, x') \in E^*$ implies $x \succeq x'$.[11] (This latter situation includes, in particular, all the lattices $\mathbb{Z}^d$, since the only vertical edges are of the form (x, x). On the other hand, it excludes the triangular lattice with *periodic* transverse boundary conditions, which needs a separate treatment.) For simplicity we describe this construction only for the cases of greatest practical interest, namely when G_n is a square or triangular lattice with free or periodic transverse boundary conditions. The single-layer vertex set is thus $V^0 = \{1, \ldots, m\}$; the horizontal edge set is either

$$E^0_{\rm free} \;=\; \{\langle x, x+1\rangle \colon\; 1 \le x \le m-1\} \tag{3.12}$$

for free transverse boundary conditions or

$$E^0_{\rm per} \;=\; \{\langle x, x+1\rangle \colon\; 1 \le x \le m\} \tag{3.13}$$

for periodic transverse boundary conditions (where site $m+1$ is of course identified with site 1); and the vertical edge set is either

$$E^0_{\rm SQ} \;=\; \{(x, x) \colon\; 1 \le x \le m\} \tag{3.14}$$

for the square lattice,

$$E^0_{\rm TRI,free} \;=\; \{(x, x) \colon\; 1 \le x \le m\} \bigcup \{(x+1, x) \colon\; 1 \le x \le m-1\} \tag{3.15}$$

for the triangular lattice with free transverse boundary conditions, or

$$E^0_{\rm TRI,per} \;=\; \{(x, x) \colon\; 1 \le x \le m\} \bigcup \{(x+1, x) \colon\; 1 \le x \le m\} \tag{3.16}$$

[11] This is equivalent to requiring that the directed graph (V^0, E^{**}) be *acyclic*, where $E^{**} = \{(x, x') \in E^* \colon\; x \ne x'\}$.

for the triangular lattice with periodic transverse boundary conditions. Note that the diagonal edges in (3.15)–(3.16) point "southeast–northwest".

We now define $q^m \times q^m$ matrices D_x and $\mathsf{J}_{xx'}$ by

$$\mathsf{D}_x(\boldsymbol{\sigma}', \boldsymbol{\sigma}) \;=\; \prod_{y \neq x} \delta(\sigma_y, \sigma'_y) \tag{3.17a}$$

$$\mathsf{J}_{xx'}(\boldsymbol{\sigma}', \boldsymbol{\sigma}) \;=\; \delta(\sigma_x, \sigma_{x'})\, \delta(\boldsymbol{\sigma}, \boldsymbol{\sigma}') \tag{3.17b}$$

Thus, D_x (for "detach" or "disconnect") is of the form $I \otimes I \otimes \cdots \otimes E \otimes \cdots \otimes I \otimes I$, where I is the $q \times q$ identity matrix, E is the $q \times q$ matrix whose entries are all 1, and the E factor occurs at position x; informally, D_x disconnects the two rows at site x. Since I and E commute, all the operators D_x commute among themselves. Likewise, $\mathsf{J}_{xx'}$ identifies ("joins") spins x and x' in a single layer. Since the operators $\mathsf{J}_{xx'}$ are diagonal in the spin basis, they also commute among themselves. Finally, D_x commutes with $\mathsf{J}_{x'x''}$ whenever x is different from both x' and x''.

We now define matrices

$$\mathsf{P}_j \;=\; v_{(j,j)} I \,+\, \mathsf{D}_j \tag{3.18}$$

$$\mathsf{Q}_j \;=\; I \,+\, v_{\langle j,j+1\rangle} \mathsf{J}_{j,j+1} \tag{3.19}$$

$$\mathsf{R}_j \;=\; I \,+\, v_{(j+1,j)} \mathsf{J}_{j,j+1} \tag{3.20}$$

corresponding to the Boltzmann factors for vertical, horizontal and diagonal edges, respectively.[12] The horizontal and vertical parts of the transfer matrix are then

$$\mathsf{H}_{\mathrm{SQ}}^{\mathrm{free}} \;=\; \mathsf{H}_{\mathrm{TRI}}^{\mathrm{free}} \;=\; \mathsf{Q}_{m-1} \cdots \mathsf{Q}_2 \mathsf{Q}_1 \tag{3.21a}$$

$$\mathsf{H}_{\mathrm{SQ}}^{\mathrm{per}} \;=\; \mathsf{Q}_m \mathsf{Q}_{m-1} \cdots \mathsf{Q}_2 \mathsf{Q}_1 \tag{3.21b}$$

and

$$\mathsf{V}_{\mathrm{SQ}}^{\mathrm{free}} \;=\; \mathsf{V}_{\mathrm{SQ}}^{\mathrm{per}} \;=\; \mathsf{P}_m \mathsf{P}_{m-1} \cdots \mathsf{P}_2 \mathsf{P}_1 \tag{3.22a}$$

$$\mathsf{V}_{\mathrm{TRI}}^{\mathrm{free}} \;=\; \mathsf{P}_m \mathsf{R}_{m-1} \mathsf{P}_{m-1} \cdots \mathsf{R}_2 \mathsf{P}_2 \mathsf{R}_1 \mathsf{P}_1 \tag{3.22b}$$

where the action of these matrices should always be read from right to left. Note that R_j corresponds to a diagonal edge whenever it is applied after P_j and before P_{j+1}.

For the *triangular* lattice with *periodic* transverse boundary conditions, a slight trick is needed in order to treat correctly the last diagonal bond joining columns m and 1 [55]. The idea is to work with $q^{m+1} \times q^{m+1}$ matrices indexed by spins $\boldsymbol{\sigma} = (\sigma_1, \ldots, \sigma_{m+1})$, and include in the horizontal matrix an operator that identifies σ_{m+1} with σ_1 on each row. Thus,

$$\mathsf{H}_{\mathrm{TRI}}^{\mathrm{per}} \;=\; \mathsf{J}_{m+1,1} \mathsf{Q}_m \mathsf{Q}_{m-1} \cdots \mathsf{Q}_2 \mathsf{Q}_1 \tag{3.23}$$

$$\mathsf{V}_{\mathrm{TRI}}^{\mathrm{per}} \;=\; \mathsf{P}_{m+1} \mathsf{R}_m \mathsf{P}_m \mathsf{R}_{m-1} \mathsf{P}_{m-1} \cdots \mathsf{R}_2 \mathsf{P}_2 \mathsf{R}_1 \mathsf{P}_1 \tag{3.24}$$

[12] In this sentence we are of course using the term "vertical edges" in its ordinary geometrical sense, not in the technical sense defined previously. We follow the notation of Baxter [55, Section 2] with some modifications.

In particular, the vertical matrix $\mathsf{V}_{\rm TRI}^{\rm per}$ is just $\mathsf{V}_{\rm TRI}^{\rm free}$ with m replaced by $m+1$.

Remarks. 1. The rewriting (3.21) of the horizontal matrix H is of course unnecessary, as H was already diagonal (hence sparse) in the spin basis. But (3.21) will be useful when we use the partition basis (see below).

2. The order of operators in (3.21), (3.22a) and (3.23) is irrelevant, as all the operators in question commute. Only in (3.22b) and (3.24) is the operator ordering crucial.

3. The operators $e_1, \ldots, e_{2m-1}$ defined by

$$e_{2j-1} \;=\; q^{-1/2}\mathsf{D}_j \qquad \text{for } 1 \le j \le m \tag{3.25a}$$

$$e_{2j} \;=\; q^{1/2}\mathsf{J}_{j,j+1} \quad \text{for } 1 \le j \le m-1 \tag{3.25b}$$

satisfy the Temperley-Lieb algebra [107, 4, 79]

$$e_i^2 \;=\; q^{1/2} e_i \tag{3.26a}$$

$$e_i e_{i\pm 1} e_i \;=\; e_i \tag{3.26b}$$

$$e_i e_j \;=\; e_j e_i \qquad \text{for } |i-j| > 1 \tag{3.26c}$$

All these operators act, of course, in the q^m-dimensional vector space consisting of all functions of $\sigma_1, \ldots, \sigma_m$.[13] But for the case of *free* longitudinal boundary conditions (3.9), we need only consider the subspace spanned by those vectors that can be obtained from the constant vector $\mathbf{1}$ by action of the operators H and V. All such functions are sums of products of delta functions $\delta(\sigma_x, \sigma_y)$, and we can take as a basis the functions $\mathbf{v}_{\mathcal{P}}$ associated to a partition $\mathcal{P} = \{P_1, \ldots, P_k\}$ of $\{1, \ldots, m\}$ by

$$\mathbf{v}_{\mathcal{P}}(\sigma_1, \ldots, \sigma_m) \;=\; \prod_{P \in \mathcal{P}} \prod_{x,y \in P} \delta(\sigma_x, \sigma_y)\;. \tag{3.27}$$

For example, for $m = 3$ we have the five basis vectors

$$\mathbf{v}_{\{\{1\},\{2\},\{3\}\}} \;=\; 1 \tag{3.28a}$$

$$\mathbf{v}_{\{\{1,2\},\{3\}\}} \;=\; \delta(\sigma_1, \sigma_2) \tag{3.28b}$$

$$\mathbf{v}_{\{\{1,3\},\{2\}\}} \;=\; \delta(\sigma_1, \sigma_3) \tag{3.28c}$$

$$\mathbf{v}_{\{\{1\},\{2,3\}\}} \;=\; \delta(\sigma_2, \sigma_3) \tag{3.28d}$$

$$\mathbf{v}_{\{\{1,2,3\}\}} \;=\; \delta(\sigma_1, \sigma_2, \sigma_3) \tag{3.28e}$$

Indeed, when the graph G is *planar*, it is not hard to see on topological grounds that only *non-crossing* partitions can arise. (A partition is said to be *non-crossing* if $a < b < c < d$ with a, c in the same block and b, d in the same block imply that

[13] Or, in the case of the triangular lattice with periodic transverse b.c., in the q^{m+1}-dimensional space of all functions of $\sigma_1, \ldots, \sigma_{m+1}$.

a, b, c, d are all in the same block.) Moreover, spatial symmetries can further restrict the subspace. Finally, when the horizontal couplings $v_{\langle xx' \rangle}$ are all equal to -1 — which is the case for the chromatic polynomial — then the horizontal operator H is a *projection*, and we can work in its image subspace by using the modified transfer matrix $\mathsf{T}' = \mathsf{HVH}$ in place of $\mathsf{T} = \mathsf{VH}$, and using the basis vectors

$$\mathbf{w}_{\mathcal{P}} \;=\; \mathsf{H}\mathbf{v}_{\mathcal{P}} \tag{3.29}$$

in place of $\mathbf{v}_{\mathcal{P}}$. Note that $\mathbf{w}_{\mathcal{P}} = 0$ if $\mathcal{P}$ has any pair of nearest neighbors in the same block. In Section 3.3 we shall compute the dimensions of all these subspaces.

The action of the operators D_x and $\mathsf{J}_{xx'}$ on the basis vectors $\mathbf{v}_{\mathcal{P}}$ is quite simple. As one might expect, $\mathsf{J}_{xx'}$ joins sites x and x', i.e.

$$\mathsf{J}_{xx'}\mathbf{v}_{\mathcal{P}} \;=\; \mathbf{v}_{\mathcal{P}\bullet xx'} \tag{3.30}$$

where $\mathcal{P}\bullet xx'$ is the partition obtained from $\mathcal{P}$ by amalgamating the blocks containing x and x' (if they were not already in the same block). D_x detaches site x from the block it currently belongs to, multiplying by a factor q if x is currently a singleton:

$$\mathsf{D}_x\mathbf{v}_{\mathcal{P}} \;=\; \begin{cases} \mathbf{v}_{\mathcal{P}\setminus x} & \text{if } \{x\} \notin \mathcal{P} \\ q\mathbf{v}_{\mathcal{P}} & \text{if } \{x\} \in \mathcal{P} \end{cases} \tag{3.31}$$

where $\mathcal{P} \setminus x$ is the partition obtained from $\mathcal{P}$ by detaching x from its block (and thus making it a singleton).

At the final stage we need to compute the inner products $\mathbf{1}^{\mathrm{T}}\mathbf{v}_{\mathcal{P}}$, which are easy:

$$\mathbf{1}^{\mathrm{T}}\mathbf{v}_{\mathcal{P}} \;=\; q^{|\mathcal{P}|} \tag{3.32}$$

where $|\mathcal{P}|$ is the number of blocks in $\mathcal{P}$.

To summarize: The Potts-model partition function (3.9) or (3.10) can always be computed by the transfer-matrix method working in the spin basis $f(\sigma_1, \ldots, \sigma_m)$, which has dimension q^m. Of course, each value of q has to be treated separately; and it goes without saying that q must be a positive integer. On the other hand, for *free* longitudinal boundary conditions, there is an alternative method for computing the partition function (3.9), using the partition basis $\mathbf{v}_{\mathcal{P}}$. In this formalism q appears only as a parameter [in (3.31) and (3.32)]; and since the final result will obviously be a polynomial in q, it must perforce be equal to the Fortuin-Kasteleyn partition function (2.4). This latter formalism is thus essentially equivalent to constructing the transfer matrix directly in the Fortuin-Kasteleyn representation, as we shall see explicitly in the next subsection.

3.2 Transfer matrix in the Fortuin-Kasteleyn representation

Let us now temporarily forget the Potts spin model — and in particular forget the transfer-matrix formalism constructed in the preceding subsection — and try instead

to devise a transfer-matrix method for computing the Fortuin-Kasteleyn partition function (2.4) when the graph G has a layered structure (3.1)–(3.6). What makes this a bit tricky is, of course, the nonlocality of the factor $q^{k(E')}$ in (2.4). The technique for handling this nonlocality was foreshadowed in the work of Lieb and Beyer [108] on percolation and was made explicit (for the case of the chromatic polynomial) in the work of Biggs and collaborators [109, 110, 111]. In the physics literature, this approach was first used (to our knowledge) by Derrida and Vannimenus [112] in their study of percolation, and was applied to the q-state Potts model (and explained very clearly) by Blöte and Nightingale [66]; it was subsequently employed by several groups [113, 114, 115, 116]. Here we limit ourselves to giving a brief summary.

The basic idea is to build up the subgraph $E' \subseteq E$ layer by layer. At the end we will need to know the number of connected components in this subgraph; in order to be able to compute this, we shall keep track, as we go along, of which sites in the current "top" layer are connected to which other sites in that layer by a path of occupied bonds (i.e. bonds of E') in lower layers. Thus, we shall work in the basis of connectivities of the top layer, whose basis elements $\mathbf{v}_{\mathcal{P}}$ are indexed by partitions $\mathcal{P}$ of the single-layer vertex set V^0. [The reader is reminded to forget (3.27) for the time being. The $\mathbf{v}_{\mathcal{P}}$ should here be thought of simply as abstract basis elements indexed by partitions $\mathcal{P}$.] The elementary operators we shall need are the *join operators*

$$\mathsf{J}_{xx'}\mathbf{v}_{\mathcal{P}} \;=\; \mathbf{v}_{\mathcal{P}\bullet xx'} \tag{3.33}$$

(note that all these operators commute) and the *detach operators*

$$\mathsf{D}_x\mathbf{v}_{\mathcal{P}} \;=\; \begin{cases} \mathbf{v}_{\mathcal{P}\setminus x} & \text{if } \{x\} \notin \mathcal{P} \\ q\mathbf{v}_{\mathcal{P}} & \text{if } \{x\} \in \mathcal{P} \end{cases} \tag{3.34}$$

where $\mathcal{P} \bullet xx'$ and $\mathcal{P} \setminus x$ were defined previously (don't forget *those* definitions!). The horizontal transfer matrix is then

$$\mathsf{H} \;=\; \prod_{\langle xx'\rangle \in E^0} [1 + v_{\langle xx'\rangle}\mathsf{J}_{xx'}] \;. \tag{3.35}$$

The vertical transfer matrix is slightly more complicated:

$$\mathsf{V}\mathbf{v}_{\mathcal{P}} \;=\; \sum_{\widetilde{E}\subseteq E^*} q^{A(\mathcal{P},\widetilde{E})} \left(\prod_{(x,x')\in\widetilde{E}} v_{(x,x')} \right) \mathbf{v}_{\mathcal{P}|\widetilde{E}} \tag{3.36}$$

where $A(\mathcal{P},\widetilde{E})$ is the number of "abandoned clusters", i.e. the number of blocks $P \in \mathcal{P}$ such that no vertex in P is an endpoint of an edge in $\widetilde{E}$; and $\mathcal{P}|\widetilde{E}$ is the partition of V^0 in which vertices x', y' lie in the same block if and only if there exist vertices x, y in the same block of $\mathcal{P}$ such that both (x, x') and (y, y') lie in $\widetilde{E}$.

In many cases (including all planar graphs), V can be written as a product of sparse matrices that correspond to the replacement of *one* site on layer i by the corresponding site on layer $i + 1$; and these sparse matrices have a simple expression

in terms of join and detach operators. Suppose, for concreteness, that the single-layer vertex set V^0 can be ordered in such a way that $(x, x') \in E^*$ implies $x \succeq x'$; using this ordering, let us number the sites of V^0 as $1, \ldots, m$. Then

$$\mathsf{V} \;=\; \mathsf{P}_m \mathsf{R}_{m-1,m} \mathsf{P}_{m-1} \left(\prod_{y > m-2} \mathsf{R}_{m-2,y} \right) \mathsf{P}_{m-2} \cdots \left(\prod_{y>2} \mathsf{R}_{2,y} \right) \mathsf{P}_2 \left(\prod_{y>1} \mathsf{R}_{1,y} \right) \mathsf{P}_1 \;, \tag{3.37}$$

where

$$\mathsf{P}_x \;=\; v_{(x,x)} I \,+\, \mathsf{D}_x \tag{3.38}$$

$$\mathsf{R}_{x,y} \;=\; I \,+\, v_{(y,x)} \mathsf{J}_{xy} \tag{3.39}$$

(The triangular lattice with periodic transverse b.c. is handled using the trick discussed in the preceding subsection.)

Finally, the partition function for *free* longitudinal boundary conditions can be obtained by sandwiching the transfer matrix between suitable vectors on right and left:

$$Z_{G_n^{\mathrm{free}}}(q, \{v_e\}) \;=\; \mathbf{u}^{\mathrm{T}} \mathsf{H} (\mathsf{V}\mathsf{H})^{n-1} \mathbf{v}_{\mathrm{id}} \;, \tag{3.40}$$

where "id" denotes the partition in which each site $x \in V^0$ is a singleton, and $\mathbf{u}^{\mathrm{T}}$ is defined by

$$\mathbf{u}^{\mathrm{T}} \mathbf{v}_{\mathcal{P}} \;=\; q^{|\mathcal{P}|} \;. \tag{3.41}$$

Of course, it will not have escaped the reader's notice that all the formulae in this subsection are *identical* to those developed in the preceding subsection; only the interpretation is different. In particular, the operators D_x and $\mathsf{J}_{xx'}$ in the FK representation act in precisely the same way as the operators of the same name act in the spin representation *with respect to the partition basis*.

Let us observe, in conclusion, that the Potts model with *free* longitudinal boundary conditions is much easier to handle than that with *periodic* longitudinal boundary conditions. We can understand the difficulty posed by periodic longitudinal b.c. from two complementary points of view. In the spin representation, the trouble is that, because of the trace in (3.10), we must compute the action of T in the entire q^m-dimensional space of functions of $\sigma_1, \ldots, \sigma_m$, not merely in the subspace spanned by sums of products of delta functions. In some cases this can be done by careful counting of subspaces and dimensions [34, 35], but it is not entirely trivial. In the FK representation, by contrast, everything is fully automated, but it is not sufficient to keep track of the connectivities of the sites in the top layer alone, as this layer will eventually need to be joined up to the bottom layer. Rather, it is necessary to keep track of the combined connectivities of the sites in the *top and bottom* layers: this method for handling periodic longitudinal b.c. will be sketched in Section 7.4 and explained in detail in a subsequent paper [88].

3.3 Dimension of the transfer matrix

Let us consider a strip of width m with free longitudinal boundary conditions. We want to know the dimension of the corresponding FK-representation transfer

matrix for different lattices (square and triangular) and different transverse boundary conditions (free and periodic). Each of these cases corresponds to a different class of allowed partitions $\mathcal{P}$. The more stringent the restrictions on the allowed partitions, the smaller the dimension of the transfer matrix.

We shall in general follow the notation of Stanley's 2-volume work *Enumerative Combinatorics* [117, 118], where more detail on various integer sequences can be found. Another useful reference is the On-Line Encyclopedia of Integer Sequences [119].

1) Let $\mathbf{P}_m$ denote the set of all partitions of $\{1, \ldots, m\}$. Its cardinality is given by the *Bell numbers* (or exponential numbers) $B(m)$, which can be computed [120, Sections 6.1 and 6.3] from the exponential generating function

$$E_B(x) \;\equiv\; \sum_{m=0}^{\infty} B(m) \, \frac{x^m}{m!} \;=\; \exp(e^x - 1) \tag{3.42}$$

or from the remarkable formula

$$B(m) \;=\; e^{-1} \sum_{k=0}^{\infty} \frac{k^m}{k!} \tag{3.43}$$

(it is far from obvious at first sight that the right-hand side defines an integer!). For example, for $m = 4$ we have $B(4) = 15$, corresponding to the partitions[14]

$$\begin{aligned} \mathbf{P}_4 \;=\; & \{1, \delta_{12}, \delta_{13}, \delta_{14}, \delta_{23}, \delta_{24}, \delta_{34}, \delta_{123}, \delta_{124}, \delta_{134}, \delta_{234}, \delta_{1234}, \\ & \delta_{12}\delta_{34}, \delta_{13}\delta_{24}, \delta_{14}\delta_{23}\} \; . \end{aligned} \tag{3.44}$$

The Bell numbers have the asymptotic behavior [120, Sections 6.1–6.3] [121, Section 5.8] [122, Examples 5.4, 5.10, 12.5 and 12.6]

$$\log B(m) \;=\; mW(m+1) \,-\, m \,+\, \frac{m+1}{W(m+1)} \,-\, \tfrac{1}{2} \log[W(m+1)+1] \,-\, 2 \,+\, O\big(\tfrac{\log m}{m}\big) \tag{3.45a}$$

$$\;=\; mW(m) \,-\, m \,+\, \frac{m}{W(m)} \,-\, \tfrac{1}{2} \log[W(m)+1] \,-\, 1 \,+\, o(1) \tag{3.45b}$$

$$\;=\; m \log m \,-\, m \log\log m \,-\, m \,+\, \frac{m \log\log m}{\log m} \,+\, \frac{m}{\log m} \,+\, O\left(\frac{m (\log\log m)^2}{(\log m)^2}\right) \tag{3.45c}$$

as $m \to \infty$, where $W(z)$ denotes the unique real solution of $we^w = z$ (this is the Lambert W function [123]) and has the (very slowly) convergent expansion in powers

[14] Henceforth we shall abbreviate delta functions $\delta(\sigma_1, \sigma_3)$ by δ_{13}, etc. Moreover, we shall usually abbreviate partitions $\mathcal{P}$ by writing instead the corresponding product $\mathbf{v}_{\mathcal{P}}$ of delta functions [cf. (3.27)]: e.g. in place of $\mathcal{P} = \{\, \{1,3\}, \{2,4\}, \{5\} \,\}$ we shall write simply $\mathcal{P} = \delta_{13}\delta_{24}$.

of $1/\log z$ and $\log\log z/\log z$:

$$W(z) \;=\; \log z \;-\; \log\log z \;+\; \sum_{n=1}^{\infty}\sum_{k=1}^{n}(-1)^{n+1}\,\frac{s(n,n-k+1)}{k!}\,\frac{(\log\log z)^k}{(\log z)^n} \tag{3.46}$$

where the $s(n,\ell)$ are the Stirling numbers of the first kind. [The expansions (3.45a,b) thus yield much better numerical approximations than (3.45c).] The Bell numbers for $1 \le m \le 14$ are shown in Table 2.

The Bell numbers can also be written as

$$B(m) \;=\; \sum_{k=1}^{m} S(m,k)\;, \tag{3.47}$$

where the *Stirling number of the second kind* $S(m,k)$ is the number of ways of partitioning the set $\{1,\ldots,m\}$ into k nonempty subsets (i.e., the number of ways of placing m labeled balls into k indistinguishable boxes, with each box containing at least one ball).

2) If the graph G is planar, then only non-crossing partitions can occur. The number of non-crossing partitions of $\{1,\ldots,m\}$ is given by the *Catalan number*[15]

$$C_m \;=\; \frac{(2m)!}{m!\,(m+1)!} \;=\; \frac{1}{m+1}\binom{2m}{m}\;. \tag{3.48}$$

Thus, for $m = 4$ we have $C_m = 14$, corresponding to the partitions

$$\begin{aligned}\mathbf{P}_{\mathrm{nc},4} \;=\; &\{1, \delta_{12}, \delta_{13}, \delta_{14}, \delta_{23}, \delta_{24}, \delta_{34}, \delta_{123}, \delta_{124}, \delta_{134}, \delta_{234}, \delta_{1234},\\ &\delta_{12}\delta_{34}, \delta_{14}\delta_{23}\}\;,\end{aligned} \tag{3.49}$$

since the only crossing partition of $\{1,2,3,4\}$ is $\delta_{13}\delta_{24}$. The Catalan numbers have the asymptotic behavior

$$C_m \;=\; 4^m m^{-3/2}\pi^{-1/2}[1 + O(1/m)] \tag{3.50}$$

as $m \to \infty$. For $1 \le m \le 14$ they are shown in Table 2.

3) For the zero-temperature antiferromagnetic model ($v = -1$), we can work in the basis $\mathbf{w}_{\mathcal{P}}$ defined by (3.29), so that partitions with nearest neighbors in the same block are also forbidden. Let us consider first the case of free transverse boundary conditions. The number of non-crossing non-nearest-neighbor partitions of $\{1,\ldots,m\}$ is given by the *Motzkin number* M_{m-1} [124, Proposition 3.6] [125].[16] Here M_n is the

[15] Stanley [118, Exercises 6.19 and 6.25] gives 66 combinatorial interpretations and 9 algebraic interpretations of the Catalan numbers C_n. See also [118, Exercise 6.24].

[16] *Warning:* Several references use the notation m_n to denote what we call M_n; and one reference [126] writes M_n to denote a *different* sequence.

number of ways of drawing any number of nonintersecting chords among n points on a circle[17]; it is given by the explicit formula

$$M_n \;=\; \sum_{j=0}^{\lfloor n/2 \rfloor} \binom{n}{2j} C_j \tag{3.51}$$

and satisfies both the linear recursion relation

$$M_n \;=\; \frac{2n+1}{n+2} M_{n-1} \;+\; \frac{3n-3}{n+2} M_{n-2} \;+\; \delta_{n0} \tag{3.52}$$

and the nonlinear recursion relation

$$M_n \;=\; M_{n-1} \;+\; \sum_{k=0}^{n-2} M_k M_{n-2-k} \;+\; \delta_{n0} \tag{3.53}$$

with initial condition $M_n = 0$ for $n < 0$ (see e.g. [127, 126, 128, 129]). The generating function $M(x) = \sum_{n=0}^{\infty} M_n x^n$ is

$$M(x) \;=\; \frac{1 - x - \sqrt{1 - 2x - 3x^2}}{2x^2} \;. \tag{3.54}$$

For example, for $m = 4$ we have $M_3 = 4$, corresponding to the partitions

$$\mathbf{P}_{\mathrm{nc+nnn},4} \;=\; \{1, \delta_{13}, \delta_{14}, \delta_{24}\} \;. \tag{3.55}$$

The Motzkin numbers have the asymptotic behavior

$$M_n \;=\; 3^n n^{-3/2} \frac{3\sqrt{3}}{2\sqrt{\pi}} [1 + O(1/n)] \tag{3.56}$$

as $n \to \infty$. The transfer matrix for a triangular-lattice strip of width m with free boundary conditions at zero temperature has dimension

$$\mathrm{TriFree}(m) \;=\; M_{m-1} \;. \tag{3.57}$$

The numbers $\mathrm{TriFree}(m) = M_{m-1}$ for $1 \le m \le 14$ are shown in Table 2.

4) Let us now consider the zero-temperature antiferromagnetic model with periodic transverse boundary conditions. The number of non-crossing non-nearest-neighbor partitions of $\{1, \ldots, m\}$ when it is considered periodically (i.e. when 1 and

[17] This interpretation of M_n arises in enumerating the "non-magnetic connectivities" of a loop model on the square lattice [114, pp. 1436–1437]. See Stanley [118, Exercises 6.38 and 6.46(b)] for 14 combinatorial interpretations of the Motzkin numbers M_n.

m also are considered to be nearest neighbors) is given by [129, Section 3.2, family R2][18]

$$d_m \;=\; \begin{cases} 1 & \text{for } m = 1 \\ R_m & \text{for } m \ge 2 \end{cases} \tag{3.58}$$

where the *Riordan numbers* (or Motzkin alternating sums) R_m [127, 126, 129][19] are defined by $R_0 = 1$, $R_1 = 0$ and

$$R_m \;=\; \sum_{k=0}^{m-1} (-1)^{m-k-1} M_k \qquad \text{for } m \ge 2 \tag{3.59}$$

and satisfy the linear recursion relations

$$R_m \;=\; -R_{m-1} \,+\, M_{m-1} \,+\, \delta_{m0} \tag{3.60}$$

$$R_m \;=\; \frac{2m-2}{m+1} R_{m-1} \,+\, \frac{3m-3}{m+1} R_{m-2} \,+\, \delta_{m0} \tag{3.61}$$

and the nonlinear recursion relation

$$R_m \;=\; \sum_{k=0}^{m-1} R_k R_{m-1-k} \,+\, (-1)^m \tag{3.62}$$

with initial condition $R_m = 0$ for $m < 0$ (see e.g. [127, 126, 129]). The generating function $R(x) = \sum_{m=0}^\infty R_m x^m$ is

$$R(x) \;=\; \frac{1 + x - \sqrt{1 - 2x - 3x^2}}{2x(1+x)} \,. \tag{3.63}$$

For example, for $m = 4$ we have $d_4 = R_4 = 3$, corresponding to the partitions

$$\mathbf{P}_{\text{nc+nnnCyl},4} \;=\; \{1, \delta_{13}, \delta_{24}\} \tag{3.64}$$

The Riordan numbers have the asymptotic behavior

$$d_m \;=\; R_m \;=\; 3^m m^{-3/2} \frac{3\sqrt{3}}{8\sqrt{\pi}} [1 + O(1/m)] \tag{3.65}$$

as $m \to \infty$. The numbers d_m for $1 \le m \le 14$ are shown in Table 2.

[18] Let d_m be the number of non-crossing non-nearest-neighbor partitions of $\{1, \ldots, m\}$ when it is considered periodically. We have $d_1 = d_2 = 1$ and $M_{m-1} = d_{m-1} + d_m$ for $m \ge 3$. [PROOF: For $m \ge 3$, a non-crossing non-nearest-neighbor partition of $\{1, \ldots, m\}$ (considered linearly) either has 1 and m in the same block or it doesn't. There are d_m partitions of the latter type. And in any partition of the former type, we can consider 1 and m to be amalgamated into a single site $1'$ that is a neighbor of both 2 and $m-1$; so there are d_{m-1} partitions of this type.] The formula (3.59) for d_m then follows by induction.

[19] In most of the literature (e.g. [127, 126]) these numbers are called γ_m. We have adopted the recent proposal of Bernhart [129] to name them after Riordan [127] and denote them R_m.

5) Further restrictions arise from spatial symmetries. For instance, if we consider the square-lattice strip with free transverse boundary conditions, then reflection with respect to the center of the strip is a symmetry of the system. We can therefore define equivalence classes of non-crossing non-nearest-neighbor partitions modulo reflection.[20] The dimension SqFree(m) of the transfer matrix is then given by the number of these equivalence classes. Since each equivalence class contains either one or two partitions (and some contain only one), we clearly have

$$\frac{\text{TriFree}(m)}{2} \;<\; \text{SqFree}(m) \;\le\; \text{TriFree}(m) \;. \tag{3.66}$$

For $m = 4$, for example, we have three equivalence classes:

$$\mathbf{P}_{\text{SqFree},4} \;=\; \{1, \delta_{13} + \delta_{24}, \delta_{14}\} \;. \tag{3.67}$$

We have been unable to compute an explicit formula for SqFree(m), or to find any known integer sequence that corresponds to SqFree(m). The asymptotic behavior is clearly the same as that of TriFree(m) within a factor 2, hence of order $3^m m^{-3/2}$. (We conjecture that SqFree(m) $\approx$ TriFree(m)/2, since "most" partitions are asymmetric. The data in Table 2 strongly suggest that this conjecture is true: the ratios SqFree(m)/TriFree(m) are roughly decreasing in m, albeit with some even-odd oscillation, and seem clearly to be approaching 1/2. Indeed, at $m = 14$ the ratio has already reached ≈ 0.5032.)

6) For the square lattice with periodic transverse boundary conditions, both reflections and translations are symmetries. We therefore define equivalence classes of non-crossing non-nearest-neighbor partitions modulo reflections and translations and the corresponding number SqCyl(m) of equivalence classes.[21] Since each equivalence class contains at most $2m$ partitions (and some contain less), we clearly have

$$\frac{d_m}{2m} \;<\; \text{SqCyl}(m) \;\le\; d_m \;. \tag{3.68}$$

For $m = 4$, there are only two such classes:

$$\mathbf{P}_{\text{SqCyl},4} \;=\; \{1, \delta_{13} + \delta_{24}\} \;. \tag{3.69}$$

We have been unable to compute an explicit formula for SqCyl(m), or to find any known integer sequence that corresponds to SqCyl(m). The asymptotic behavior is clearly the same as that of d_m within a factor $2m$, hence the leading behavior is $\sim 3^m$. (We conjecture that SqCyl(m) $\approx d_m/(2m)$, since "most" partitions are asymmetric. The data in Table 2 strongly suggest that this conjecture is true: the ratios $2m$SqCyl(m)/d_m are roughly decreasing in m, albeit with some even-odd oscillation,

[20] One could also drop the non-nearest-neighbor condition; this would be relevant at nonzero temperature.

[21] One could also drop the non-nearest-neighbor condition; this would be relevant at nonzero temperature.

and seem to be approaching a value near 1. At $m = 14$ the ratio has already reached ≈ 1.14.)

7) For the triangular lattice, reflection is not a symmetry; but if we have periodic transverse boundary conditions, then translations are symmetries. We therefore define equivalence classes of non-crossing non-nearest-neighbor partitions modulo translations, and the corresponding number TriCyl(m) of equivalence classes.[22] Since each equivalence class contains at most m partitions (and some contain less), we clearly have

$$\frac{d_m}{m} \;<\; \mathrm{TriCyl}(m) \;\le\; d_m \;. \tag{3.70}$$

For $m = 4$, there are again only two such classes:

$$\mathbf{P}_{\mathrm{TriCyl},4} \;=\; \{1, \delta_{13} + \delta_{24}\} \;. \tag{3.71}$$

Indeed, we have found that TriCyl(m) = SqCyl(m) for $m \le 7$; only for $m \ge 8$ does reflection symmetry impose additional constraints beyond those imposed by translation symmetry, so that TriCyl(m) > SqCyl(m). We have been unable to compute an explicit formula for TriCyl(m), or to find any known integer sequence that corresponds to TriCyl(m). The asymptotic behavior is clearly the same as that of d_m within a factor m, hence the leading behavior is $\sim 3^m$. (We conjecture that TriCyl(m) $\approx d_m/m$, since "most" partitions are asymmetric. The data in Table 2 strongly suggest that this conjecture is true: the ratios $m\mathrm{TriCyl}(m)/d_m$ are roughly decreasing in m, albeit with strong even-odd oscillation, and seem clearly to be approaching 1. At $m = 14$ the ratio has already reached ≈ 1.01.)

Although the dimension of the transfer matrix is given by SqCyl(m), SqFree(m), TriCyl(m) or TriFree(m), the basis with respect to which the vectors are expressed is considerably larger, namely the set $\mathbf{P}_{\mathrm{nc},m}$ of all non-crossing partitions (or $\mathbf{P}_m$ in case G is non-planar). Thus, the vectors produced at intermediate stages of the computation can be rather long; this is the main limiting factor in our numerical work. In order to save memory, we use the following tricks:

- Label the partitions by an integer variable $k = 1, \ldots, B(m)$. (For large widths m, however, it is vastly more efficient to include only the smaller set of the *non-crossing* partitions $k = 1, \ldots, C_m$ [66, 115]; this approach will be taken in future work in collaboration with Jesper-Lykke Jacobsen [86, 87].)

- Represent the vectors in sparse-vector format (i.e. representing explicitly only nonzero coefficients). This is automatic in MATHEMATICA. (If, however, we consider only the set of non-crossing partitions, then typical intermediate vectors are dense, so that sparse-vector format is actually a disadvantage.)

[22] One could also drop the non-nearest-neighbor condition; this would be relevant at nonzero temperature.

- The coefficients of the chromatic polynomial are extremely large integers, which grow rapidly with the width and length of the strip. We can reduce the magnitude of these coefficients (and therefore save memory) by performing a change of variables $u = q - q_0$, where q_0 lies at or near the barycenter of the roots. This barycenter lies at $|E|/|V|$, where $|E|$ (resp. $|V|$) is the number of edges (resp. vertices) in the graph G; that is, it lies at half the average coordination number. It is therefore convenient to take $q_0 = 2$ (resp. $q_0 = 3$) for the square (resp. triangular) lattice; this vastly reduces the size of the coefficients of the chromatic polynomial, as was noted already by Baxter [55].

Remark. As explained in Section 3.1, when computing the transfer matrix for a triangular-lattice strip of width m and cylindrical boundary conditions, we use the following technical trick [55]: To take account of the diagonal bond joining the sites m and 1, it is convenient to consider a triangular strip of width $m + 1$ and, at the end of the computation, identify the spins at sites $m + 1$ and 1. This means that the number of partitions arising in intermediate steps of the computation is not C_m, but C_{m+1}. However, the dimension of the transfer matrix is still TriCyl(m).

4 Eigenvalue Crossing and Isolated Limiting Points

4.1 Computation of eigenvalue-crossing curves

The limiting curve $\mathcal{B}$ is the locus of points in the q-plane where there are two or more dominant eigenvalues. Our approach is to compute first the locus of q values where there are two or more equimodular eigenvalues, *dominant or not*; we then check the corresponding eigenvalues one-by-one for dominance. We have used two methods to compute the locus of equimodularity: the resultant method, and the direct-search method.

4.1.1 The resultant method

The resultant of two polynomials $P(x) = A\prod_{i=1}^{M}(x-x_i)$ and $Q(y) = B\prod_{i=1}^{N}(y-y_i)$ is defined to be the product of all the differences of roots, scaled suitably by the two leading coefficients:

$$\mathrm{Res}(P,Q) \;=\; A^N B^M \prod_{i=1}^{M}\prod_{j=1}^{N}(x_i - y_j)\;. \tag{4.1}$$

Thus, the resultant vanishes if and only if P and Q have at least one root in common (or one or both of the leading coefficients vanishes). It is a nontrivial fact that the resultant $\mathrm{Res}(P,Q)$ can be expressed as an $(M+N)\times(M+N)$ determinant involving the coefficients of P and Q; it is *not* necessary to know explicitly the roots $\{x_i\}$ and $\{y_j\}$.

Likewise, the discriminant of a polynomial $P(x) = A \prod_{i=1}^{M} (x - x_i)$ is defined as

$$\mathrm{Disc}(P) \;=\; A^{2M-2} \prod_{i<j} (x_i - x_j)^2 \;=\; (-1)^{M(M-1)/2} A^{2M-2} \prod_{i \neq j} (x_i - x_j) \;. \tag{4.2}$$

(For a quadratic $P(x) = ax^2 + bx + c$, we have $\mathrm{Disc}(P) = b^2 - 4ac$, which agrees with the definition used in high-school algebra.) It is not difficult to show that

$$\mathrm{Disc}(P) \;=\; (-1)^{M(M-1)/2} A^{-1} \mathrm{Res}(P, P') \;, \tag{4.3}$$

so that the discriminant vanishes if and only if P has at least one multiple root.[23]

For further information on resultants and discriminants and algorithms for computing them, see e.g. [131, Chapter 3].

Consider now the characteristic polynomial of the transfer matrix $T(q)$:

$$P(\lambda, q) \;=\; \det[\lambda I - T(q)] \;=\; \prod_{i=1}^{\dim T} [\lambda - \lambda_i(q)] \;, \tag{4.4}$$

where $\{\lambda_i(q)\}$ are the eigenvalues of $T(q)$. Consider next the polynomial

$$P_\theta(\lambda, q) \;=\; P(e^{i\theta}\lambda, q) \;. \tag{4.5}$$

P and P_θ are polynomials in λ whose coefficients are polynomials in q (and in $e^{i\theta}$), and they have a root in common if and only if $T(q)$ has eigenvalues λ_1 and λ_2 satisfying $\lambda_1 = e^{i\theta}\lambda_2$. (Note that, in addition to the desired case of an equimodular pair of eigenvalues, this also occurs whenever $T(q)$ has a zero eigenvalue.) We can therefore compute the locus of equimodularity by sweeping over a closely spaced set of points $\theta \in (0, \pi]$, and computing for each θ the roots of

$$R_\theta(q) \;=\; \mathrm{Res}_\lambda(P, P_\theta) \;, \tag{4.6}$$

which is a polynomial in q and $e^{i\theta}$.[24]

Of course, $\theta = 0$ is a special case: here we are looking for the multiple roots of P, which can be located by computing the zeros of the discriminant

$$\widetilde{R}_0(q) \;=\; \mathrm{Res}_\lambda(P, P') \;=\; \lim_{\theta \to 0} \frac{R_\theta(q)}{(-i\theta)^{\dim T} P(0, q)} \tag{4.7}$$

where $P'(\lambda, q) = \partial P(\lambda, q)/\partial\lambda$. As we shall see, the zeros corresponding to $\theta = 0$ are very important because they correspond to the endpoints of the curves of equimodularity.

---

[23] Lang [130, p. 204] warns that many books (including his own first edition!) contain sign errors (i.e. fail to include the factor $(-1)^{M(M-1)/2}$) either in the definition of the discriminant or in the formula relating it to the resultant.

[24] This method was presumably known already to Beraha, Kahane and Weiss: see [38, footnote 2].

After finding a set of q values for which $T(q)$ has a pair of equimodular eigenvalues, we check them one-by-one by solving the characteristic equation $P(\lambda, q) = 0$ and testing whether the pair of equimodular eigenvalues is dominant or subdominant. The limiting curve $\mathcal{B}$ of partition-function zeros corresponds only to the crossing in modulus of *dominant* eigenvalues; nevertheless, it is sometimes of interest to depict the loci of subdominant eigenvalue-crossing as well. Whenever we do so in this paper, we shall draw the dominant eigenvalue-crossing curves using solid black lines and the subdominant curves with dashed red lines.

In practice, we first use MATHEMATICA to compute $R_\theta(q)$ symbolically as a polynomial in q and $e^{i\theta}$ with integer coefficients. To minimize the effect of round-off errors in the subsequent computation, we use instead of θ the real variable $t = \tan(\theta/2) \in (0, \infty]$ defined by

$$e^{i\theta} \;=\; \frac{1+it}{1-it}\,, \tag{4.8}$$

and we always choose t to be a rational number. In this way, $e^{i\theta}$ is a complex rational number whose modulus is always exactly equal to 1, and the polynomial $R_\theta(q)$ has complex rational coefficients. This allows us to take advantage of arbitrary-precision polynomial root-finders such as MATHEMATICA's `NSolve` or (better yet) the package MPSolve 2.0 developed by Bini and Fiorentino [132, 133].[25]

The drawback of the resultant method is that the degree of the resultant polynomial $R_\theta(q)$ grows very rapidly with the width of the lattice strip; moreover, the coefficients in $R_\theta(q)$ also grow very rapidly (even if we use the variable $u = q - q_0$). This limits in practice the widths we can study: $L_x \le 6$ for free transverse boundary conditions and $L_x \le 8$ for periodic transverse boundary conditions.

Remark. In some cases (notably with periodic and twisted-periodic boundary conditions in the longitudinal direction [26, 27, 29, 31, 32, 33]), the amplitude corresponding to one or more eigenvalues can vanish identically. If this occurs for one of the dominant eigenvalues, blind application of the foregoing procedure can lead to erroneous results. As a safeguard against this phenomenon, we numerically computed the corresponding amplitudes for a selected value of q, by numerically diagonalizing the transfer matrix and rotating the corresponding vectors on left and right. It suffices to find at least one value of q for which none of the amplitudes vanishes. In all the cases considered in this paper, an identically-vanishing amplitude never arises.

Example. In the simple special case of a 2×2 transfer matrix

$$T(q) \;=\; \begin{pmatrix} a(q) & b(q) \\ c(q) & d(q) \end{pmatrix} \tag{4.9}$$

[25] MPSolve 2.0 is much faster than MATHEMATICA's `NSolve` for high-degree polynomials (this is reported in [133], and we confirm it); it gives guaranteed error bounds for the roots, based on rigorous theorems [133]; its algorithms are publicly documented [133]; and its source code is freely available [132].

with left and right vectors

$$\vec{u} \;=\; \begin{pmatrix} f(q) \\ g(q) \end{pmatrix} \tag{4.10a}$$

$$\vec{v} \;=\; \begin{pmatrix} 1 \\ 0 \end{pmatrix} \tag{4.10b}$$

and partition function

$$Z_n \;=\; \vec{u}^{\,\mathrm{T}} T^{n-1} \vec{v} \tag{4.11}$$

for a strip of length n (where $^{\mathrm{T}}$ denotes transpose), we can obtain explicit expressions. We have

$$Z_n(q) \;=\; \alpha_-(q)\lambda_-(q)^{n-1} \,+\, \alpha_+(q)\lambda_+(q)^{n-1} \;, \tag{4.12}$$

where the eigenvalues $\lambda_\pm$ and their corresponding amplitudes $\alpha_\pm$ are

$$\lambda_\pm(q) \;=\; \frac{1}{2}\left(\mathrm{tr}\, T(q) \pm \sqrt{\mathrm{tr}^2\, T(q) - 4 \det T(q)}\right) \tag{4.13a}$$

$$\equiv\; \frac{1}{2}\left(P_1(q) \pm \sqrt{P_2(q)}\right) \tag{4.13b}$$

and

$$\alpha_\pm(q) \;=\; \frac{1}{2}\left(f(q) \pm \frac{[a(q)-d(q)]f(q) + 2c(q)g(q)}{\sqrt{\mathrm{tr}^2\, T(q) - 4 \det T(q)}}\right) \tag{4.14a}$$

$$\equiv\; \frac{1}{2}\left(f(q) \pm \frac{P_3(q)}{\sqrt{P_2(q)}}\right) \;. \tag{4.14b}$$

Note that even though the eigenvalues and the amplitudes are non-polynomial algebraic functions of q, the partition function $Z_n(q)$ is always a polynomial in q. From these equations it is not difficult to prove the recurrence relation

$$Z_{n+2}(q) \,-\, [\mathrm{tr}\, T(q)] Z_{n+1}(q) \,+\, [\det T(q)] Z_n(q) \;=\; 0 \;. \tag{4.15}$$

According to the Beraha–Kahane–Weiss theorem (Theorem 2.1), the limit points as $n \to \infty$ of the partition-function zeros are of two types: the isolated limiting points, which occur where one eigenvalue is dominant and its amplitude vanishes; and curves of non-isolated limiting points, where there is a crossing in modulus of two or more dominant eigenvalues. In our simple case, the limiting curves are given by the condition $|\lambda_-(q)| = |\lambda_+(q)|$, which means that $P_2(q)/P_1(q)^2$ should be a negative real number (call it $-t^2$), or in other words

$$\mathrm{tr}^2\, T(q) \;=\; 4\widetilde{t} \det T(q) \quad \text{with } 0 \,\le\, \widetilde{t} \equiv \frac{1}{1+t^2} \,\le\, 1 \;. \tag{4.16}$$

An identical result is obtained using the resultant method (4.6)/(4.7): we have

$$P(\lambda, q) \;=\; \lambda^2 \,-\, [\mathrm{tr}\, T(q)]\lambda \,+\, \det T(q) \tag{4.17}$$

and hence

$$R_\theta(q) \;=\; (1-e^{i\theta})^2\,[\det T(q)]\,\left[(1+e^{i\theta})^2 \det T(q) - e^{i\theta}\,\mathrm{tr}^2\,T(q)\right] \tag{4.18a}$$

$$\widetilde{R}_0(q) \;=\; 4\det T(q) - \mathrm{tr}^2\,T(q) \;=\; -P_2(q) \tag{4.18b}$$

We see that (4.18a) vanishes precisely on the curve (4.16): it suffices to insert (4.8) and note that

$$\frac{(1+e^{i\theta})^2}{e^{i\theta}} \;=\; \frac{4}{1+t^2} \;=\; 4\widetilde{t} \tag{4.19}$$

[equivalently, $\widetilde{t} = \cos^2(\theta/2)$].

The isolated limiting points of zeros are given by the condition that the amplitude of the leading eigenvalue vanishes. We first compute the product of the two amplitudes:

$$\alpha_-(q)\alpha_+(q) \;=\; \frac{P_4(q)}{P_2(q)} \tag{4.20}$$

where

$$P_4(q) \;\equiv\; \frac{f(q)^2 P_2(q) - P_3(q)^2}{4} \;=\; Z_1(q)Z_3(q) - Z_2(q)^2\;. \tag{4.21}$$

[Note that (4.20)/(4.21) is just Lemma 2.2 specialized to the case $M = 2$.] We now observe that a root of P_4 corresponds to the vanishing of α_- (resp. α_+) in case $f\sqrt{P_2} = P_3$ (resp. $f\sqrt{P_2} = -P_3$); and λ_- (resp. λ_+) is dominant in case $\mathrm{Re}(P_1/\sqrt{P_2}) < 0$ (resp. > 0). It follows that a root of P_4 corresponds to the vanishing of the amplitude corresponding to the *dominant* eigenvalue in case

$$\mathrm{Re}\,\frac{f(q)P_1(q)}{P_3(q)} \;<\; 0 \tag{4.22}$$

there. If $P_3(q) = 0$ at a root of P_4, then *both* amplitudes vanish there.

4.1.2 Direct-search method

When we were unable to apply the resultant method (i.e. for large lattice widths), or when we wanted to study in detail a small region in the q-plane (for any lattice width), we used a direct-search method to obtain the curves of equimodularity. The idea is to define a function that measures the difference between the moduli of the two dominant eigenvalues of the transfer matrix. Since an explicit expression of the eigenvalues as a function of q is usually not available, the eigenvalues are obtained numerically for each value of q. Then we extract the two eigenvalues of largest modulus and compute

$$F(q) \;\equiv\; |\lambda_1(q)| - |\lambda_2(q)| \tag{4.23}$$

where $\omega\lambda_1(q) \preceq \omega\lambda_2(q)$ in lexicographic order (here ω is some arbitrarily chosen nonzero complex number). Clearly $F(q)$ vanishes if and only if the two dominant eigenvalues are equimodular; moreover, because generically the two dominant eigenvalues will *not* satisfy $\mathrm{Re}[\omega\lambda_1(q)] = \mathrm{Re}[\omega\lambda_2(q)]$ precisely where they also satisfy

$|\lambda_1(q)| = |\lambda_2(q)|$, they will generically *not* interchange roles at the eigenvalue crossing, and hence $F(q)$ will be a *smooth* function of q there.[26] We then search for the zeros of $F(q)$ using a Newton method in the complex q-plane.

Once a good approximation for a zero is found, we also compute the phase $e^{i\theta} = \lambda_1/\lambda_2$ [or equivalently, the number t defined by (4.8)]. Knowledge of θ is very useful in trying to understand the topology of the limiting curve.

4.2 Qualitative structure of eigenvalue-crossing curves

In this section we want to discuss the types of qualitative behaviors that can arise when studying the eigenvalue-crossing curves. Recall first [134, Chapter 2] that the eigenvalues $\lambda_i(q)$ of the transfer matrix $T(q)$ are analytic functions of q except possibly where two or more eigenvalues collide. Indeed, this can be seen by expanding the characteristic polynomial $P(\lambda, q) = \det[\lambda I - T(q)]$ around a root (λ_0, q_0):

$$P(\lambda, q) \;=\; a(\lambda{-}\lambda_0) + b(q{-}q_0) + c(\lambda{-}\lambda_0)^2 + d(q{-}q_0)^2 + e(\lambda{-}\lambda_0)(q{-}q_0) + \ldots \quad (4.24)$$

Provided that λ_0 is not a multiple eigenvalue of $T(q_0)$, we have $a \equiv (\partial P/\partial\lambda)(\lambda_0, q_0) \neq 0$; the implicit function theorem then guarantees that in a neighborhood of $q = q_0$ there exists an analytic function $\lambda(q)$ solving $P(\lambda(q), q) = 0$ with $\lambda(q_0) = \lambda_0$, and it has the convergent expansion

$$\lambda(q) \;=\; \lambda_0 \;-\; \frac{b}{a}(q - q_0) \;+\; \frac{abe - a^2 d - b^3 c}{a^3}(q - q_0)^2 \;+\; \mathcal{O}((q - q_0)^3)\,. \quad (4.25)$$

If, on the other hand, λ_0 is a k-fold eigenvalue of $T(q_0)$ with $k \geq 2$, then $\lambda(q)$ can have an l^{th}-root branch point at q_0 for any $l \leq k$. More precisely, near $q = q_0$ the eigenvalues divide into groups of cardinalities $l_1, \ldots, l_M$ (with $l_1 + \cdots + l_M = \dim T$) such that the eigenvalues of the i^{th} group are the l_i distinct determinations of an analytic function of $(q - q_0)^{1/l_i}$, i.e. they have an l_i^{th}-root branch point at q_0 [134, pp. 65–66]. For example, for $k = 2$ we have $a = 0$ and $c \neq 0$: if $b \neq 0$, then a pair of eigenvalues $\lambda_\pm(q)$ bifurcate off λ_0 with a square-root branch point,

$$\lambda_\pm(q) \;=\; \lambda_0 \;\pm\; \left(-\frac{b}{c}\right)^{1/2} (q - q_0)^{1/2} \;-\; \frac{e}{2c}(q - q_0) \;+\; \mathcal{O}((q - q_0)^{3/2})\,; \quad (4.26)$$

while if $b = 0$, then $\lambda_\pm(q)$ are analytic functions in a neighborhood of q_0,

$$\lambda_\pm(q) \;=\; \lambda_0 \;+\; \frac{-e \pm \sqrt{e^2 - 4cd}}{2c}(q - q_0) \;+\; \mathcal{O}((q - q_0)^2)\,. \quad (4.27)$$

[26] There is nothing special about lexicographic order; virtually any order will do, *except* ordering by moduli. In practice, we used MATHEMATICA's default ordering, which is slightly different from lexicographic. Note also that any nonzero $\omega \in \mathbb{C}$ will do; but when studying an eigenvalue crossing on the real q axis (for which λ_1 and λ_2 will be complex conjugates), it is advantageous to choose ω non-real.

4.2.1 Crossing of two simple eigenvalues

Generically, the equimodularity of two eigenvalues defines an analytic curve in the complex q-plane, along which the parameter θ (or t) varies smoothly. To see this, suppose that at $q = q_0$ we have a pair of *simple* (i.e. non-multiple) eigenvalues $\lambda_{1,0}$ and $\lambda_{2,0}$ that have equal modulus ($|\lambda_{1,0}| = |\lambda_{2,0}| \neq 0$); they satisfy $\lambda_{1,0} = e^{i\theta}\lambda_{2,0}$ with $\theta \neq 0 \pmod{2\pi}$. Each of these eigenvalues then extends to a single-valued analytic function of q in a neighborhood of $q = q_0$, as in (4.25):

$$\lambda_i(q) \;=\; \lambda_{i,0} \;-\; \frac{b_i}{a_i}(q-q_0) \;+\; \frac{a_i b_i e_i - a_i^2 d_i - b_i^3 c_i}{a_i^3}(q-q_0)^2 \;+\; \mathcal{O}((q-q_0)^3) \tag{4.28}$$

for $i = 1, 2$. Their ratio is then

$$\frac{\lambda_1(q)}{\lambda_2(q)} \;=\; e^{i\theta}\left[1 - \left(\frac{b_1}{a_1\lambda_{1,0}} - \frac{b_2}{a_2\lambda_{2,0}}\right)(q-q_0) + \mathcal{O}((q-q_0)^2)\right] \tag{4.29a}$$

$$\equiv\; e^{i\theta}\left[1 + \rho e^{i\phi}(q-q_0) + \mathcal{O}((q-q_0)^2)\right] \tag{4.29b}$$

Provided that $\rho \neq 0$, the equimodularity locus $|\lambda_1(q)/\lambda_2(q)| = 1$ defines near $q = q_0$ an analytic curve that passes through $q = q_0$ at angle $-\phi \pm \pi/2$.

If, however, $\rho = 0$ [i.e. the term in (4.29a) that is linear in $q - q_0$ vanishes], then the equimodularity locus can have multiple points. (A *sufficient* though not necessary condition for this to occur is for the linear terms to vanish in each eigenvalue separately, i.e. $b_1 = b_2 = 0$.) If the first nonvanishing term in (4.29a) is the one of order $(q-q_0)^k$, then we have a k-fold multiple point in the sense of algebraic geometry [135, Section 6.2]: that is, the equimodularity locus $|\lambda_1(q)/\lambda_2(q)| = 1$ defines near $q = q_0$ an analytic image of the set $\operatorname{Re} z^k = 0$ near $z = 0$. In particular, this set can be interpreted locally as k analytic curves crossing at angles π/k.

Remark. Let us consider the partition function $Z_n(q)$ near a point q_0 where there are exactly two dominant simple eigenvalues:

$$Z_n(q) \;=\; \alpha_1(q)\,\lambda_1(q)^n \;+\; \alpha_2(q)\,\lambda_2(q)^n \;+\; \ldots \tag{4.30}$$

where the dots indicate the contributions of subdominant eigenvalues. Let us assume for simplicity that $\alpha_1(q_0), \alpha_2(q_0) \neq 0$ and insert the expansions

$$\log\frac{\lambda_1(q)}{\lambda_2(q)} \;=\; 2\pi i\psi \;+\; A(q-q_0) \;+\; \mathcal{O}((q-q_0)^2) \tag{4.31}$$

$$\log\frac{\alpha_1(q)}{-\alpha_2(q)} \;=\; 2\pi i B \;+\; C(q-q_0) \;+\; \mathcal{O}((q-q_0)^2) \tag{4.32}$$

where $\psi \equiv \theta/2\pi \in \mathbb{R}$ and $A, B, C \in \mathbb{C}$. [From (4.29) we have $A = \rho e^{i\phi} \equiv (b_2/a_2\lambda_{2,0}) - (b_1/a_1\lambda_{1,0})$.] Then (4.30) can be written as

$$\begin{aligned} Z_n(q) \;&=\; 2i\,[\alpha_1(q)\,\alpha_2(q)\,\lambda_1(q)^n\,\lambda_2(q)^n]^{1/2} \;\times \\ &\qquad \sinh\left[\pi i(n\psi + B) \;+\; \frac{An + C}{2}(q-q_0) \;+\; \mathcal{O}((q-q_0)^2)\right], \end{aligned} \tag{4.33}$$

which agrees with [55, eqn. (3.3)] by trivial renaming of variables. When n is large, (4.33) has zeros at

$$q \;=\; q_0 \;-\; \frac{2\pi i}{An}\,[k + B + R(n\psi)] \;+\; \mathcal{O}(1/n^2) \tag{4.34}$$

where $k \in \mathbb{Z}$ is an arbitrary integer and $R(x) \equiv x - \lfloor x \rfloor$ is x modulo 1. Therefore, we see that near a regular point q_0 of the limiting curve $\mathcal{B}$, the finite-volume partition function $Z_n(q)$ has a sequence of evenly spaced zeros [spacing $= 2\pi/(|A|n)$] lying parallel to $\mathcal{B}$. These zeros lie a distance $2\pi|\mathrm{Im}\, B|/(|A|n)$ away from $\mathcal{B}$, hence converge to it generically at rate $1/n$.

In addition to this generic behavior, there are other features exhibited by the limiting curves that are worth studying in detail:

4.2.2 Endpoints (collision of two eigenvalues)

Suppose that $\lambda_0 \neq 0$ is a two-fold eigenvalue of $T(q_0)$. Then generically (i.e. if $b \neq 0$) a pair of eigenvalues $\lambda_\pm(q)$ bifurcates off λ_0 with a square-root branch point, as in (4.26). The ratio of the two eigenvalues is

$$\frac{\lambda_+(q)}{\lambda_-(q)} \;=\; 1 \;+\; A(q-q_0)^{1/2} \;+\; \frac{A^2}{2}(q-q_0) \;+\; \mathcal{O}((q-q_0)^{3/2}) \tag{4.35}$$

where $A = (2/\lambda_0)(-b/c)^{1/2} \neq 0$. Setting

$$\frac{\lambda_+(q)}{\lambda_-(q)} \;=\; e^{i\theta} \;=\; \frac{1+it}{1-it} \tag{4.36}$$

with t real, we see that the equimodularity locus is given by

$$q \;=\; q_0 \;-\; \frac{4}{A^2}t^2 \;+\; \mathcal{O}(t^4)\;. \tag{4.37}$$

Only even powers of t appear in this expansion, since λ_+ and λ_- interchange roles as we go around the branch point, and $\lambda_+/\lambda_- = e^{i\theta}$ if and only if $\lambda_-/\lambda_+ = e^{-i\theta}$. Writing $A = \rho e^{i\phi}$, we see that the equimodularity locus is an analytic curve ending at $q = q_0$ and tangent there to the ray $\arg(q - q_0) = \pi - 2\phi$.

Because the two eigenvalues are equal at $q = q_0$, the parameter θ (or t) takes the value 0 at endpoints. Each such endpoint corresponds to a simple root of the $t = 0$ resultant $\widetilde{R}_0(q)$: indeed, (4.26) implies that for q near q_0 we have $\lambda_+ - \lambda_- \sim (q-q_0)^{1/2}$ and hence $\widetilde{R}_0(q) \sim (\lambda_+ - \lambda_-)^2 \sim q - q_0$. For this reason, the simple zeros of the $t = 0$ resultant play an essential role when we try to determine with high accuracy the topology of the limiting curve.

By contrast, in the non-generic case $b = 0$, where the eigenvalues $\lambda_\pm(q)$ are analytic functions in a neighborhood of q_0 [cf. (4.27)], the formulae (4.28)/(4.29) of the preceding subsection apply with $\theta = 0$. In this case, the root $q = q_0$ is a

double zero of the $t = 0$ resultant $\widetilde{R}_0(q)$, as $\lambda_+ - \lambda_- \sim q - q_0$ by (4.27), so that $\widetilde{R}_0(q) \sim (\lambda_+ - \lambda_-)^2 \sim (q - q_0)^2$.

Example. Consider a two-dimensional transfer matrix as in (4.9). Collision of the two eigenvalues (4.13) occurs whenever $P_2(q) = 0$, i.e. whenever $\operatorname{tr}^2 T(q) = 4 \det T(q)$. Suppose this occurs at $q = q_0$, with $\lambda_0 \equiv \lambda_\pm(q_0) = \frac{1}{2} \operatorname{tr} T(q_0)$, and let us expand the eigenvalues (4.13) around $q = q_0$:

$$\lambda_\pm = \frac{1}{2} \operatorname{tr} T(q_0) \pm C_1 (q - q_0)^{1/2} + C_2 (q - q_0) + \mathcal{O}((q - q_0)^{3/2}) \tag{4.38}$$

where

$$C_1 = \left(\frac{1}{2} \operatorname{tr} T(q_0) \left. \frac{d \operatorname{tr} T(q)}{dq} \right|_{q=q_0} - \left. \frac{d \det T(q)}{dq} \right|_{q=q_0} \right)^{1/2} \tag{4.39a}$$

$$C_2 = \frac{1}{2} \left. \frac{d \operatorname{tr} T(q)}{dq} \right|_{q=q_0} \tag{4.39b}$$

The ratio of the two eigenvalues is therefore

$$\frac{\lambda_+(q)}{\lambda_-(q)} = 1 + A(q - q_0)^{1/2} + \frac{A^2}{2}(q - q_0) + \mathcal{O}((q - q_0)^{3/2}) \tag{4.40}$$

with $A = 4C_1/[\operatorname{tr} T(q_0)]$.

Remark. Let us return now to the general case, and consider the partition function $Z_n(q)$ close to an endpoint $q = q_0$ where two dominant eigenvalues collide:

$$Z_n(q) = \alpha_+(q) \lambda_+(q)^n + \alpha_-(q) \lambda_-(q)^n + \dots \tag{4.41}$$

where the dots indicate the contributions of subdominant eigenvalues. From (4.26) [cf. also (4.13)/(4.14)] we have

$$\log \frac{\lambda_+(q)}{\lambda_-(q)} = A(q - q_0)^{1/2} + \mathcal{O}(q - q_0) \tag{4.42}$$

$$\log \frac{\alpha_+(q)}{-\alpha_-(q)} = 2\pi i B + C(q - q_0)^{1/2} + \mathcal{O}(q - q_0) \tag{4.43}$$

where $A = 2(-b/c)^{1/2}/\lambda_0$. Then (4.41) can be written as

$$Z_n(q) = 2i \left[\alpha_+(q) \alpha_-(q) \lambda_+(q)^n \lambda_-(q)^n \right]^{1/2} \times \sinh\left[i\pi B + \frac{An + C}{2}(q - q_0)^{1/2} + \mathcal{O}(q - q_0) \right] . \tag{4.44}$$

When n is large, the zeros of (4.44) are given by

$$q = q_0 - \frac{4\pi^2 (k + B)^2}{A^2 n^2} + \mathcal{O}(1/n^3) \tag{4.45}$$

where $k \in \mathbb{Z}$, in agreement with (4.37). Therefore, the convergence close to an endpoint is generically of order $1/n^2$, in contrast with the $1/n$ convergence near a regular point of the limiting curve [cf. (4.34)].

4.2.3 Crossing of three simple eigenvalues (T points)

Suppose that at $q = q_0$ we have three dominant simple eigenvalues (call them $\lambda_1, \lambda_2, \lambda_3$): then three smooth curves of equimodularity, corresponding to the three pairs of eigenvalues $\lambda_{1/2}, \lambda_{1/3}, \lambda_{2/3}$, pass through $q = q_0$. One half of each curve of equimodularity corresponds to a dominant pair of eigenvalues, while one half corresponds to a subdominant pair; therefore the locus of dominant equimodularity looks like a T, so we call these crossings *T points* (see Figure 1). They are complex analogues of "triple points" in the thermodynamic sense (but they are *not* multiple points in the sense of algebraic geometry: see Remark 2 below).

More precisely, the eigenvalues $\lambda_i(q)$ for $i = 1, 2, 3$ define single-valued analytic functions (4.28) in a neighborhood of q_0, so that their ratios are

$$\frac{\lambda_1(q)}{\lambda_2(q)} \;=\; \frac{\lambda_{1,0}}{\lambda_{2,0}} \left[1 - \left(\frac{a_1}{b_1 \lambda_{1,0}} - \frac{a_2}{b_2 \lambda_{2,0}} \right) (q - q_0) + \mathcal{O}((q - q_0)^2) \right] \tag{4.46a}$$

$$\frac{\lambda_1(q)}{\lambda_3(q)} \;=\; \frac{\lambda_{1,0}}{\lambda_{3,0}} \left[1 - \left(\frac{a_1}{b_1 \lambda_{1,0}} - \frac{a_3}{b_3 \lambda_{3,0}} \right) (q - q_0) + \mathcal{O}((q - q_0)^2) \right] \tag{4.46b}$$

$$\frac{\lambda_2(q)}{\lambda_3(q)} \;=\; \frac{\lambda_{2,0}}{\lambda_{3,0}} \left[1 - \left(\frac{a_2}{b_2 \lambda_{2,0}} - \frac{a_3}{b_3 \lambda_{3,0}} \right) (q - q_0) + \mathcal{O}((q - q_0)^2) \right] \tag{4.46c}$$

Provided that the coefficients of $q - q_0$ in (4.46a–c) are not collinear, there are six possible phases for $q - q_0$ that render one of the ratios unimodular to leading order in $q - q_0$; three of these correspond to a dominant crossing, while the three complementary phases correspond to a subdominant crossing. If, on the curve where $|\lambda_i/\lambda_j| = 1$, we define

$$\frac{\lambda_i(q)}{\lambda_j(q)} \;=\; e^{i\theta_{ij}(q)} \;, \tag{4.47}$$

then the phase $\theta_{ij}(q)$ varies smoothly along this curve. No *pair* of these three phases obeys in general any relation, even as $q \to q_0$; but at the T point we obviously have the relation

$$\theta_{12} + \theta_{23} + \theta_{31} \;=\; 2\pi n \tag{4.48}$$

for some integer n. If we take $-\pi < \theta_{ij} \le \pi$, then n must be -1, 0 or $+1$. In particular, the absolute values of the θ_{ij} (which are what we actually calculate in practice) must satisfy either $|\theta_{12}| + |\theta_{23}| + |\theta_{31}| = 2\pi$ or some permutation of $|\theta_{12}| + |\theta_{23}| - |\theta_{31}| = 0$. In practice, one way of detecting a T point is by noticing the discontinuity in θ as we pass from one piece of the limiting curve to another.

Remarks. 1. We frequently find that the limiting curve $\mathcal{B}$ contains an arc starting at an endpoint ($t = 0$) and ending at a T point ($t = t_0$).[27] If we are able to compute the $t = 0$ resultant, then all endpoints can be detected, so that the corresponding

[27] Similar features were found in the complex-temperature zeros of the two-dimensional spin-s Ising model [136], in the complex-temperature zeros of the Potts model on the hexagonal, Kagomé and triangular lattices [15, 16], and in the complex-q zeros of the Potts antiferromagnet on some families of strip graphs [20].

arcs can be detected as well. But using the direct-search method, a short arc can easily be overlooked: for since the parameter t grows smoothly as we move along the arc towards the T point, a short arc corresponds to a small value of t_0; and if t_0 is smaller than our step size, we may fail to detect the discontinuity in t along the other two arcs merging at the T point (unless we are very lucky!). This means that in the cases where we were unable to obtain the zeros of the $t = 0$ resultant (namely, widths $7_{\rm F}$ and $8_{\rm F}$), we may have missed some such "close pairs" of endpoints and T points; so the lists of endpoints and T points reported in Sections 5.6 and 5.7 may be incomplete, and the counts reported in Table 5 must be understood as *lower bounds* on the true value.

2. Roček, Shrock and Tsai [17, p. 528 top, item (ii)] state erroneously that a T point is a "multiple point" in the technical sense of algebraic geometry, i.e. a point where two or more branches of the *same* irreducible algebraic curve meet. In fact, a T point corresponds to the crossing *in modulus* of three usually *unrelated* analytic functions. Our aim here is not to quibble about definitions, but to emphasize a radical difference in behavior: at a k-fold multiple point the branches always intersect at angles π/k, while at a T point they can (and in general do) intersect at *arbitrary* angles. (By contrast, the crossing (4.29) with $\rho = 0$ is a true multiple point, as correctly observed by Roček *et al.* [17, p. 528 top, item (i)].)

4.3 Computation of isolated limiting points of zeros

According to case (a) of the Beraha–Kahane–Weiss theorem, the isolated limiting points of partition-function zeros correspond to points where there is a unique dominant eigenvalue whose amplitude vanishes. We locate such points by a two-step process: First we determine, using Lemma 2.2, the (finite) set of q values where *at least one* amplitude vanishes. Then we check these q values one by one, by diagonalizing $T(q)$, rotating the left and right vectors $\vec{u}(q)$ and $\vec{v}(q)$, and checking whether the vanishing amplitude(s) corresponds to the dominant eigenvalue. In the special case $\dim T = 2$, we can test dominance using the analytic criterion (4.22).

5 Numerical Results for the Square-Lattice Chromatic Polynomial: Free Transverse Boundary Conditions

We have computed the transfer matrix $T(q)$ and the limiting curves $\mathcal{B}$ for square-lattice strips of widths $2 \le L_x \le 8$ with free boundary conditions in the transverse direction. We have checked the self-consistency of our finite-lattice results using the trivial identity

$$Z(m_{\rm F} \times n_{\rm F}) \;=\; Z(n_{\rm F} \times m_{\rm F}) \tag{5.1}$$

for all pairs $2 \le m, n \le 8$.

5.1 $L_x = 2_{\rm F}$

In this case the transfer matrix is one-dimensional, and the result is trivial:

$$Z(2_{\rm F} \times n_{\rm F}) \;=\; q(q-1)(q^2-3q+3)^{n-1} \;. \tag{5.2}$$

Since there is only one eigenvalue, there is obviously no crossing, hence $\mathcal{B} = \emptyset$. However, there are zeros for all n at $q = 0, 1$ (trivially) and for all $n \geq 2$ at $q = (3 \pm \sqrt{3}\, i)/2$.

5.2 $L_x = 3_{\rm F}$

In this case the transfer matrix is two-dimensional. The allowed partitions are given by $\mathbf{P} = \{1, \delta_{13}\}$. In this basis the transfer matrix is equal to[28]

$$T(3_{\rm F}) \;=\; \begin{pmatrix} q^3 - 5q^2 + 10q - 8 & q^2 - 4q + 5 \\ 1 & q-2 \end{pmatrix} \;, \tag{5.3}$$

and the partition function is equal to

$$Z(3_{\rm F} \times n_{\rm F}) \;=\; q(q-1) \begin{pmatrix} q-1 \\ 1 \end{pmatrix}^{\rm T} \cdot T(3_{\rm F})^{n-1} \cdot \begin{pmatrix} 1 \\ 0 \end{pmatrix} \tag{5.4}$$

where $^{\rm T}$ denotes transpose.

We can rewrite the above expression for the partition function as in (4.12). The polynomials P_1, P_2, P_3 and P_4 entering the definitions of the eigenvalues and amplitudes (4.13)/(4.14)/(4.20) are given by

$$P_1(q) \;=\; (q^2 - 3q + 5)(q-2) \tag{5.5a}$$
$$P_2(q) \;=\; (q^2 - 5q + 7)(q^4 - 5q^3 + 11q^2 - 12q + 8) \tag{5.5b}$$
$$P_3(q) \;=\; q(q-1)(q^4 - 6q^3 + 14q^2 - 15q + 8) \tag{5.5c}$$
$$P_4(q) \;=\; q^2(q-1)^2(q-2) \tag{5.5d}$$

The limiting curve $\mathcal{B}$ (see Figure 2) consists of three disjoint arcs.[29] One of them crosses the real axis at $q_0 = 2$, and is invariant under complex conjugation; the other two lie in the first and fourth quadrants, respectively, and are complex conjugates of each other. There are six endpoints:

$$q \;\approx\; 0.5865699800 \pm 1.1400627519\, i \tag{5.6a}$$
$$q \;\approx\; 1.9134300200 \pm 1.0979688996\, i \tag{5.6b}$$
$$q \;=\; \frac{5 \pm \sqrt{3}\, i}{2} \;\approx\; 2.5 \pm 0.8660254038\, i \tag{5.6c}$$

[28] As was found a quarter of a century ago by Biggs and Meredith [111, p. 11].

[29] This curve is also depicted in [17, Figure 3(a)].

These endpoints are the six roots of the $t = 0$ resultant $\widetilde{R}_0(q) = -P_2(q)$ given by (5.5b).

The zeros of the amplitudes can be found by solving the equation $P_4(q) = 0$. There are two trivial zeros $q = 0, 1$, where both amplitudes vanish simultaneously; both these zeros lie in the region where the eigenvalue λ_- is dominant. The non-trivial zero $q = B_4 = 2$ is a zero of α_-, but not of α_+ [$\alpha_+(q = 2) = 2$]. However, this point happens to lie on an dominant-eigenvalue-crossing curve [$\lambda_+(q = 2) = -\lambda_-(q = 2) = 1$], so it actually belongs to case (b) of the Beraha–Kahane–Weiss theorem. Indeed, from Table 3 we see that the first non-trivial real zero of the partition function seems to converge to $q = 2$, but at the slow (roughly $1/n$) rate characteristic of non-isolated limiting points rather than at the fast (exponential) rate characteristic of isolated limiting points.

5.3 $L_x = 4_{\mathrm{F}}$

The transfer matrix is three-dimensional. In the basis $\mathbf{P} = \{1, \delta_{13} + \delta_{24}, \delta_{14}\}$ it can be written as

$$T(4_{\mathrm{F}}) = \begin{pmatrix} q^4 - 7q^3 + 21q^2 - 32q + 21 & 2(q^3 - 6q^2 + 14q - 12) & q^3 - 7q^2 + 19q - 20 \\ q - 2 & q^2 - 4q + 5 & 3 - q \\ -1 & -2(q - 2) & q^2 - 5q + 7 \end{pmatrix}, \tag{5.7}$$

and the partition function is equal to

$$Z(4_{\mathrm{F}} \times n_{\mathrm{F}}) \;=\; q(q-1) \begin{pmatrix} (q-1)^2 \\ 2(q-1) \\ q-2 \end{pmatrix}^{\mathrm{T}} \cdot T(4_{\mathrm{F}})^{n-1} \cdot \begin{pmatrix} 1 \\ 0 \\ 0 \end{pmatrix} . \tag{5.8}$$

The limiting curve $\mathcal{B}$ (see Figure 3) has three connected components: again, one crosses the real axis and is self-conjugate, while the other two stay away from the real axis and are a pair of mutually conjugate arcs.[30] This time, however, the component that crosses the real axis is rather complicated: there is a pair of T points at $q \approx 2.327 \pm 0.9113\,i$, and there is a double point on the real axis at $q \approx 2.2649418565$.

There are ten endpoints:

$$q \;\approx\; 0.3254743549 \pm 1.1048503376\,i \tag{5.9a}$$
$$q \;\approx\; 2.0555822564 \pm 1.5703029256\,i \tag{5.9b}$$
$$q \;\approx\; 2.2283590792 \tag{5.9c}$$
$$q \;\approx\; 2.2823594125 \pm 1.5512247035\,i \tag{5.9d}$$
$$q \;\approx\; 2.3014157308 \tag{5.9e}$$
$$q \;\approx\; 2.6674264726 \pm 0.7845284722\,i \tag{5.9f}$$

[30] This curve is also depicted in [17, Figure 3(b)].

The horizontal segment emerging from the double point ends at the pair of real endpoints (5.9c,e).

Using Lemma 2.2 we find that the points where at least one amplitude vanishes are given by the zeros of the polynomial

$$\det D(q) \;=\; 2q^3(q-1)^3(q-2)^2(q^2-3q+1)(2q^3-13q^2+27q-17)^2\,. \qquad (5.10)$$

The values $q = 0, 1$ are trivial zeros where all three amplitudes vanish simultaneously. At $q = 2$ the amplitude corresponding to the leading eigenvalue vanishes (as does one of the two subdominant amplitudes). The other roots $q = (3 \pm \sqrt{5})/2$ and $q \approx 1.170516, 2.664742 \pm 0.401127\,i$ all correspond to the vanishing of a subdominant amplitude. Therefore, according to case (a) of the Beraha–Kahane–Weiss theorem, the isolated limiting points for this strip are $q = 0, 1, 2$.

From Table 3, we see that the first non-trivial real zero converges rapidly to the Beraha number $B_4 = 2$. In addition, there are further real zeros (whose number increases with n) that tend to the segment $[2.2283590792\ldots, 2.3014157308\ldots]$ of the limiting curve and in the limit $n \to \infty$ become dense on that segment.

It is curious that (5.10) vanishes also at the Beraha number $B_5 = (3+\sqrt{5})/2$ and its conjugate $B_5^* = (3-\sqrt{5})/2$, even though both of these correspond to the vanishing of a subdominant amplitude.

5.4 $L_x = 5_{\mathrm{F}}$

The transfer matrix is seven-dimensional, and can be expressed in the basis $\mathbf{P} = \{1, \delta_{13}+\delta_{35}, \delta_{24}, \delta_{14}+\delta_{25}, \delta_{15}, \delta_{135}, \delta_{15}\delta_{24}\}$. We refrain from giving here the full transfer matrix; instead, we refer the reader to the MATHEMATICA file `transfer1.m` included in the electronic version of this article at xxx.lanl.gov.

The limiting curve $\mathcal{B}$ (see Figure 5) has five connected components. One of them crosses the real axis at $q_0 \approx 2.4284379020$ and is a self-conjugate arc; there is a pair of mutually conjugate arcs; and finally, there is a pair of mutually conjugate components exhibiting T points at $q \approx 2.423 \pm 0.1067\,i$ and $q \approx 2.291 \pm 1.561\,i$.

There are 14 endpoints:

$$q \;\approx\; 0.1708973690 \pm 1.0464583589\,i \qquad (5.11a)$$
$$q \;\approx\; 1.9065720451 \pm 1.9339587717\,i \qquad (5.11b)$$
$$q \;\approx\; 1.9748200483 \pm 1.9395387106\,i \qquad (5.11c)$$
$$q \;\approx\; 2.3024178902 \pm 1.6190810539\,i \qquad (5.11d)$$
$$q \;\approx\; 2.3990745384 \pm 0.8206408701\,i \qquad (5.11e)$$
$$q \;\approx\; 2.4983799650 \pm 0.8199051472\,i \qquad (5.11f)$$
$$q \;\approx\; 2.7692051339 \pm 0.7143320949\,i \qquad (5.11g)$$

Please note that the endpoints $q \approx 1.9065720451 \pm 1.9339587717\,i$ and $q \approx 1.9748200483 \pm 1.9395387106\,i$ define a pair of small gaps in the limiting curve. Likewise, the curves emerging from the endpoints $q \approx 2.3024178902 \pm 1.6190810539\,i$ and $q \approx 2.3990745384 \pm$

$0.8206408701\,i$ do not cross, but define another pair of very small gaps (see Figure 6 for detail).

By Lemma 2.2, the points where at least one amplitude vanishes are given by the zeros of the polynomial

$$\det D(q) \;=\; q^7(q-1)^{13}(q-2)^6(q^2-3q+1)^5(q-3)^7 P(q)^2 \tag{5.12}$$

where $P(q)$ is a polynomial of degree 37 with integer coefficients that we report in the file `transfer1.m`; as far as we can tell, $P(q)$ cannot be factored further over the integers. The values $q = 0, 1$ are trivial zeros where all seven amplitudes vanish simultaneously. (Two of the amplitudes have in fact *multiple* roots at $q = 1$.) At $q = 2$ the amplitude corresponding to the leading eigenvalue vanishes (as do the amplitudes of five of the six subdominant eigenvalues). In addition, one complex-conjugate pair of zeros of $P(q)$, namely $q \approx 2.2866147868 \pm 1.0116506019\,i$, corresponds to the vanishing of a dominant amplitude (shown with a $\times$ in Figure 5). This is the first time we find a nonreal isolated limiting zero. The remaining zeros of $\det D(q)$ correspond to the vanishing of subdominant amplitudes.

The first non-trivial real zero (see Table 3) converges quickly to the Beraha number $B_4 = 2$. The next real zero appears to be converging slowly (at a roughly $1/n$ rate) to the value $q_0 \approx 2.4284379020$ where the limiting curve $\mathcal{B}$ intersects the real axis, which is smaller than the next Beraha number B_5. The convergence to the complex isolated limiting points at $q \approx 2.2866147868 \pm 1.0116506019\,i$ is quite again rapid. Indeed, if we select for each strip length n the zero closest to the limiting point, and fit the distance from the limiting point to an inverse power of n, the effective power seems to grow with n; this is compatible with the expected exponential convergence.

It is curious that (5.12) vanishes also at the Beraha numbers $B_5 = (3+\sqrt{5})/2$ and $B_6 = 3$ — and hence also at the conjugate $B_5^* = (3-\sqrt{5})/2$ — even though all of these correspond to the vanishing of a subdominant amplitude.

5.5 $L_x = 6_{\mathrm{F}}$

The transfer matrix is 13-dimensional; it can be found in the MATHEMATICA file `transfer1.m`.

The limiting curve $\mathcal{B}$ (see Figure 7) has five connected components. One of the components is self-conjugate and crosses the real axis with a double point at $q \approx 2.5328721401$, from which there emerges a small horizontal segment running from $2.5286467909 \lesssim q \lesssim 2.5370979311$ (see Figure 8a for detail). The other four connected components form two mutually conjugate pairs. One pair consists of arcs running from $q \approx 0.0689480595 \pm 0.9874383424\,i$ to $q \approx 1.6648104050 \pm 2.1404062947\,i$. The other pair exhibits T points at $q \approx 2.039 \pm 1.964\,i$, $q \approx 2.332 \pm 1.638\,i$ and $q \approx 2.478 \pm 1.213\,i$, the latter of which is the end of a small bulb-like region enclosed by the limiting curve (see Figures 8b,c). There are two small gaps at $q \approx 1.67 \pm 2.14\,i$.

There are 14 endpoints:

$$q \;\approx\; 0.0689480595 \pm 0.9874383424\,i \tag{5.13a}$$

$$q \;\approx\; 1.6648104050 \pm 2.1404062947\,i \tag{5.13b}$$

$$q \approx 1.6870381566 \pm 2.1423501191\,i \quad (5.13c)$$
$$q \approx 2.0370674106 \pm 1.9742433636\,i \quad (5.13d)$$
$$q \approx 2.3334923547 \pm 1.6492963460\,i \quad (5.13e)$$
$$q \approx 2.5286467909 \quad (5.13f)$$
$$q \approx 2.8373380200 \pm 0.6533586125\,i \quad (5.13g)$$
$$q \approx 2.5370979311 \quad (5.13h)$$

The bulb-like region is rather unusual. The point at which it starts, $q \approx 2.478 \pm 1.213\,i$, really is a T point: computations show that each of the three curves of dominant equimodularity arriving at the T point has a smooth continuation into the region beyond the T point, where it becomes a curve of *subdominant* equimodularity (see Figure 8c, where the dominant curves are shown with solid black lines and the subdominant curves with dashed red lines); moreover, the t value varies continuously along each of these three curves. One of the subdominant curves lies entirely within the enclosed bulb-like region and ends at a $t = 0$ subdominant endpoint $q \approx 2.5018915620 \pm 1.1501464506\,i$. This means that there is a branch cut for these two subdominant eigenvalues, which become the dominant eigenvalues outside the bulb-like region.

By Lemma 2.2, the points where at least one amplitude vanishes are given by the condition $\det D(q) = 0$. This determinant can be written as

$$\det D(q) \;=\; q^{13}(q-1)^{23}(q-2)^{12}(q^2-3q+1)^8(q-3)^{27}(q^3-5q^2+6q-1)P(q)^2 \quad (5.14)$$

where $P(q)$ is a polynomial of degree 218 with integer coefficients that we report in the file `transfer1.m`. There are two trivial zeros $q = 0, 1$ where all the amplitudes vanish simultaneously. There are five non-trivial zeros of $\det D(q)$ that correspond to the vanishing of the dominant amplitude: $q = 2$, $q \approx 2.0617791396 \pm 1.7315562279\,i$, $q \approx 2.3406021969 \pm 1.3825644365\,i$ (shown with a $\times$ in Figure 7).

The first non-trivial real zero converges rapidly to the Beraha number $B_4 = 2$ (see Table 3), while the second non-trivial zero appears to be converging (at a roughly $1/n^2$ rate) to the real endpoint $q \approx 2.5286467909$. We expect that there will be further real zeros (whose number increases with n) that tend to the segment $[2.5286467909\ldots, 2.5370979311\ldots]$ of the limiting curve and in the limit $n \to \infty$ become dense on that segment. The convergence to the complex isolated limiting points at $q \approx 2.0617791396 \pm 1.7315562279\,i$ and $q \approx 2.3406021969 \pm 1.3825644365\,i$ is in both cases very fast and is compatible with an exponential rate.

It is curious that (5.14) vanishes also at the Beraha numbers $B_5 = (3+\sqrt{5})/2$, $B_6 = 3$ and $B_7 \approx 3.246979603717$ — and hence also at their conjugates $B_5^* = (3-\sqrt{5})/2$, $B_7^{(2)} \approx 1.5549581321$ and $B_7^{(3)} \approx 0.1980622642$ — though all of these correspond to the vanishing of a subdominant amplitude.

5.6 $L_x = 7_{\mathrm{F}}$

The transfer matrix is 32-dimensional; it can be found in the MATHEMATICA file `transfer1.m`.

The limiting curve $\mathcal{B}$ (see Figure 9) appears to have seven connected components (but there may be more: we cannot be sure, as we were unable to compute the $t = 0$ resultant). One of these components is a self-conjugate arc, and crosses the real axis at $q_0 \approx 2.6062482130$; it has endpoints at $q \approx 2.622974 \pm 0.609548\,i$. The other six components form three mutually conjugate pairs. One pair consists of arcs running from $q \approx -0.002412 \pm 0.933080\,i$ to $q \approx 1.425603 \pm 2.248902\,i$. A very small gap (see Figure 10a for detail) separates these arcs from the second pair, which starts at the endpoint $q \approx 1.433184 \pm 2.248834\,i$ and ends in a tiny bulb-like region with a T point at $q \approx 2.415 \pm 1.497\,i$ (see Figure 10b). A small gap (see Figure 10c) separates these components from the third pair, which exhibits T points at $q \approx 2.577 \pm 1.133\,i$ and endpoints at $q \approx 2.616006 \pm 0.616910\,i$; the latter is in turn separated by a very small gap from the self-conjugate arc (see Figure 10d).

Please note that $\mathcal{B}$ enters for the first time into the half-plane $\mathrm{Re}\, q < 0$; we conjecture that this occurs for *all* lattice widths $L_x \geq 7_{\mathrm{F}}$.

There are probably 14 endpoints:

$$q \approx -0.002412 \pm 0.933080\,i \tag{5.15a}$$
$$q \approx 1.425603 \pm 2.248902\,i \tag{5.15b}$$
$$q \approx 1.433184 \pm 2.248834\,i \tag{5.15c}$$
$$q \approx 2.445207 \pm 1.471332\,i \tag{5.15d}$$
$$q \approx 2.616006 \pm 0.616910\,i \tag{5.15e}$$
$$q \approx 2.622974 \pm 0.609548\,i \tag{5.15f}$$
$$q \approx 2.886041 \pm 0.602908\,i \tag{5.15g}$$

We have determined these endpoints by the direct-search method; therefore, they are less accurate than endpoints computed by the resultant method, and the list is possibly incomplete.

Due to limitations of CPU time, we were unable to obtain the explicit expression for $\det D(q)$ as a polynomial in q; we were therefore unable to obtain all its roots. Instead, we evaluated $\det D(q)$ numerically at selected values of q. In particular, motivated by the results of the preceding subsections, we computed $\det D(q)$ numerically at the first 50 Beraha numbers; and in those cases where $\det D(q) = 0$, we numerically diagonalized the transfer matrix in order to ascertain *which* amplitude(s) are the one(s) that vanish. We find two trivial zeros $q = 0, 1$ where all the amplitudes vanish simultaneously, and one non-trivial real zero $q = 2$ where the dominant amplitude vanishes (along with others). In addition, $\det D(q)$ vanishes at the Beraha numbers $B_5 = (3 + \sqrt{5})/2$, $B_6 = 3$, $B_7 \approx 3.246979603717$ and $B_8 = 2 + \sqrt{2}$ (and hence also at their conjugates); these all correspond to the vanishing of a subdominant amplitude. Finally, inspection of Figure 9 suggests the existence of at least two pairs of complex-conjugate isolated limiting points, $q \approx 2.48873 \pm 0.75416\,i$ and $q \approx 1.65436 \pm 2.01881\,i$; and we confirm that the absolute value of the dominant amplitude is very small in both cases (2.9×10^{-11} and 2.1×10^{-6}, respectively), suggesting that this amplitude does indeed have a zero nearby. There might exist further isolated limiting points not found here.

The first non-trivial real zero converges quickly to the Beraha number $B_4 = 2$ (see Table 3), and the next real zero converges (at a roughly $1/n$ rate) to the value of $q_0 \approx 2.6062482130$ for this lattice, which is slightly smaller than the Beraha number B_5.

5.7 $L_x = 8_{\mathrm{F}}$

The transfer matrix is 70-dimensional; it can be found in the MATHEMATICA file `transfer1.m`.

The limiting curve $\mathcal{B}$ (see Figure 11) appears to consist of six connected components that form three mutually conjugate pairs (but there may be more). One pair is defined by arcs running from $q \approx -0.054426 \pm 0.884363\,i$ to $q \approx 1.211959 \pm 2.301760\,i$. A very small gap (see Figure 12a) separates these arcs from the second pair of arcs, which run from $q \approx 1.214531 \pm 2.301385\,i$ to $q \approx 2.326565 \pm 1.753667\,i$. Another small gap (see Figure 12b) separates these arcs from the third pair of components, which run from $q \approx 2.330755 \pm 1.737504\,i$ to $q \approx 2.660260 \pm 0.001257\,i$ and also have T points at $q \approx 2.640 \pm 1.114\,i$ (see Figure 12c). Note that the limiting curve does *not* cross the real axis: the closest approach is $q \approx 2.660260 \pm 0.001257\,i$ (see Figure 12d).

There are probably 14 endpoints:

$$q \approx -0.054426 \pm 0.884363\,i \tag{5.16a}$$
$$q \approx 1.211959 \pm 2.301760\,i \tag{5.16b}$$
$$q \approx 1.214531 \pm 2.301385\,i \tag{5.16c}$$
$$q \approx 2.326565 \pm 1.753667\,i \tag{5.16d}$$
$$q \approx 2.330755 \pm 1.737504\,i \tag{5.16e}$$
$$q \approx 2.660260 \pm 0.001257\,i \tag{5.16f}$$
$$q \approx 2.921658 \pm 0.560969\,i \tag{5.16g}$$

We have again determined these endpoints by the direct-search method.

Once again we were unable to compute the determinant $\det D(q)$ as a polynomial in q, so we followed the same numerical method as in Section 5.6 to locate at least some of the isolated limiting points. There are of course two trivial isolated real zeros at $q = 0, 1$ where all the amplitudes vanish simultaneously. In addition, $\det D(q)$ vanishes at the Beraha numbers $B_4 = 2$, $B_5 = (3 + \sqrt{5})/2$, $B_6 = 3$, $B_7 \approx 3.246979603717$, $B_8 = 2 + \sqrt{2}$ and $B_9 \approx 3.5320888862$ (and hence also at their conjugates). Unfortunately, we were unable to compute the corresponding amplitudes: even using 4000-digit numerical precision, the inverse of the change-of-basis matrix was obtained with no precision at all! Nevertheless, by inspection of Figure 9 we can guess that B_4 and B_5 are indeed isolated limiting points (see also the discussion below about the rate of convergence to those points), while B_6, B_7, B_8, B_9 are not. Inspection of Figure 9 also suggests that there are two possible pairs of complex-conjugate isolated limiting points, namely $q \approx 1.33321 \pm 2.15164\,i$ and $q \approx 2.39242 \pm 1.11180\,i$; but we are again unable to confirm this by a direct evaluation of the amplitudes at those points.

The convergence of the first non-trivial real zero to $B_4 = 2$ is very rapid (see Table 3). The second non-trivial real zero converges fairly rapidly to the Beraha

number $B_5 = (3+\sqrt{5})/2$, which lies slightly below the point $q \approx 2.66$ where the limiting curve comes close to (but does not cross) the real axis. This rapid convergence suggests that B_4 and B_5 are indeed isolated limiting points. This is the first square-lattice strip with free b.c. for which B_5 appears as an isolated limiting point.

6 Numerical Results for the Square-Lattice Chromatic Polynomial: Periodic Transverse Boundary Conditions

We have also computed the transfer matrix $T(q)$ and the limiting curves $\mathcal{B}$ for square-lattice strips of widths $2 \le L_x \le 8$ with periodic boundary conditions in the transverse direction. We have checked our results for widths $2 \le m_{\rm P} \le 8$ and lengths $n_{\rm F} = 2, 3$ by comparing to the results of Biggs–Damerell–Sands [109] (resp. Shrock–Tsai [24, 29]) for *width* $n_{\rm F} = 2$ (resp. $n_{\rm F} = 3$) and *length* $m_{\rm P}$, using the trivial identity

$$Z(m_{\rm P} \times n_{\rm F}) \;=\; Z(n_{\rm F} \times m_{\rm P}) \;. \tag{6.1}$$

6.1 $L_x = 2_{\rm P}$

This is of course identical to $L_x = 2_{\rm F}$ (Section 5.1).

6.2 $L_x = 3_{\rm P}$

This case is also trivial, as the transfer matrix is one-dimensional. The result is

$$Z(3_{\rm P} \times n_{\rm F}) = q(q-1)(q-2)(q^3 - 6q^2 + 14q - 13)^{n-1} \tag{6.2}$$

The dominant-eigenvalue-crossing curve is of course the empty set $\mathcal{B} = \emptyset$. However, there are zeros for all n at $q = 0, 1, 2$ (trivially) and for all $n \ge 2$ at $q \approx 1.7733011742 \pm 1.4677115087\,i$ and $q \approx 2.4533976515$.

6.3 $L_x = 4_{\rm P}$

The transfer matrix is two-dimensional. In the basis $\mathbf{P} = \{1, \delta_{13} + \delta_{24}\}$ it can be written as

$$T(4_{\rm P}) \;=\; \begin{pmatrix} q^4 - 8q^3 + 28q^2 - 51q + 41 & 2(q^3 - 6q^2 + 14q - 12) \\ 2q - 5 & q^2 - 4q + 5 \end{pmatrix} \;, \tag{6.3}$$

and the partition function is equal to

$$Z(4_{\rm P} \times n_{\rm F}) \;=\; q(q-1) \begin{pmatrix} q^2 - 3q + 3 \\ 2(q-1) \end{pmatrix}^{\rm T} \cdot T(4_{\rm P})^{m-1} \cdot \begin{pmatrix} 1 \\ 0 \end{pmatrix} \;. \tag{6.4}$$

The eigenvalues of the transfer matrix $T(4_{\rm P})$ and their corresponding amplitudes are given by (4.13)/(4.14)/(4.20) with[31]

$$\begin{aligned}
P_1(q) &= q^4 - 8q^3 + 29q^2 - 55q + 46 && \text{(6.5a)}\\
P_2(q) &= q^8 - 16q^7 + 118q^6 - 526q^5 + 1569q^4 - 3250q^3 + 4617q^2 \\
&\quad -4136q + 1776 && \text{(6.5b)}\\
P_3(q) &= q(q-1)(q^6 - 11q^5 + 54q^4 - 152q^3 + 266q^2 - 277q + 128) && \text{(6.5c)}\\
P_4(q) &= 2q^2(q-1)^2(q-2)(q^2 - 3q + 1)(2q-5)^2 && \text{(6.5d)}
\end{aligned}$$

The limiting curve $\mathcal{B}$ (see Figure 13) contains three pieces.[32] It crosses the real axis at the double point $q \approx 2.3026282864$ (with $t \approx 0.092$), from which there emerges a horizontal segment running from $q \approx 2.2533697671$ to $q \approx 2.3516882809$.

There are eight endpoints given by the zeros of the resultant at $t = 0$ $[= -P_2(q)]$:

$$\begin{aligned}
q &\approx 0.7098031013 \pm 2.0427103451\,i && \text{(6.6a)}\\
q &\approx 1.9923366166 \pm 1.5941556425\,i && \text{(6.6b)}\\
q &\approx 2.2533697671 && \text{(6.6c)}\\
q &\approx 2.3516882809 && \text{(6.6d)}\\
q &\approx 2.9953312581 \pm 1.4266372190\,i && \text{(6.6e)}
\end{aligned}$$

The zeros of the amplitudes can be found by solving $P_4(q) = 0$. There are trivial zeros $q = 0, 1$, where both amplitudes vanish simultaneously; both these zeros lie in the region where the eigenvalue λ_+ is dominant. There are five non-trivial zeros: $q = 2$, $5/2$ (double) and $(3 \pm \sqrt{5})/2$. All of them lie in regions where there is a unique dominant eigenvalue; but only for $q = 2$ does the amplitude corresponding to the dominant eigenvalue vanish. The Beraha–Kahane–Weiss theorem thus implies that the isolated limiting points of zeros are precisely $q = 0, 1, 2$. From Table 4 we see that the first non-trivial real zero does indeed converge rapidly to the Beraha number $B_4 = 2$. In addition, there are further real zeros (whose number increases with n) that tend to the segment $[2.2533697671\ldots, 2.3516882809\ldots]$ of the limiting curve and in the limit $n \to \infty$ become dense on that segment.

It is again curious that the amplitude corresponding to the subdominant eigenvalue vanishes at the Beraha number $B_5 = (3 + \sqrt{5})/2$ and its conjugate $B_5^* = (3 - \sqrt{5})/2$.

6.4 $L_x = 5_{\rm P}$

The transfer matrix is again two-dimensional. In the basis $\mathbf{P} = \{1,\ \delta_{13} + \delta_{24} + \delta_{35} + \delta_{41} + \delta_{52}\}$ it can be written as

$$T(5_{\rm P}) =$$

[31] Our results are in agreement with those of [19, eqns. (7.1)–(7.4)]. In particular, we have $b_{sq(4),c,1} = -\operatorname{tr} T$ and $b_{sq(4),c,2} = \det T$.

[32] This curve is also depicted in [19, Figure 3(a)].

$$\begin{pmatrix} q^5 - 10q^4 + 45q^3 - 115q^2 + 169q - 116 & 5(q^4 - 9q^3 + 34q^2 - 63q + 47) \\ q^2 - 6q + 10 & q^3 - 9q^2 + 29q - 32 \end{pmatrix}, \tag{6.7}$$

and the partition function is equal to

$$Z(5_{\rm P} \times m_{\rm F}) \;=\; q(q-1)(q-2) \begin{pmatrix} q^2 - 2q + 2 \\ 5(q-1) \end{pmatrix}^{\rm T} \cdot T(5_{\rm P})^{m-1} \cdot \begin{pmatrix} 1 \\ 0 \end{pmatrix} . \tag{6.8}$$

The eigenvalues of the transfer matrix $T(5_{\rm P})$ and their corresponding amplitudes are given by (4.13)/(4.14)/(4.20) with[33]

$$\begin{aligned} P_1(q) &= q^5 - 10q^4 + 46q^3 - 124q^2 + 198q - 148 && \text{(6.9a)} \\ P_2(q) &= q^{10} - 20q^9 + 188q^8 - 1092q^7 + 4356q^6 - 12596q^5 + 27196q^4 \\ &\quad -44212q^3 + 52708q^2 - 41760q + 16456 && \text{(6.9b)} \\ P_3(q) &= q(q-1)(q-2)(q^7 - 12q^6 + 66q^5 - 214q^4 + 450q^3 \\ &\quad -646q^2 + 608q - 268) && \text{(6.9c)} \\ P_4(q) &= 5q^2(q-1)^2(q-2)^2(q^2 - 3q + 1)(q-3)(q^2 - 6q + 10)^2 && \text{(6.9d)} \end{aligned}$$

The limiting curve contains five pieces, and it crosses the real axis at $q_0 \approx 2.6916837012$.[34] There are ten endpoints given by the zeros of the resultant at $t = 0$ $[= -P_2(q)]$:

$$\begin{aligned} q &\approx 0.1650212134 \pm 1.9190897717\,i && \text{(6.10a)} \\ q &\approx 2.0895893895 \pm 1.9436539472\,i && \text{(6.10b)} \\ q &\approx 2.5034648023 \pm 2.0851731765\,i && \text{(6.10c)} \\ q &\approx 2.5680063227 \pm 0.4886738235\,i && \text{(6.10d)} \\ q &\approx 2.6739182721 \pm 0.5983324603\,i && \text{(6.10e)} \end{aligned}$$

The zeros of the amplitudes can be found by solving $P_4(q) = 0$. There are trivial zeros at $q = 0, 1, 2$, where both amplitudes vanish simultaneously; all of them lie in the region where the eigenvalue λ_- is dominant. The non-trivial zeros of P_4 are $q = 3$, $3 \pm i$ (each of them double) and $(3 \pm \sqrt{5})/2$. Only for $q = (3 + \sqrt{5})/2 = B_5$ does the amplitude corresponding to the leading eigenvalue vanish. So the isolated zeros are expected to converge when the strip length goes to infinity to the first four Beraha numbers $B_2, \ldots, B_5 = 0, 1, 2, (3 + \sqrt{5})/2$.

From Table 4 we see that the third real zero is trivially equal to $B_4 = 2$ (a cylindrical square lattice of odd width is not 2-colorable). The first non-trivial zero converges rapidly to the Beraha number B_5, while the last real zero seems to be converging slowly (at a roughly $1/n$ rate) to the value $q_0 \approx 2.6916837012$ where the limiting curve $\mathcal{B}$ crosses the real axis.

The next Beraha number $B_6 = 3$ is also a zero of $P_4(q)$, but this corresponds to the vanishing of the subdominant amplitude.

[33] Our results are in agreement with those of [32, eqns. (3.8)–(3.10)].

[34] This curve is also depicted in [32, Figure 2].

6.5 $L_x = 6_{\rm P}$

The transfer matrix is five-dimensional; it can be found in the MATHEMATICA file `transfer1.m`.

The limiting curve $\mathcal{B}$ (see Figure 15) has three connected components. Two of them form a pair of mutually conjugate arcs, which extend for the first time into the half-plane $\mathrm{Re}\, q < 0$. The third component is self-conjugate and crosses the real axis with a double point at $q \approx 2.6110856839$, from which there emerges a small horizontal segment running from $2.6089429411 \lesssim q \lesssim 2.6132283584$ (see Figure 16a for detail). Note that this crossing lies slightly *below* the Beraha number $B_5 = (3+\sqrt{5})/2 \approx 2.6180339887$. This component also has T points at $q \approx 2.650 \pm 1.240\, i$ (see Figures 16b,c for detail).

Inspection of Figure 15 might lead one to think that the self-conjugate component also exhibits a cusp at $q \approx 2.568 \pm 1.395\, i$: indeed, the curve $\mathcal{B}$ seems to have a discontinuous derivative there. Moreover, there is no nearby dominant endpoint (which rules out the alternative hypothesis of a T point from which there emerges a very short curve terminating at a dominant endpoint); and anyway the value of t is also reasonably continuous around the alleged cusp (providing further evidence against the idea of a T point). However, by zooming on this region we can see that it is actually a single smooth curve (see Figure 16b,c,d). What happens is that there is a *subdominant* endpoint very close to this curve (the subdominant curve is shown with dashed red lines); moreover, the subdominant eigenvalues are very close in modulus to the dominant ones. In particular, at the subdominant endpoint we have

$$\lambda_{\rm dom} = 10.4372144110 \exp(-0.9719979634\, i) \tag{6.11a}$$

$$\lambda_{\rm sub} = 10.4046337888 \exp(-2.8500677201\, i) \tag{6.11b}$$

Near the subdominant endpoint, the two subdominant eigenvalues are very rapidly changing (as they have a square-root branch point), so that their crossing in modulus with the dominant eigenvalue occurs on a curve $\mathcal{B}$ of rapidly changing slope.

There are ten endpoints:

$$q \approx -0.1318891429 \pm 1.7132242811\, i \tag{6.12a}$$

$$q \approx 1.9257517021 \pm 2.2876287010\, i \tag{6.12b}$$

$$q \approx 2.0571168133 \pm 2.3885607275\, i \tag{6.12c}$$

$$q \approx 2.6089429411 \tag{6.12d}$$

$$q \approx 2.6132283584 \tag{6.12e}$$

$$q \approx 3.1711921718 \pm 0.8639071723\, i \tag{6.12f}$$

By Lemma 2.2, the points where at least one amplitude vanishes are given by the condition $\det D(q) = 0$. This determinant can be written as

$$\det D(q) = q^5(q-1)^5(q-2)^4(q^2-3q+1)^2(q-3)^3(q^3-5q^2+6q-1)P(q)^2 \tag{6.13}$$

where $P(q)$ is a polynomial of degree 28 with integer coefficients that we report in the file `transfer1.m`. We find two trivial zeros $q = 0, 1$ where all the amplitudes

vanish simultaneously. There are three points where a dominant amplitude vanishes: $q = 2$ and $q \approx 2.4813444277 \pm 1.7147613188\,i$ (shown with a $\times$ in Figure 15). The complex-conjugate pair of isolated limiting zeros lies extremely near, *but not on*, the limiting curve $\mathcal{B}$ (namely, about 0.006 to the left of $\mathcal{B}$). The rate of convergence to the complex isolated limiting points is roughly $1/n$ instead of the expected exponential rate. This may be due to the fact that they are extremely close to the limiting curve $\mathcal{B}$.

From Table 4 we see that the first non-trivial real zero converges rapidly to the Beraha number $B_4 = 2$, while the second non-trivial zero appears to be converging slowly (at a rate somewhere between $1/n$ and $1/n^2$) to the real endpoint $q \approx 2.6089429411$. We expect that there will be further real zeros (whose number increases with n) that tend to the segment $[2.6089429411\ldots, 2.6132283584\ldots]$ of the limiting curve and in the limit $n \to \infty$ become dense on that segment.

It is curious that (6.13) vanishes also at the Beraha numbers $B_5 = (3+\sqrt{5})/2$, $B_6 = 3$ and $B_7 \approx 3.246979603717$ and their conjugates, even though all of these correspond to the vanishing of a subdominant amplitude.

6.6 $L_x = 7_{\rm P}$

The transfer matrix is six-dimensional; it can be found in the MATHEMATICA file `transfer1.m`.

The limiting curve $\mathcal{B}$ (see Figure 17) has seven connected components. One of them is a self-conjugate arc that crosses the real axis at $q_0 \approx 2.7883775115$, which lies for the first time *above* the Beraha number $B_5 = (3+\sqrt{5})/2 \approx 2.6180339887$; this arc has endpoints at $q \approx 2.7618995071 \pm 0.4693560083\,i$. The other six components form three pairs of mutually conjugate components. The first pair are arcs running from $q \approx -0.2962497164 \pm 1.5256077564\,i$ to $q \approx 1.6542262925 \pm 2.4866235231\,i$, and thus have support on $\mathrm{Re}\,q < 0$. The second pair are also arcs, running from $q \approx 1.6947007027 \pm 2.5327609879\,i$ to $q \approx 2.6589962013 \pm 1.5245516751\,i$. The last pair of components has endpoints at $q \approx 2.7275004011 \pm 1.4172937300\,i$, $q \approx 2.7873170476 \pm 0.4754613769\,i$ and $q \approx 2.8390155832 \pm 1.3872842928\,i$, and T points at $q \approx 2.737 \pm 1.405\,i$ (see Figure 18a,b); it is separated from the self-conjugate arc by a very small gap (see Figure 18c).

There are 16 endpoints:

$$q \approx -0.2962497164 \pm 1.5256077564\,i \tag{6.14a}$$
$$q \approx 1.6542262925 \pm 2.4866235231\,i \tag{6.14b}$$
$$q \approx 1.6947007027 \pm 2.5327609879\,i \tag{6.14c}$$
$$q \approx 2.6589962013 \pm 1.5245516751\,i \tag{6.14d}$$
$$q \approx 2.7275004011 \pm 1.4172937300\,i \tag{6.14e}$$
$$q \approx 2.7618995071 \pm 0.4693560083\,i \tag{6.14f}$$
$$q \approx 2.7873170476 \pm 0.4754613769\,i \tag{6.14g}$$
$$q \approx 2.8390155832 \pm 1.3872842928\,i \tag{6.14h}$$

By Lemma 2.2, the points where at least one amplitude vanishes are given by the condition $\det D(q) = 0$. This determinant can be written as

$$\begin{aligned} \det D(q) &= q^6(q-1)^6(q-2)^6(q^2-3q+1)^4(q-3)^3(q^3-5q^2+6q-1) \times \\ &\quad (q^2-4q+2)P(q)^2 \end{aligned} \tag{6.15}$$

where $P(q)$ is a polynomial of degree 56 with integer coefficients. This polynomial can be found in the file `transfer1.m`. The trivial isolated limiting points are $q = 0, 1, 2$, where all the amplitudes vanish simultaneously. The non-trivial isolated limiting points are the Beraha number $B_5 = (3+\sqrt{5})/2$ and the pair of complex-conjugate roots $q \approx 2.1027473746 \pm 2.2083820861\,i$. This is the first square-lattice strip with cylindrical b.c. for which B_5 appears as an isolated limiting point.

There is trivially a real zero at $q = 2$ (because the strip width is odd). The first non-trivial real zero (see Table 4) converges rapidly to the Beraha number $B_5 = (3+\sqrt{5})/2$, while the next real zero appears to converge slowly (at a roughly $1/n$ rate) to the value $q_0 \approx 2.7883775115$ where the limiting curve $\mathcal{B}$ crosses the real axis. The rate of convergence to the complex isolated limiting points $q \approx 2.1027473746 \pm 2.2083820861\,i$ is very fast and is compatible with an exponential rate.

It is curious that (6.15) vanishes also at the Beraha numbers $B_6 = 3$, $B_7 \approx 3.246979603717$ and $B_8 = 2+\sqrt{2}$ and their conjugates, even though all of these correspond to the vanishing of a subdominant amplitude.

6.7 $L_x = 8_{\mathrm{P}}$

The transfer matrix is 14-dimensional; it can be found in the MATHEMATICA file `transfer1.m`.

The limiting curve $\mathcal{B}$ (see Figure 19) has six connected components, which define three pairs of mutually conjugate components. The first pair is defined by arcs running from $q \approx -0.3908638747 \pm 1.3698634697\,i$ to $q \approx 1.3863697070 \pm 2.5801346584\,i$, which thus have support on $\mathrm{Re}\,q < 0$. A small gap (see Figure 20a) separates these components from the second pair, which consists of arcs running from $q \approx 1.3989312933 \pm 2.5988401222\,i$ to $q \approx 2.5297861557 \pm 1.8426263238\,i$. The last pair has endpoints at $q \approx 2.5810431815 \pm 1.8106192070\,i$, $q \approx 2.7515311636 \pm 0.0025313231\,i$, $q \approx 2.7812812528 \pm 1.0876657311\,i$ and $q \approx 3.2111321566 \pm 0.6498638896\,i$, and T points at $q \approx 2.801 \pm 1.043\,i$ and $q \approx 2.783 \pm 1.088\,i$. Note that the T points at $q \approx 2.783 \pm 1.088\,i$ might look like cusps if we fail to use enough magnification (see Figure 20b). But if we magnify the region sufficiently, we observe that it is indeed an ordinary T point (see Figure 20c). Note also that $\mathcal{B}$ does not cross the real axis at any point; rather, there is a very tiny gap between $q \approx 2.7515311636 \pm 0.0025313231\,i$ (see Figure 20d).

There are 16 endpoints:

$$q \approx -0.3908638747 \pm 1.3698634697\,i \tag{6.16a}$$

$$q \approx 1.3863697070 \pm 2.5801346584\,i \tag{6.16b}$$

$$q \approx 1.3989312933 \pm 2.5988401222\,i \tag{6.16c}$$

$$q \approx 2.5297861557 \pm 1.8426263238\,i \tag{6.16d}$$
$$q \approx 2.5810431815 \pm 1.8106192070\,i \tag{6.16e}$$
$$q \approx 2.7515311636 \pm 0.0025313231\,i \tag{6.16f}$$
$$q \approx 2.7812812528 \pm 1.0876657311\,i \tag{6.16g}$$
$$q \approx 3.2111321566 \pm 0.6498638896\,i \tag{6.16h}$$

By Lemma 2.2, the points where at least one amplitude vanishes are given by the condition $\det D(q) = 0$. This determinant is given by

$$\begin{aligned} \det D(q) \;=\; & q^{14}(q-1)^{20}(q-2)^{13}(q^2-3q+q^2)^{11}(q-3)^{18}(q^3-5q^2+6q-1)^4 \times \\ & (q^2-4q+2)(q^3-6q^2+9q-1)P(q)^2 \end{aligned} \tag{6.17}$$

where $P(q)$ is a polynomial of degree 396 with integer coefficients (see file `transfer1.m`). The trivial isolated limiting points are $q = 0, 1$: at these points all the amplitudes vanish simultaneously. The non-trivial isolated limiting points are the Beraha numbers $B_4 = 2$ and $B_5 = (3+\sqrt{5})/2$ and the complex-conjugate pairs $q \approx 1.6836371202 \pm 2.4533856271\,i$ and $q \approx 2.6775096551 \pm 1.2084144891\,i$ (see Figure 19).

The first non-trivial real zero converges rapidly to the Beraha number $B_4 = 2$, and the next real zero converges rapidly to the Beraha number $B_5 = (3+\sqrt{5})/2$ (see Table 4). The convergence to the complex isolated limiting points $q \approx 1.6836371202 \pm 2.4533856271\,i$ and $q \approx 2.6775096551 \pm 1.2084144891\,i$ is also very fast and is compatible with an exponential rate.

It is curious that (6.17) vanishes also at the Beraha numbers $B_6 = 3$, $B_7 \approx 3.246979603717$, $B_8 = 2+\sqrt{2}$ and $B_9 \approx 3.532088886238$ and their conjugates, even though all of these correspond to the vanishing of a subdominant amplitude.

7 Discussion and Open Questions

7.1 Behavior of dominant-eigenvalue-crossing curves $\mathcal{B}$

In this paper we have computed the chromatic polynomials (= zero-temperature antiferromagnetic Potts-model partition functions) $P_G(q)$ and their zeros for square-lattice strips of width $2 \le L_x \le 8$ and arbitrary length L_y with free and cylindrical boundary conditions. In particular, we have extracted the limiting curves $\mathcal{B}$ of partition-function zeros when the length L_y goes to infinity at fixed width L_x. By studying the finite-width limiting curves and their behavior as we increase the width L_x, we hope to shed light on the thermodynamic limit $L_x, L_y \to \infty$.

In Table 5 we summarize the main properties of the limiting curves $\mathcal{B}$ (and of the isolated limiting points) for all the lattices studied in the previous sections. Note the identity

$$\begin{aligned} \text{endpoints} \;=\; & (2 \times \text{components}) + (2 \times \text{double points}) + (\text{T points}) - \\ & (2 \times \text{enclosed regions})\,, \end{aligned} \tag{7.1}$$

which can be derived by simple topological/graph-theoretic arguments.

Our first conclusion is that the limiting curves become in general more complicated as the strip width L_x grows. In particular, the number of connected components, the number of endpoints, and the number of T points all tend to increase with the width L_x. (Note that our counts for $L_x = 7_{\rm F}, 8_{\rm F}$ are only lower bounds on the true values.) Moreover, the size of the gaps between connected components, and the lengths of the protruding arcs associated to some of the T points, both seem to decrease with the strip width L_x. The approach to the thermodynamic limit thus appears to be rather complicated.

A second point deals with the existence or not of enclosed regions. Shrock [28, Section III, point 3] conjectured that for families of graphs with a well-defined lattice structure, a *sufficient* condition for $\mathcal{B}$ to separate the q-plane into two or more regions is that the graphs contain at least one "global circuit", defined as a route following a lattice direction which has the topology of S^1 and a length that goes to infinity as $L_y \to \infty$. (For strip graphs, this condition is equivalent to having periodic boundary conditions in the longitudinal direction.) Our results for $L_x = 6_{\rm F}, 7_{\rm F}$ show that this condition, whether or not it is in fact sufficient for the existence of enclosed regions, is in any case not *necessary*: enclosed regions can arise also with *free* longitudinal b.c.[35] In both these cases, the enclosed regions are small bulb-like regions located at the end of one of the components of $\mathcal{B}$. Enclosed regions do, however, seem to be atypical for square-lattice strips with free longitudinal b.c.

A third point concerns the existence of chromatic zeros with $\mathrm{Re}\, q < 0$, and more specifically of limiting curves $\mathcal{B}$ that intersect the half-plane $\mathrm{Re}\, q < 0$. In 1980, Farrell [137] conjectured, based on computations with small graphs, that all chromatic roots have $\mathrm{Re}\, q \ge 0$. We now know that this conjecture is false [138]; indeed, there are families of graphs whose chromatic roots, taken together, are dense in the whole complex q-plane [40]. Nevertheless, chromatic roots do seem to have a tendency to avoid the left half-plane, and it would be interesting to know why. Our computations show that for $L_x = 7_{\rm F}, 8_{\rm F}$ and $L_x = 6_{\rm P}, 7_{\rm P}, 8_{\rm P}$, the locus $\mathcal{B}$ does intersect the half-plane $\mathrm{Re}\, q < 0$. Indeed, we conjecture that this happens for square-lattice strips of *all* widths $L_x \ge 7$ (free b.c.) or $L_x \ge 6$ (cylindrical b.c.).

Although the limiting curves get more complicated as the strip width L_x grows, they do exhibit some regularities, as can be seen in Table 5 and Figures 21 and 22. In Figure 21 we superpose the limiting curves for all the square-lattice strips with free boundary conditions. In the leftmost part of the plot ($\mathrm{Re}\, q \lesssim 2$), we see that the arcs behave monotonically: as the width L_x increases, the corresponding arc moves outwards. In particular, $\min \mathrm{Re}\, q$ decreases monotonically with the width L_x (see Table 5). A similar behavior is observed in the right part of the plot for $L_x \ge 4$: the limiting curves have similar shapes and they move monotonically to the right as L_x grows. In particular, the point q_0 where $\mathcal{B}$ crosses the real axis increases monotonically with the strip width, as does $\max \mathrm{Re}\, q$ (see again Table 5). In general, the shapes of the limiting curves look roughly similar to those obtained by Baxter [55, Figures 5 and

[35] For earlier examples showing that enclosed regions can arise also with free longitudinal b.c., see [19, Figures 2(b), 3(b) and 4(a,b)].

6] for the triangular lattice. We conjecture that the rightmost endpoints of $\mathcal{B}$, which lie at $q \approx 2.92 \pm 0.56\,i$ for $L_x = 8$, will tend (slowly) to close up at the critical value $q_c = 3$ as $L_x \to \infty$. We also conjecture, in analogy with the triangular lattice, that the values q_0 will tend to a number strictly less than 3, probably somewhere around 2.9. However, our strip widths are still too small to give unambiguous evidence for or against these conjectures.

In Figure 22 we show the limiting curves for all the square-lattice strips with cylindrical boundary conditions. In the leftmost part of the plot ($\mathrm{Re}\, q \lesssim 2$), the behavior of the arcs is again monotonic in the strip width; in particular, $\min \mathrm{Re}\, q$ is again a decreasing function of L_x (see Table 5). However, the qualitative behavior of the limiting curves on the right side of the plot ($\mathrm{Re}\, q \gtrsim 2.3$) is clearly *not* monotonic: there is a notorious difference between strips with even width and those with odd width. This difference is, in fact, to be expected: with periodic transverse boundary conditions, odd widths are in some sense "unnatural" as they introduce frustration in the antiferromagnetic Ising system (i.e. they make the chromatic number 3 rather than 2, thereby forcing a chromatic zero at $q = 2$). It is curious that the difference between even and odd widths is significant only on the rightmost part of the limiting curve (namely, the part nearest $q = 2$ and $q = 3$). In any case, if we consider the even and odd subsequences separately, then q_0 and $\max \mathrm{Re}\, q$ are again monotonically increasing functions of L_x (see Table 5). Moreover, the limiting curves for the square-lattice strips with *even* width and cylindrical boundary conditions have, apart from the case $L_x = 4$, a qualitative shape in agreement with that for free boundary conditions.

Finally, let us compare the limiting curves for free and cylindrical boundary conditions (Figures 21 and 22). If we focus on the leftmost part of the plots, we see that both sets of curves tend to larger values of $|\mathrm{Im}\, q|$ as L_x grows, but the curves for cylindrical boundary conditions reach large values of $|\mathrm{Im}\, q|$ much faster. Likewise, on the rightmost part of the plots, both sets of curves tend to larger values of $\mathrm{Re}\, q$ as L_x grows (modulo the even-odd oscillation for cylindrical b.c.), but the curves for cylindrical boundary conditions do so somewhat faster. This suggests that the thermodynamic limit is achieved faster with cylindrical boundary conditions than with free boundary conditions.

Let us conclude by mentioning briefly the work of Bakaev and Kabanovich [139], who computed the large-q series for the infinite-volume limiting chromatic polynomial through order z^{36} [where $z = 1/(q-1)$], using the finite-lattice method. Tony Guttmann (private communication) has kindly analyzed their series using differential approximants. He finds that the nearest singularity to $z = 0$ lies at $z \approx (0.155 \pm 0.005) \pm (0.37 \pm 0.03)i$, corresponding to $q \approx (1.96 \pm 0.15) \pm (2.30 \pm 0.15)i$. Curiously enough, this corresponds quite closely to a gap (pair of nearby endpoints) for width 6_{P} (see Section 6.5), where the limiting chromatic polynomial is indeed singular. But this may be a coincidence, as there is no corresponding endpoint for width 8_{P}, and the nearby endpoints for strips with free b.c. do not seem to be converging to this value.[36] The large-q series shows no hint of singularity at $q_c = 3$, which is very

[36] For 5_{F} there is a gap around $z \approx 0.20 \pm 0.41\,i$, but as the width increases, the real part decreases *beyond* the predicted singularity (0.13 for 6_{F}, 0.08 for 7_{F}, 0.04 for 8_{F}).

likely a weak essential singularity.

7.2 Behavior of amplitudes and the Beraha conjecture

For all the lattices we studied (up to width $L = 8$), we observed empirically that there is at least one vanishing amplitude $\alpha_i(q)$ at each of the Beraha numbers up to B_{L+1}. It is reasonable to conjecture that this holds for all L:

Conjecture 7.1 *For a square-lattice strip of width L with free or cylindrical boundary conditions, at each Beraha number $q = B_2, \ldots, B_{L+1}$ there is at least one vanishing amplitude $\alpha_i(q)$. That is,* $\det D(q) = 0$ *for $q = B_2, \ldots, B_{L+1}$.*

For all the cases we studied except $7_{\rm F}$ and $8_{\rm F}$ [where we were unable to compute an explicit expression for $\det D(q)$], we also verified that none of the roots of $\det D(q)$ correspond to Beraha numbers *beyond* B_{L+1}. We conjecture that this holds for all L:

Conjecture 7.2 *For a square-lattice strip of width L with either free or cylindrical boundary conditions,* $\det D(q) \neq 0$ *for all $q = B_k$ with $k > L + 1$. [We assume, of course, that the chromatic polynomial is written in such a way that there are no* identically *vanishing amplitudes.]*

In some cases we found real roots of $\det D(q)$ that are *very close to* Beraha numbers: for instance, the strip with $L = 5_{\rm F}$ (resp. $L = 6_{\rm F}$) has a zero of $\det D(q)$ very close to B_7 (resp. B_9 and B_{29}). Moreover, $\det D(q)$ does in general have many real roots with $q > B_{L+1}$ (and indeed with $q > 4$), as well as real roots with $q < 0$.

We can strengthen the preceding conjecture to assert that $\det D(q)$ is *strictly positive* at the Beraha numbers beyond B_{L+1}:

Conjecture 7.3 *For a square-lattice strip of width L with either free or cylindrical boundary conditions,* $\det D(q) > 0$ *for all $q = B_k$ with $k > L + 1$.*

We have verified this conjecture for all square-lattice strips with $L \leq 7_{\rm F}$ and $L \leq 8_{\rm P}$ up to $k = 50$. Furthermore, the function $f(k) = \det D(B_k)$ seems to be a monotonically increasing function of k for $k > L + 1$.

Conjecture 7.1 asserts that at each of the Beraha numbers $B_2, \ldots, B_{L+1}$ there is at least one vanishing amplitude $\alpha_i(q)$, but it says nothing about whether the vanishing amplitude belongs to a dominant or a subdominant eigenvalue. Basing ourselves on a suggestion of Baxter [55, p. 5255], we conjectured that at each Beraha number $q = B_2, \ldots, B_{L+1}$, the amplitude $\alpha_*(q)$ corresponding to the eigenvalue $\lambda_*(q)$ vanishes: here $\lambda_*(q)$ is the eigenvalue that is dominant at small real q (e.g. at $q = 1$), analytically continued up the real axis (or, if there is a branch point on the real axis, then just above or below the real axis). [Note that $\lambda_*(q)$ remains dominant until the path of analytic continuation crosses $\mathcal{B}$; after that, it becomes in general subdominant.] We tested this conjecture numerically as follows: Choose a path in the complex q-plane starting at $q = 1$ and proceeding to the right just above or below the

real axis (note that for 8_F and 8_P we must keep $|\mathrm{Im}\, q| \lesssim 0.001$ in order to avoid going around an endpoint).[37] Subdivide this path into very small steps, and at each point compute the eigenvalues of the transfer matrix, following $\lambda_*(q)$ "by continuity" (that is, starting with $\lambda_*(1)$, choose at each q value the eigenvalue that is closest to the one chosen at the preceding q value). Then, when the Beraha number B_k is reached, diagonalize the transfer matrix, rotate the left and right vectors $\vec{u}(q)$ and $\vec{v}(q)$, and test whether the amplitude $\alpha_*(q)$ vanishes.

We were unable to carry out this computation for $L = 7_F$ and 8_F: in the former case, because of CPU-time limitations, and in the latter case, because of loss of numerical precision in diagonalizing the matrices (even when we used 1000-digit arithmetic). In all but one of the other cases (namely, for $L \le 6_F$ and $L \le 7_P$), we found that $\alpha_*(q)$ does indeed vanish (sometimes along with other amplitudes) at all the Beraha numbers up to B_{L+1}. The strips with $L = 8_F$ and 8_P are, however, a different case, as the limiting curve $\mathcal{B}$ does not cross the real axis. If we follow a path from $q = 1$ to $q = +\infty$ along the real axis, we do not cross $\mathcal{B}$; so $\lambda_*(q)$ stays dominant everywhere on the real axis (and in particular at the Beraha numbers $B_6, \ldots, B_9$). Therefore, if $\alpha_*(q)$ were to vanish at $B_6, \ldots, B_9$, as our conjecture asserts, then those Beraha numbers would be isolated limiting points. But Figures 11 and 19 show clearly that they are not! So our conjecture must be *false* for the strips 8_F and 8_P. (Indeed, for 8_P we confirmed explicitly that α_* vanishes at $B_2, \ldots, B_5$ but *not* at $B_6, \ldots, B_9$; rather, it is a *subdominant* amplitude that vanishes at the latter points.) More generally, we can expect our conjecture to be false whenever $\mathcal{B}$ does not cross the real axis.[38] We are therefore obliged to modify our conjecture as follows:

Conjecture 7.4 *For a square-lattice strip of width L with free or cylindrical boundary conditions, let $\lambda_*(q)$ be the eigenvalue that is dominant at small real q (e.g. at $q = 1$),analytically continued up the real axis (or, if there is a branch point on the real axis, then just above or below the real axis). Then,* provided that the limiting curve $\mathcal{B}$ crosses the real axis, *at each Beraha number $q = B_2, \ldots, B_{L+1}$, the corresponding amplitude $\alpha_*(q)$ vanishes. [Other amplitudes may vanish as well.]*

All our numerical evidence is consistent with Conjecture 7.4.

Remark. In the case $L = 8_P$, suppose that we follow a path that *does* cross the limiting curve $\mathcal{B}$ slightly above the endpoint at $q \approx 2.7515 + 0.0025\, i$. Then the eigenvalue λ_* will cease to be dominant to the right of $\mathcal{B}$; and we find that the

[37] Any two such paths give the same analytic continuation provided that there are no endpoints in the region between them.

[38] For the same reason, if in the cases $L \le 6_F$ and $L \le 7_P$ we analytically continue the dominant eigenvalue at $q = 1$ (namely, λ_*) to the region $q > q_0(L)$ by following a path that does *not* cross $\mathcal{B}$ — e.g., by going through one of the gaps in $\mathcal{B}$ — then the analytic continuation of λ_* will remain dominant everywhere. But then, the analytic continuation of the amplitude α_* will *not* vanish at any of the Beraha numbers to the right of $\mathcal{B}$, since we know that these are *not* isolated limiting points. Rather, the analytic continuation of one or more *sub*dominant amplitudes at $q = 1$ will vanish at those Beraha numbers. We have numerically tested this behavior of the eigenvalues and amplitudes along paths that do not cross $\mathcal{B}$ in the same way we did for the paths that do cross $\mathcal{B}$.

corresponding amplitude α_* *does* vanish at all the Beraha numbers $B_6, \ldots, B_9$! So a variant of Conjecture 7.4 applies in this case as well. But we are unable to see what general principle might be at work.

Conjecture 7.4 "explains" why the first few Beraha numbers — but *only* the first few — arise as limiting points of chromatic roots, at least in those cases where the limiting curve $\mathcal{B}$ crosses the real axis at some point $q_0(L)$. Indeed, those Beraha numbers that satisfy both $q \le B_{L+1}$ and $q < q_0(L)$ correspond to the vanishing of the dominant amplitude, hence are isolated limiting points of chromatic roots. By contrast, the remaining Beraha numbers correspond either to the vanishing of a subdominant amplitude (in case $q_0(L) < q \le B_{L+1}$) or do not correspond to the vanishing of any amplitude (in case $q > B_{L+1}$, assuming the validity of Conjecture 7.2).[39] As the strip width L grows, the limiting curve $\mathcal{B}$ moves to the right and "uncovers" more Beraha numbers; $q_0(L)$ presumably tends to a limiting value $q_0(\infty)$. For the triangular lattice, Baxter's [55] analytic solution predicts that $q_0(\infty) \approx 3.81967$, which lies between B_{14} and B_{15} and in particular lies strictly below the critical point $q_c = 4$. For the square lattice, an analytic solution is lacking, but our results in Table 5 suggest (assuming monotonicity in L) that $q_0(\infty) > 2.788$, and analogy with the triangular lattice suggests that $q_0(\infty) < q_c = 3$. It follows that $q_0(\infty)$ lies between B_5 and B_6, so that the first four Beraha numbers $B_2, \ldots, B_5$ — *but only these* — will be isolated limiting points.

7.3 Upper zero-free interval for bipartite planar graphs

Let G be a loopless planar graph. Then it is not hard to prove that $P_G(q) > 0$ for all *integers* $q \ge 5$;[40] moreover, one of the most famous theorems of graph theory — the Four-Color Theorem [141, 142, 143, 144, 145] — asserts that $P_G(q) > 0$ holds in fact for all integers $q \ge 4$.

It is natural to ask whether these results can be extended from integer q to *real* q. The answer is yes, at least in part: Birkhoff and Lewis [101] proved in 1946 that if G is a loopless planar graph, then $P_G(q) > 0$ for all real numbers $q \ge 5$.[41] Furthermore, they conjectured that $P_G(q) > 0$ also for $4 < q < 5$; and while no one has yet found a proof, no one has found a counterexample either, so it seems plausible (in the light of the Four-Color Theorem) that the conjecture is true.

[39] In case $q_0(L)$ is itself a Beraha number $\le B_{L+1}$ (as happens e.g. for $L = 3_{\rm F}$), it corresponds to case (b) of the Beraha–Kahane–Weiss theorem, hence to a non-isolated limiting point. More generally, if $\mathcal{B}$ intersects the real axis in an interval $[q_{0,-}(L), q_{0,+}(L)]$, then all the points in this interval correspond to non-isolated limiting points, even if a dominant amplitude should happen to vanish.

[40] This is the Five-Color Theorem, which goes back to Heawood in 1890. For a proof, see e.g. [140, Theorem V.8, pp. 154–155]; or for an elegant alternate proof of an even stronger result, see [140, Theorem V.12, pp. 161–163].

[41] See also Woodall [102, Theorem 1] and Thomassen [103, Theorem 3.1 ff.] for alternate proofs of a more general result.

Now some planar graphs can be colored with three or even two colors; their chromatic polynomials $P_G(q)$ are strictly positive for integers $q \geq 3$ or $q \geq 2$, respectively. Can *these* bounds can be extended to real q? That is, if G is a k-colorable planar graph, do we have $P_G(q) > 0$ for all real $q \geq k$? Woodall [102, p. 142] conjectured that the answer is yes. For $k = 4$, this is the conjecture of Birkhoff and Lewis mentioned above. For $k = 3$, however, Thomassen [103, pp. 505–506] has shown that Woodall's conjecture is false: there exist 3-colorable planar graphs with real chromatic roots greater than 3.[42] We can now show that Woodall's conjecture is false also for $k = 2$: there exist 2-colorable (i.e. bipartite) planar graphs with real chromatic roots greater than 2. For example, the $4_P \times 6_F$ square lattice has chromatic roots at $q \approx 2.009978$ and $q \approx 2.168344$; and the same pattern persists for larger lattices, with both free and periodic transverse boundary conditions (see Tables 3 and 4). Indeed, for the cases $8_F \times n_F$ and $8_P \times n_F$, we see numerically (Tables 3 and 4) that there are real chromatic roots tending to $B_5 = (3 + \sqrt{5})/2 \approx 2.618034$ from below as $n \to \infty$.[43] This leads us to modify Woodall's conjecture as follows:

Conjecture 7.5 *Let G be a bipartite planar graph. Then $P_G(q) > 0$ for real $q \geq B_5 = (3 + \sqrt{5})/2$.*

Let us make two remarks:

1) Planarity here is crucial, as non-planar bipartite graphs can have arbitrarily large real chromatic roots. Indeed, the complete bipartite graphs K_{n_1,n_2}, in the limit $n_2 \to \infty$ with n_1 fixed, have real chromatic roots arbitrarily close to all the integers from 2 through $\lfloor n_1/2 \rfloor$ [104, Theorem 8].

2) Initially we conjectured that not only $P_G(q)$ but also *all its derivatives* are positive for $q \geq B_5$. But this turns out to be false: for example, the $8_P \times 16_F$ lattice has $P''_G(B_5) < 0$; and the $8_P \times 24_F$ lattice has $P'_G(q) < 0$ for $2.638337 \lesssim q \lesssim 2.687058$.

[42] Start with a graph K and a real number q_0 for which $P_K(q_0) < 0$. Then Thomassen [103, Theorem 3.9] constructs a 2-degenerate (and hence 3-colorable [140, Theorem V.1, p. 148]) graph $K(m)$ such that $P_{K(m)}(q_0) < 0$; moreover, $K(m)$ can be chosen to be planar if K is. Since there exist planar graphs K with real chromatic roots q_1 greater than 3, and since the 3-colorability of $K(m)$ [or alternatively the Four-Color Theorem] implies that $P_{K(m)}(4) > 0$, we can take $q_0 = q_1 - \epsilon$ and conclude that $K(m)$ has a chromatic root in the interval $q_0 < q < 4$. Thus, the upper zero-free interval for 3-colorable planar graphs is the same as that for all planar graphs.

In presenting this result, Thomassen [103, p. 506] further asserted that there exist planar graphs K with real chromatic roots *arbitrarily close to 4*; but this assertion apparently arises from a misunderstanding of the Beraha–Kahane [38] theorem that $4_P \times n_F$ triangular lattices have *complex* chromatic roots arbitarily close to 4. In fact we do not know of any planar graphs with real chromatic roots arbitarily close to 4. In our study of triangular-lattice strips [87] we have thus far found chromatic roots up to ≈ 3.51; and Baxter's [55] result $q_0(\infty) \approx 3.81967$ suggests that sufficiently wide and long pieces of the triangular lattice will have real chromatic roots up to at least $B_{14} \approx 3.801938$. But we do not know of any planar graphs with chromatic roots in the interval $[B_{14}, \infty)$.

We thank Carsten Thomassen and Douglas Woodall for correspondence concerning these questions.

[43] The $5_P \times n_F$ and $7_P \times n_F$ lattices have chromatic roots larger than B_5, but graphs of odd strip width with periodic b.c. are not bipartite.

7.4 Prospects for future work

One very interesting extension of this work is the computation of the chromatic polynomials for strips with *periodic* boundary conditions in the *longitudinal* direction [88]. Such computations have been performed for strip widths $m = 2, 3$ by *ad hoc* methods [109, 34, 35, 23, 24, 26, 27, 29], but a systematic transfer-matrix formalism has heretofore been lacking. In fact, the needed formalism can be obtained by a slight extension of the methods explained in this paper. Suppose we want to obtain the chromatic polynomial for a square-lattice strip $m_{\mathrm{F/P}} \times n_{\mathrm{P}}$ (i.e., either free or periodic transverse b.c., and periodic longitudinal b.c.). The idea is simple: instead of just keeping track of the connectivities among the m sites on the current top row, we keep track of the connectivities among the $2m$ sites on the current top row *and* the bottom row. Let us call these sites $1, 2, \ldots, m$ and $1', 2', \ldots, m'$, respectively. Initially the top and bottom rows are identical. We then enlarge the lattice one site at a time, exactly as in Section 3.2; the join and detach operations act on the sites of the top row, with those of the bottom row simply "going along for the ride". At the end, when we have obtained a lattice with $n + 1$ rows, we identify the top and bottom rows. The partition function for periodic longitudinal boundary conditions can thus be written as

$$Z_{G_n^{\mathrm{per}}}(q, \{v_e\}) \;=\; \widehat{\mathbf{u}}^{\mathrm{T}} (\mathsf{VH})^n \mathbf{v}_{\mathrm{equiv}} \;, \tag{7.2}$$

where "equiv" denotes the partition $\{ \{1, 1'\}, \{2, 2'\}, \ldots \{m, m'\} \}$ and $\widehat{\mathbf{u}}^{\mathrm{T}}$ is defined by

$$\widehat{\mathbf{u}}^{\mathrm{T}} \;=\; \mathbf{u}^{\mathrm{T}} \mathsf{J}_{11'} \mathsf{J}_{22'} \cdots \mathsf{J}_{mm'} \tag{7.3}$$

where $\mathbf{u}^{\mathrm{T}}$ is defined in (3.41).

In future work in collaboration with Jesper-Lykke Jacobsen, we will extend the results of the present paper to wider strip widths [86], to the triangular lattice [87], to periodic boundary conditions in the longitudinal direction [88], and to nonzero temperature [65].

Acknowledgments

We wish to thank Dario Bini for supplying us the MPSolve 2.0 package and for many discussions about its use; Tony Guttmann for analyzing the large-q series; Jesper-Lykke Jacobsen for independently confirming our transfer matrices and for pointing out some typographical errors in an early draft; Hubert Saleur for emphasizing the importance of the Beraha numbers; Dan Segal for helping us with algebra and number theory; Norman Weiss for suggesting that we study the resultant; and Robert Shrock for many helpful conversations throughout the course of this work.

The authors' research was supported in part by U.S. National Science Foundation grant PHY-9900769 (J.S. and A.D.S.) and CICyT (Spain) grant AEN97-1680 (J.S.). It was completed while the second author was a Visiting Fellow at All Souls College, Oxford, where he was supported in part by Engineering and Physical Sciences Research Council grant GR/M 71626 and aided by the warm hospitality of John Cardy and the Department of Theoretical Physics.

References

[1] R.B. Potts, Proc. Cambridge Philos. Soc. **48**, 106 (1952).

[2] F.Y. Wu, Rev. Mod. Phys. **54**, 235 (1982); **55**, 315 (E) (1983).

[3] F.Y. Wu, J. Appl. Phys. **55**, 2421 (1984).

[4] R.J. Baxter, *Exactly Solved Models in Statistical Mechanics* (Academic Press, London–New York, 1982).

[5] C. Itzykson, H. Saleur and J.-B. Zuber, eds., *Conformal Invariance and Applications to Statistical Mechanics* (World Scientific, Singapore, 1988).

[6] P. Di Francesco, P. Mathieu and D. Sénéchal, *Conformal Field Theory* (Springer-Verlag, New York, 1997).

[7] B. Nienhuis, J. Stat. Phys. **34**, 731 (1984).

[8] C.N. Yang and T.D. Lee, Phys. Rev. **87**, 404 (1952).

[9] P.W. Kasteleyn and C.M. Fortuin, J. Phys. Soc. Japan **26** (Suppl.), 11 (1969).

[10] C.M. Fortuin and P.W. Kasteleyn, Physica **57**, 536 (1972).

[11] R. Shrock and S.-H. Tsai, Phys. Rev. E **55**, 5165 (1997), cond-mat/9612249.

[12] R. Shrock and S.-H. Tsai, Phys. Rev. E **56**, 1342 (1997), cond-mat/9703249.

[13] R. Shrock and S.-H. Tsai, Phys. Rev. E **56**, 3935 (1997), cond-mat/9707096.

[14] R. Shrock and S.-H. Tsai, Phys. Rev. E **56**, 4111 (1997), cond-mat/9707306.

[15] H. Feldmann, R. Shrock and S.-H. Tsai, Phys. Rev. E **57**, 1335 (1998), cond-mat/9711058.

[16] H. Feldmann, A.J. Guttmann, I. Jensen, R. Shrock and S.-H. Tsai, J. Phys. A **31**, 2287 (1998), cond-mat/9801305.

[17] M. Roček, R. Shrock and S.-H. Tsai, Physica A **252**, 505 (1998), cond-mat/9712148.

[18] R. Shrock and S.-H. Tsai, Physica A **259**, 315 (1998), cond-mat/9807105.

[19] M. Roček, R. Shrock and S.-H. Tsai, Physica A **259**, 367 (1998), cond-mat/9807106.

[20] S.-H. Tsai, Physica A **259**, 349 (1998), cond-mat/9807107.

[21] R. Shrock and S.-H. Tsai, J. Phys. A **31**, 9641 (1998), cond-mat/9810057.

[22] R. Shrock and S.-H. Tsai, Physica A **265**, 186 (1999), cond-mat/9811410.

[23] R. Shrock and S.-H. Tsai, J. Phys. A **32**, L195 (1999), cond-mat/9903233.

[24] R. Shrock and S.-H. Tsai, Phys. Rev. E **60**, 3512 (1999), cond-mat/9910377.

[25] R. Shrock and S.-H. Tsai, J. Phys. A **32**, 5053 (1999), cond-mat/9905431.

[26] N. Biggs and R. Shrock, J. Phys. A **32**, L489 (1999), cond-mat/0001407.

[27] R. Shrock, Phys. Lett. A **261**, 57 (1999), cond-mat/9908323.

[28] R. Shrock, Chromatic polynomials and their zeros and asymptotic limits for families of graphs, to appear in the proceedings of the 1999 British Combinatorial Conference (University of Kent, Canterbury, July 1999), cond-mat/9908307.

[29] R. Shrock and S.-H. Tsai, Physica A **275**, 429 (2000), cond-mat/9907403.

[30] R. Shrock, Physica A **283**, 388 (2000), cond-mat/0001389.

[31] S.-C. Chang and R. Shrock, Ground state entropy of the Potts antiferromagnet on triangular lattice strips, cond-mat/0004129.

[32] S.-C. Chang and R. Shrock, Ground state entropy of the Potts antiferromagnet on strips of the square lattice, cond-mat/0004161.

[33] S.-C. Chang and R. Shrock, Physica A **286**, 189 (2000), cond-mat/0004181.

[34] N. Biggs, A matrix method for chromatic polynomials, London School of Economics CDAM Research Report LSE-CDAM-99-03 (1999).

[35] N. Biggs, The chromatic polynomial of the $3 \times n$ toroidal lattice, London School of Economics CDAM Research Report LSE-CDAM-99-05 (1999).

[36] S. Beraha, J. Kahane and N.J. Weiss, Proc. Nat. Acad. Sci. USA **72**, 4209 (1975).

[37] S. Beraha, J. Kahane and N.J. Weiss, in *Studies in Foundations and Combinatorics* (Advances in Mathematics Supplementary Studies, Vol. 1), ed. G.-C. Rota (Academic Press, New York, 1978).

[38] S. Beraha and J. Kahane, J. Combin. Theory B **27**, 1 (1979).

[39] S. Beraha, J. Kahane and N.J. Weiss, J. Combin. Theory B **28**, 52 (1980).

[40] A.D. Sokal, Chromatic roots are dense in the whole complex plane, in preparation.

[41] J. Salas and A.D. Sokal, J. Stat. Phys. **86**, 551 (1997), cond-mat/9603068.

[42] R.J. Baxter, Proc. Roy. Soc. London A **383**, 43 (1982).

[43] L. Onsager, Phys. Rev. **65**, 117 (1944).

[44] A. Lenard, cited in E.H. Lieb, Phys. Rev. **162**, 162 (1967) at pp. 169–170.

[45] R.J. Baxter, J. Math. Phys. **11**, 3116 (1970).

[46] M. den Nijs, M.P. Nightingale and M. Schick, Phys. Rev. B **26**, 2490 (1982).

[47] J.K. Burton Jr. and C.L. Henley, J. Phys. A **30**, 8385 (1997), cond-mat/9708171.

[48] J. Salas and A.D. Sokal, J. Stat. Phys. **92**, 729 (1998), cond-mat/9801079.

[49] S.L.A. de Queiroz, T. Paiva, J.S. de Sá Martins and R.R. dos Santos, Phys. Rev. E **59**, 2772 (1999), cond-mat/9812341.

[50] S.J. Ferreira and A.D. Sokal, J. Stat. Phys. **96**, 461 (1999), cond-mat/9811345.

[51] H. Saleur, Commun. Math. Phys. **132**, 657 (1990).

[52] H. Saleur, Nucl. Phys. B **360**, 219 (1991).

[53] R.J. Baxter, H.N.V. Temperley and S.E. Ashley, Proc. Roy. Soc. London A **358**, 535 (1978).

[54] R.J. Baxter, J. Phys. A **19**, 2821 (1986).

[55] R.J. Baxter, J. Phys. A **20**, 5241 (1987).

[56] B. Nienhuis, Phys. Rev. Lett. **49**, 1062 (1982).

[57] J. Stephenson, J. Math. Phys. **5**, 1009 (1964).

[58] H.W.J. Blöte and H.J. Hilhorst, J. Phys. A **15**, L631 (1982).

[59] B. Nienhuis, H.J. Hilhorst and H.W.J. Blöte, J. Phys. A **17**, 3559 (1984).

[60] R.J. Baxter, J. Math. Phys. **11**, 784 (1970).

[61] C.L. Henley, private communications.

[62] J. Salas and A.D. Sokal, unpublished.

[63] A.C.D. van Enter, R. Fernández and A.D. Sokal, unpublished (1996).

[64] J. Adler, A. Brandt, W. Janke and S. Shmulyan, J. Phys. A **28**, 5117 (1995).

[65] J.L. Jacobsen, J. Salas and A.D. Sokal, Transfer matrices and partition-function zeros for antiferromagnetic Potts models. V. Nonzero temperature, work in progress.

[66] H.W.J. Blöte and M.P. Nightingale, Physica **112A**, 405 (1982).

[67] S. Beraha, unpublished, circa 1974.

[68] G. Berman and W.T. Tutte, J. Combin. Theory **6**, 301 (1969).

[69] W.T. Tutte, J. Combin. Theory **9**, 289 (1970).

[70] W.T. Tutte, Ann. New York Acad. Sci. **175**, 391 (1970).

[71] W.T. Tutte, Canad. J. Math. **26**, 893 (1974).

[72] W.T. Tutte, in *Studies in Graph Theory*, Part II, ed. D.R. Fulkerson, Studies in Mathematics #12 (Mathematical Association of America, Washington, 1975), pp. 361–377.

[73] W.T. Tutte, Canad. J. Math. **34**, 741 (1982).

[74] W.T. Tutte, Canad. J. Math. **34**, 952 (1982).

[75] P.P. Martin, J. Phys. A **20**, L399 (1987).

[76] P.P. Martin, J. Phys. A **22**, 3991 (1989).

[77] P.P. Martin, *Potts Models and Related Problems in Statistical Mechanics*. (World Scientific, Singapore, 1991).

[78] F. Jaeger, J. Combin. Theory B **52**, 259 (1991).

[79] L.H. Kauffmann and H. Saleur, Commun. Math. Phys. **152**, 565 (1993).

[80] H.N.V. Temperley, in *Low-Dimensional Topology and Quantum Field Theory* (Cambridge, 1992), ed. H. Osborn, NATO Advanced Science Institutes Series B: Physics #315 (Plenum, New York, 1993), pp. 203–212.

[81] W.T. Tutte, J. Combin. Theory. B **57**, 269 (1993).

[82] D.M. Jackson, European J. Combin. **15**, 245 (1994).

[83] J.-M. Maillard, G. Rollet and F.Y. Wu, J. Phys. A **27**, 3373 (1994).

[84] J.-M. Maillard and G. Rollet, J. Phys. A **27**, 6963 (1994).

[85] J.-M. Maillard, Math. Comput. Modelling **26**, 169 (1997).

[86] J.L. Jacobsen and J. Salas, Transfer matrices and partition-function zeros for antiferromagnetic Potts models. II. Extended results for square-lattice chromatic polynomial, cond-mat/0011456.

[87] J.L. Jacobsen, J. Salas and A.D. Sokal, Transfer matrices and partition-function zeros for antiferromagnetic Potts models. III. Triangular-lattice chromatic polynomial, in preparation.

[88] J.L. Jacobsen, J. Salas and A.D. Sokal, Transfer matrices and partition-function zeros for antiferromagnetic Potts models. IV. Periodic boundary conditions in the longitudinal direction, work in progress.

[89] G.D. Birkhoff, Ann. Math. **14**, 42 (1912).

[90] H. Whitney, Bull. Amer. Math. Soc. **38**, 572 (1932).

[91] W.T. Tutte, Proc. Cambridge Philos. Soc. **43**, 26 (1947).

[92] W.T. Tutte, Canad. J. Math. **6**, 80 (1954).

[93] R.G. Edwards and A.D. Sokal, Phys. Rev. D **38**, 2009 (1988).

[94] R.C. Read, J. Combin. Theory **4**, 52 (1968).

[95] R.C. Read and W.T. Tutte, in *Selected Topics in Graph Theory 3*, ed. L.W. Beineke and R.J. Wilson (Academic Press, London, 1988).

[96] G.L. Chia, Discrete Math. **172**, 175 (1997).

[97] I. Stewart and D. Tall, *Algebraic Number Theory*, 2^{nd} ed. (Chapman and Hall, London–New York, 1987).

[98] P.M. Cohn, *Algebra*, 2^{nd} ed., vol. 2 (Wiley, Chichester, 1989).

[99] I. Stewart, *Galois Theory*, 2^{nd} ed. (Chapman and Hall, London–New York, 1989).

[100] B. Jackson, Combin. Probab. Comput. **2**, 325 (1993).

[101] G.D. Birkhoff and D.C. Lewis, Trans. Amer. Math. Soc. **60**, 355 (1946).

[102] D.R. Woodall, Discrete Math. **172**, 141 (1997).

[103] C. Thomassen, Combin. Probab. Comput. **6**, 497 (1997).

[104] D.R. Woodall, in *Combinatorial Surveys: Proceedings of the Sixth British Combinatorial Conference*, ed. P.J. Cameron (Academic Press, London, 1977).

[105] D.R. Woodall, Discrete Math. **101**, 327 (1992).

[106] D.R. Woodall, Discrete Math. **101**, 333 (1992).

[107] H.N.V. Temperley and E.H. Lieb, Proc. Roy. Soc. London A **322**, 251 (1971).

[108] E.H. Lieb and W.A. Beyer, Stud. Appl. Math. **48**, 77 (1969).

[109] N.L. Biggs, R.M. Damerell and D.A. Sands, J. Combin. Theory B **12**, 123 (1972).

[110] D.A. Sands, Dichromatic polynomials of linear graphs, Ph.D. thesis, University of London (1972).

[111] N.L. Biggs and G.H.J. Meredith, J. Combin. Theory B **20**, 5 (1976).

[112] B. Derrida and J. Vannimenus, J. Physique Lett. **41**, L-473 (1980).

[113] H.W.J. Blöte and M.P. Nightingale, Physica **129A**, 1 (1984).

[114] H.W.J. Blöte and B. Nienhuis, J. Phys. A **22**, 1415 (1989).

[115] J.L. Jacobsen and J. Cardy, Nucl. Phys. B **515**[FS], 701 (1998), cond-mat/9711279.

[116] V. Dotsenko, J.L. Jacobsen, M.-A. Lewis and M. Picco, Nucl. Phys. B **546**[FS], 505 (1999), cond-mat/9812227.

[117] R.P. Stanley, *Enumerative Combinatorics*, vol. 1 (Wadsworth & Brooks/Cole, Monterey, CA, 1986). Reprinted by Cambridge University Press, 1999.

[118] R.P. Stanley, *Enumerative Combinatorics*, vol. 2 (Cambridge University Press, Cambridge–New York, 1999).

[119] N.J.A. Sloane, Sloane's On-Line Encyclopedia of Integer Sequences, `http://www.research.att.com/~njas/sequences/index.html`

[120] N.G. De Bruijn, *Asymptotic Methods in Analysis*, 2^{nd} ed. (North-Holland, Amsterdam, 1961).

[121] V.N. Sachkov, *Combinatorial Methods in Discrete Mathematics*, Encyclopedia of Mathematics and its Applications #55 (Cambridge University Press, Cambridge, 1996).

[122] A.M. Odlyzko, in *Handbook of Combinatorics*, vol. 2, ed. R.L. Graham, M. Grötschel and L. Lovász (Elsevier/MIT Press, Amsterdam/Cambridge, 1995), pp. 1063–1229.

[123] R.M. Corless, G.H. Gonnet, D.E.G. Hare, D.J. Jeffrey and D.E. Knuth, Adv. Comput. Math. **5**, 329 (1996).

[124] R. Simion and D. Ullman, Discrete Math. **98**, 193 (1991).

[125] M. Klazar, Discrete Appl. Math. **82**, 263 (1998).

[126] R. Donaghey and L.W. Shapiro, J. Combin. Theory A **23**, 291 (1977).

[127] J. Riordan, J. Combin. Theory A **19**, 214 (1975).

[128] D. Gouyou-Beauchamps and G. Viennot, Adv. Appl. Math. **9**, 334 (1988).

[129] F.R. Bernhart, Discrete Math. **204**, 73 (1999).

[130] S. Lang, *Algebra*, 3^{rd} ed. (Addison-Wesley, Reading, Mass., 1993).

[131] D. Cox, J. Little and D. O'Shea, *Using Algebraic Geometry* (Springer-Verlag, New York, 1998).

[132] D.A. Bini and G. Fiorentino, Numerical computation of polynomial roots: MPSolve – Version 2.0. FRISCO report (1998). Available at `http://www.dm.unipi.it/pages/bini/public_html/papers/mpsolve.ps.Z`. Software package available at `http://www.dm.unipi.it/pages/bini/public_html/software/mps2.tar.gz`.

[133] D.A. Bini and G. Fiorentino, Numer. Algorithms **23**, 127 (2000).

[134] T. Kato, *Perturbation Theory for Linear Operators*, 2^{nd} ed., corrected printing (Springer-Verlag, Berlin–New York, 1980).

[135] C.G. Gibson, *Elementary Geometry of Algebraic Curves* (Cambridge University Press, Cambridge, 1998).

[136] V. Matveev and R. Shrock, J. Phys. A **28**, L533 (1995).

[137] E.J. Farrell, Discrete Math. **29**, 161 (1980).

[138] R.C. Read and G.F. Royle, in *Graph Theory, Combinatorics, and Applications* (Proceedings of the Sixth Quadrennial International Conference on the Theory and Applications of Graphs, Western Michigan University, 1988), Volume 2, ed. Y. Alavi *et al.* (Wiley, New York, 1991).

[139] A.V. Bakaev and V.I. Kabanovich, J. Phys. A **27**, 6731 (1994).

[140] B. Bollobas, *Modern Graph Theory* (Springer-Verlag, New York–Berlin–Heidelberg, 1998).

[141] K. Appel and W. Haken, Illinois J. Math. **21**, 429 (1977).

[142] K. Appel, W. Haken and J. Koch, Illinois J. Math. **21**, 491 (1977).

[143] K. Appel and W. Haken, *Every Planar Map is Four Colorable*, Contemporary Mathematics #98 (American Mathematical Society, Providence RI, 1989).

[144] N.Robertson, D.P. Sanders, P.D. Seymour and R.Thomas, J. Combin. Theory B **70**, 2 (1997).

[145] R. Thomas, Notices Amer. Math. Soc. **45**, 848 (1998).

n	B_n (exact)	B_n (num)	$p_n(q)$	Other $B_n^{(k)}$
2	0	0	q	
3	1	1	$q-1$	
4	2	2	$q-2$	
5	$(3+\sqrt{5})/2$	2.6180339887	q^2-3q+1	$(3-\sqrt{5})/2$
6	3	3	$q-3$	
7		3.2469796037	q^3-5q^2+6q-1	0.1980622642 1.5549581321
8	$2+\sqrt{2}$	3.4142135624	q^2-4q+2	$2-\sqrt{2}$
9		3.5320888862	q^3-6q^2+9q-1	0.1206147584 2.3472963553
10	$(5+\sqrt{5})/2$	3.6180339887	q^2-5q+5	$(5-\sqrt{5})/2$
11		3.6825070657	$q^5-9q^4+28q^3-35q^2+15q-1$	0.0810140528 0.6902785321 1.7153703235 2.8308300260
12	$2+\sqrt{3}$	3.7320508076	q^2-4q+1	$2-\sqrt{3}$
13		3.7709120513	$q^6-11q^5+45q^4-84q^3+70q^2$ $-21q+1$	0.0581163651 0.5029785037 1.2907902259 2.2410733605 3.1361294935
14		3.8019377358	$q^3-7q^2+14q-7$	0.7530203963 2.4450418679
15	$(9+\sqrt{5}+\sqrt{30-6\sqrt{5}})/4$	3.8270909153	$q^4-9q^3+26q^2-24q+1$	0.0437047985 1.7909430735 3.3382612127
16	$2+\sqrt{2+\sqrt{2}}$	3.8477590650	$q^4-8q^3+20q^2-16q+2$	0.1522409350 1.2346331353 2.7653668647

Table 1: Beraha numbers $B_n = 4\cos^2(\pi/n)$ and their minimal polynomials $p_n(q)$. For each n we give the exact expression of the Beraha number B_n whenever it can be expressed in terms of square roots alone; its numerical value to 10 decimal places; the unique irreducible monic polynomial $p_n(q)$ with integer coefficients having B_n as a root; and the other zeros of $p_n(q)$, which are the generalized Beraha numbers $B_n^{(k)} = 4\cos^2(k\pi/n)$ with k relatively prime to n.

m	$B(m)$	C_m	TriFree(m)	SqFree(m)	d_m	TriCyl(m)	SqCyl(m)
1	1	1	1	1	1	1	1
2	2	2	1	1	1	1	1
3	5	5	2	2	1	1	1
4	15	14	4	3	3	2	2
5	52	42	9	7	6	2	2
6	203	132	21	13	15	5	5
7	877	429	51	32	36	6	6
8	4140	1430	127	70	91	15	14
9	21147	4862	323	179	232	28	22
10	115975	16796	835	435	603	67	51
11	678570	58786	2188	1142	1585	145	95
12	4213597	208012	5798	2947	4213	368	232
13	27644437	742900	15511	7889	11298	870	499
14	190899322	2674440	41835	21051	30537	2211	1241

Table 2: Dimension of the transfer matrix. For each strip width m we give the number $B(m)$ of all partitions, the number C_m of non-crossing partitions, the number TriFree(m) = M_{m-1} of non-crossing non-nearest-neighbor partitions with free boundary conditions, and the number SqFree(m) of equivalence classes of non-crossing non-nearest-neighbor partitions modulo reflection in the center of the strip. We also give the number d_m ($= R_m$ for $m \geq 2$) of non-crossing non-nearest-neighbor partitions with periodic boundary conditions, the number TriCyl(m) of equivalence classes of such partitions modulo translations, and the number SqCyl(m) of equivalence classes of such partitions modulo translations and reflections.

Lattice	3rd Zero	4th Zero	5th Zero	6th Zero
$3_F \times 3_F$	1.646039212420			
$3_F \times 6_F$				
$3_F \times 9_F$	1.862295803794			
$3_F \times 12_F$				
$3_F \times 15_F$	1.910244567418			
$3_F \times 18_F$				
$3_F \times 21_F$	1.932253338339			
$3_F \times 24_F$				
$3_F \times 27_F$	1.945103511556			
$3_F \times 30_F$				
$4_F \times 4_F$				
$4_F \times 8_F$				
$4_F \times 12_F$	2.000607664038	2.183434328589		
$4_F \times 16_F$	2.000017521546	2.226186181588		
$4_F \times 20_F$	2.000000515361	2.248253640526		
$4_F \times 24_F$	2.000000015170	2.261494080470		
$4_F \times 28_F$	2.000000000447	2.270172437566		
$4_F \times 32_F$	2.000000000013	2.276213662199		
$4_F \times 36_F$	2.000000000000	2.280609243979		
$4_F \times 40_F$	2.000000000000	2.283918256290		
$4_F \times 100_F$	2.000000000000	2.236070288638	2.284202920228	2.297805980307
$5_F \times 5_F$	1.955073615801			
$5_F \times 10_F$	2.000022457863	2.243311545349		
$5_F \times 15_F$	1.999999994509			
$5_F \times 20_F$	2.000000000001	2.335823711578		
$5_F \times 25_F$	2.000000000000			
$5_F \times 30_F$	2.000000000000	2.365828458342		
$5_F \times 35_F$	2.000000000000			
$5_F \times 40_F$	2.000000000000	2.381070502769		
$5_F \times 45_F$	2.000000000000			
$5_F \times 50_F$	2.000000000000	2.390328275726		
$6_F \times 6_F$	2.001381451484	2.196830038914		
$6_F \times 12_F$	2.000000000760	2.390498998123		
$6_F \times 18_F$	2.000000000000	2.448434501424		
$6_F \times 24_F$	2.000000000000	2.475714120608		
$6_F \times 30_F$	2.000000000000	2.491245543049		
$6_F \times 36_F$	2.000000000000	2.501126630104		
$6_F \times 42_F$	2.000000000000	2.507892809644		
$6_F \times 48_F$	2.000000000000	2.512775536891		
$6_F \times 54_F$	2.000000000000	2.516440469487		
$6_F \times 60_F$	2.000000000000	2.519276871603		
$6_F \times 240_F$	2.000000000000	2.534921463459		
$7_F \times 7_F$	1.999994176430			
$7_F \times 14_F$	2.000000000000	2.451966225086		
$7_F \times 21_F$	2.000000000000			
$7_F \times 28_F$	2.000000000000	2.523291736983		
$7_F \times 35_F$	2.000000000000			
$7_F \times 42_F$	2.000000000000	2.548814353555		
$7_F \times 49_F$	2.000000000000			
$7_F \times 56_F$	2.000000000000	2.562226841180		
$7_F \times 63_F$	2.000000000000			
$7_F \times 70_F$	2.000000000000	2.570504933475		
$8_F \times 8_F$	2.000000005426	2.391719919086		
$8_F \times 16_F$	2.000000000000	2.531414423190		
$8_F \times 24_F$	2.000000000000	2.576747844784		
$8_F \times 32_F$	2.000000000000	2.597790566370		
$8_F \times 40_F$	2.000000000000	2.609001821476		
$8_F \times 48_F$	2.000000000000	2.614901253573		
$8_F \times 56_F$	2.000000000000	2.617322619879		
$8_F \times 64_F$	2.000000000000	2.617921204353		
$8_F \times 72_F$	2.000000000000	2.618018253506		
$8_F \times 80_F$	2.000000000000	2.618031848556		
Beraha	2	2.618033988750		

Table 3: Real zeros of the chromatic polynomials of finite square-lattice strips with free boundary conditions in both directions, to 12 decimal places. A blank means that the zero in question is absent. The first two real zeros $q = 0, 1$ are exact on all lattices. "Beraha" indicates the Beraha numbers $B_4 = 2$ and $B_5 = (3 + \sqrt{5})/2$.

Lattice	3rd Zero	4th Zero	5th Zero	6th Zero	7th Zero	8th Zero
$4_P \times 4_F$						
$4_P \times 8_F$	2.000937646653	2.233582851404				
$4_P \times 12_F$	2.000011295331	2.285151240169				
$4_P \times 16_F$	2.000000139385	2.307528225343				
$4_P \times 20_F$	2.000000001721	2.319813608989				
$4_P \times 24_F$	2.000000000021	2.327431319510				
$4_P \times 28_F$	2.000000000000	2.332533058471				
$4_P \times 32_F$	2.000000000000	2.336139224928				
$4_P \times 36_F$	2.000000000000	2.338792911735				
$4_P \times 40_F$	2.000000000000	2.340807853864				
$4_P \times 100_F$	2.000000000000	2.257013014819	2.270836682396	2.325455510831	2.341961199927	2.349426156978
$5_P \times 5_F$	2					
$5_P \times 10_F$	2	2.579692798743				
$5_P \times 15_F$	2					
$5_P \times 20_F$	2	2.615053742246				
$5_P \times 25_F$	2	2.618482995587	2.643045814623			
$5_P \times 30_F$	2	2.617994992234				
$5_P \times 35_F$	2	2.618037696771	2.658908973824			
$5_P \times 40_F$	2	2.618033639521				
$5_P \times 45_F$	2	2.618034021676	2.666710728680			
$5_P \times 50_F$	2	2.618033985646				
$6_P \times 6_F$	2.000004484676	2.407498857052				
$6_P \times 12_F$	2.000000000000	2.516516196247				
$6_P \times 18_F$	2.000000000000	2.551495362906				
$6_P \times 24_F$	2.000000000000	2.568645710453				
$6_P \times 30_F$	2.000000000000	2.578747609077				
$6_P \times 36_F$	2.000000000000	2.585363032613				
$6_P \times 42_F$	2.000000000000	2.590008147965				
$6_P \times 48_F$	2.000000000000	2.593435585192				
$6_P \times 54_F$	2.000000000000	2.596060266523				
$6_P \times 60_F$	2.000000000000	2.598129161537				
$6_P \times 240_F$	2.000000000000	2.610780621890				
$7_P \times 7_F$	2					
$7_P \times 14_F$	2	2.617937723253				
$7_P \times 21_F$	2	2.618034017737	2.721810707015			
$7_P \times 28_F$	2	2.618033988741				
$7_P \times 35_F$	2	2.618033988750	2.748882762812			
$7_P \times 42_F$	2	2.618033988750				
$7_P \times 49_F$	2	2.618033988750	2.760230036513			
$7_P \times 56_F$	2	2.618033988750				
$7_P \times 63_F$	2	2.618033988750	2.766499503035			
$7_P \times 70_F$	2	2.618033988750				
$8_P \times 8_F$	2.000000000001	2.551072878420				
$8_P \times 16_F$	2.000000000000	2.616714700486				
$8_P \times 24_F$	2.000000000000	2.618032009068				
$8_P \times 32_F$	2.000000000000	2.618033986108				
$8_P \times 40_F$	2.000000000000	2.618033988746				
$8_P \times 48_F$	2.000000000000	2.618033988750				
$8_P \times 56_F$	2.000000000000	2.618033988750				
$8_P \times 64_F$	2.000000000000	2.618033988750				
$8_P \times 72_F$	2.000000000000	2.618033988750				
$8_P \times 80_F$	2.000000000000	2.618033988750				
Beraha	2	2.618033988750				

Table 4: Real zeros of the chromatic polynomials of finite square-lattice strips with periodic boundary conditions in the transverse direction and free boundary conditions in the longitudinal direction, to 12 decimal places. A blank means that the zero in question is absent. The first two real zeros $q = 0, 1$ are exact on all lattices; the third real zero $q = 2$ is exact on all lattices of odd width. "Beraha" indicates the Beraha numbers $B_4 = 2$ and $B_5 = (3 + \sqrt{5})/2$.

	Eigenvalue-Crossing Curves $\mathcal{B}$								Isolated Points	
Lattice	# C	# E	# T	# D	# ER	$\min \mathrm{Re}\, q$	q_0	$\max \mathrm{Re}\, q$	# RI	# CI
2_F	0	0	0	0	0				2	0
3_F	3	6	0	0	0	0.586570	2	2.5	2	0
4_F	3	10	2	1	0	0.325474	$[2.228359, 2.301416]$	2.667426	3	0
5_F	5	14	4	0	0	0.170897	2.428438	2.769205	3	0
6_F	5	14	6	1	2	0.063142	$[2.528647, 2.537098]$	2.837338	3	2
7_F	$7^\dagger$	$14^\dagger$	$4^\dagger$	$0^\dagger$	$2^\dagger$	-0.044443	2.606248	2.886041	$3^\dagger$	$2^\dagger$
8_F	$6^\dagger$	$14^\dagger$	$2^\dagger$	$0^\dagger$	$0^\dagger$	-0.130642	$2.660260 \pm 0.001257\, i^*$	2.921658	$4^\dagger$	$2^\dagger$
3_P	0	0	0	0	0				3	0
4_P	3	8	0	1	0	0.709803	$[2.253370, 2.351688]$	2.995331	3	0
5_P	5	10	0	0	0	0.165021	2.691684	2.691684	4	0
6_P	3	10	2	1	0	-0.131889	$[2.608943, 2.613228]$	3.171192	3	1
7_P	7	16	2	0	0	-0.296250	2.788378	2.839016	4	1
8_P	6	16	4	0	0	-0.390864	$2.751531 \pm 0.002531\, i^*$	3.211132	4	2

Table 5: Summary of qualitative results for the eigenvalue-crossing curves $\mathcal{B}$ and for the isolated limiting points of zeros. For each square-lattice strip considered in this paper, we give the number of connected components of $\mathcal{B}$ (# C), the number of endpoints (# E), the number of T points (# T), the number of double points (# D), and the number of enclosed regions (# ER); we give the minimum value of $\mathrm{Re}\, q$ on $\mathcal{B}$, the value(s) q_0 where $\mathcal{B}$ intersects the real axis (* denotes an almost-crossing), and the maximum value of $\mathrm{Re}\, q$ on $\mathcal{B}$. We also report the number of real isolated limiting points of zeros (# RI) [which are always successive Beraha numbers B_2, B_3, ...] and the number of complex-conjugate pairs of isolated limiting points (# CI). The symbol † indicates uncertain results.

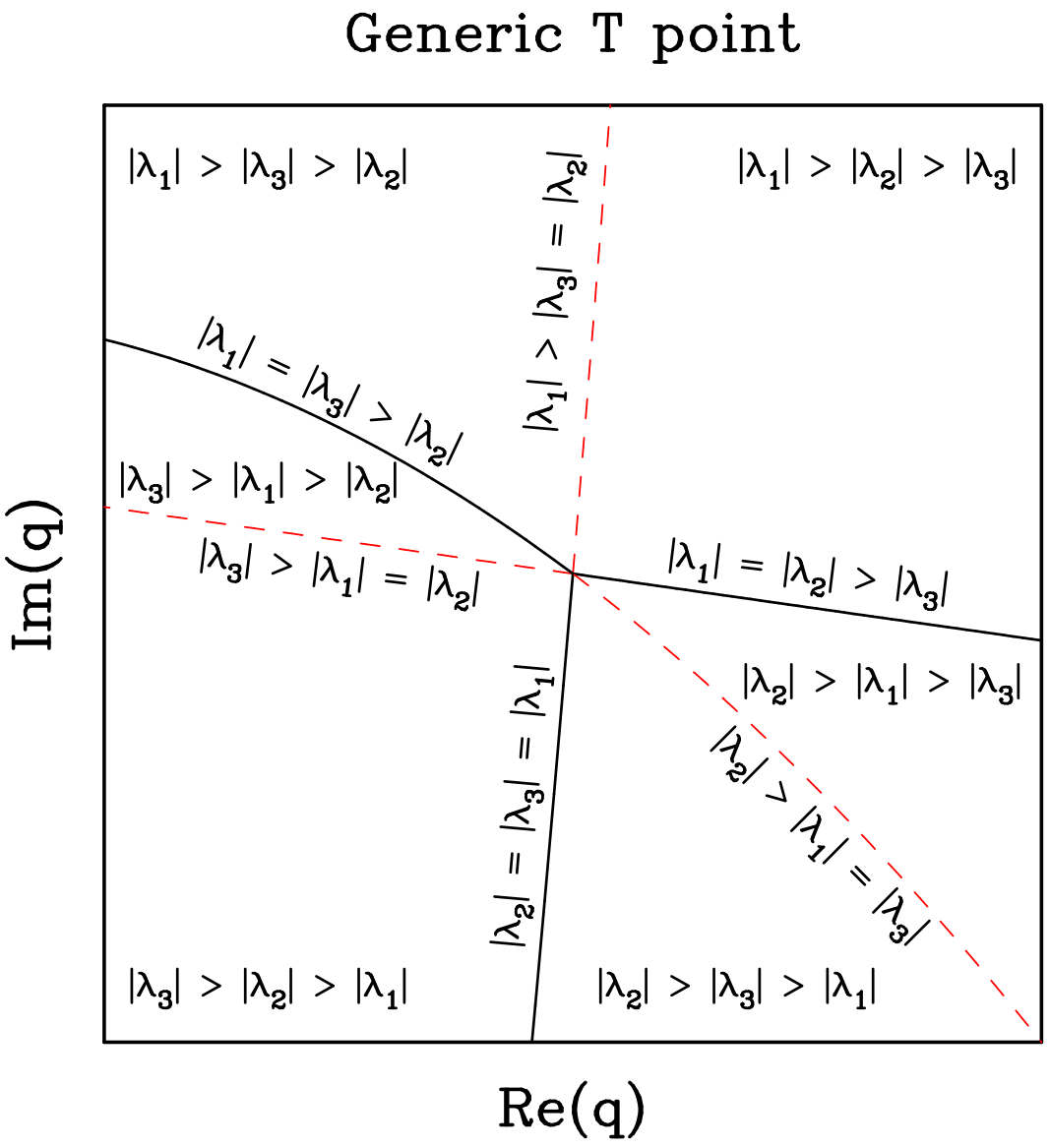

Figure 1: Schematic representation of a generic T point where three eigenvalues $\lambda_1, \lambda_2, \lambda_3$ are simultaneously dominant. The solid black lines represent the loci of dominant eigenvalue crossings, while the dashed red lines represent the loci of subdominant eigenvalue crossings. Each line has been labeled by the inequalities and equalities it satisfies, and each region has been labeled by the inequalities it satisfies.

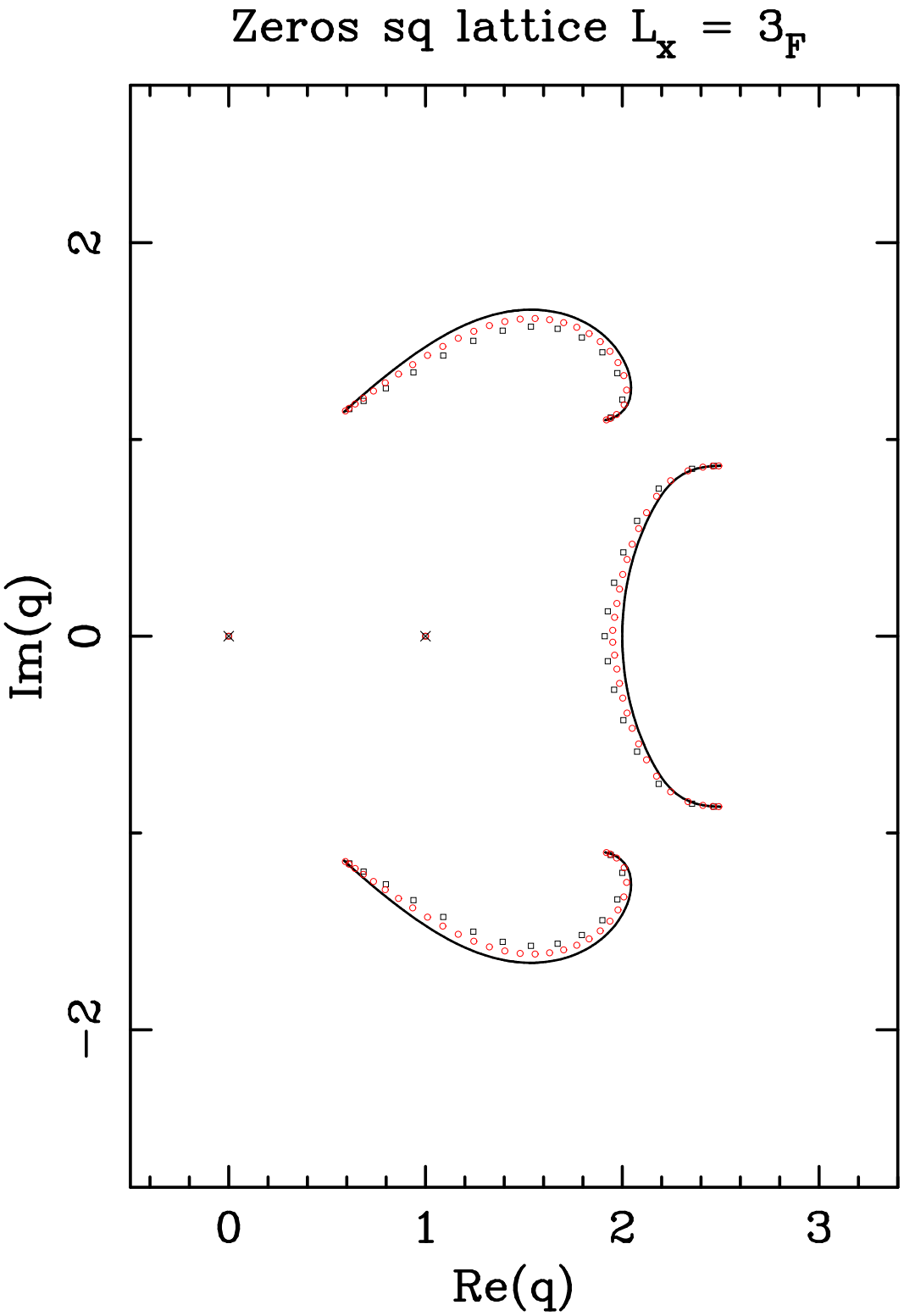

Figure 2: Zeros of the partition function of the q-state Potts antiferromagnet on the square lattices $3_F \times 15_F$ (squares), $3_F \times 30_F$ (circles) and $3_F \times \infty_F$ (solid line). The isolated limiting zeros are depicted by a $\times$. The limiting curve was computed using the resultant method.

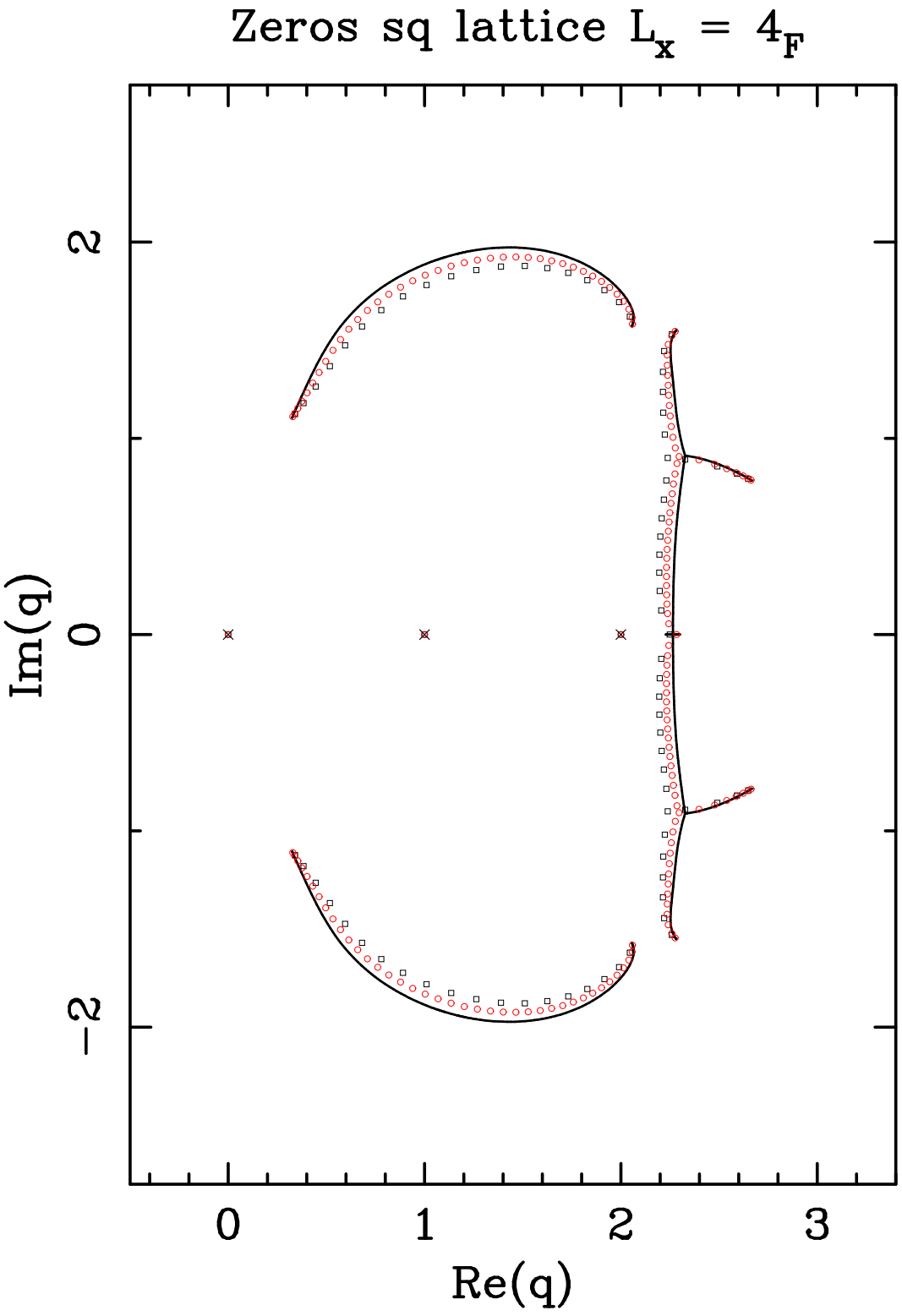

Figure 3: Zeros of the partition function of the q-state Potts antiferromagnet on a square lattices $4_F \times 20_F$ (squares), $4_F \times 40_F$ (circles) and $4_F \times \infty_F$ (solid line). The isolated limiting zeros are depicted by a $\times$. The limiting curve was computed using the resultant method.

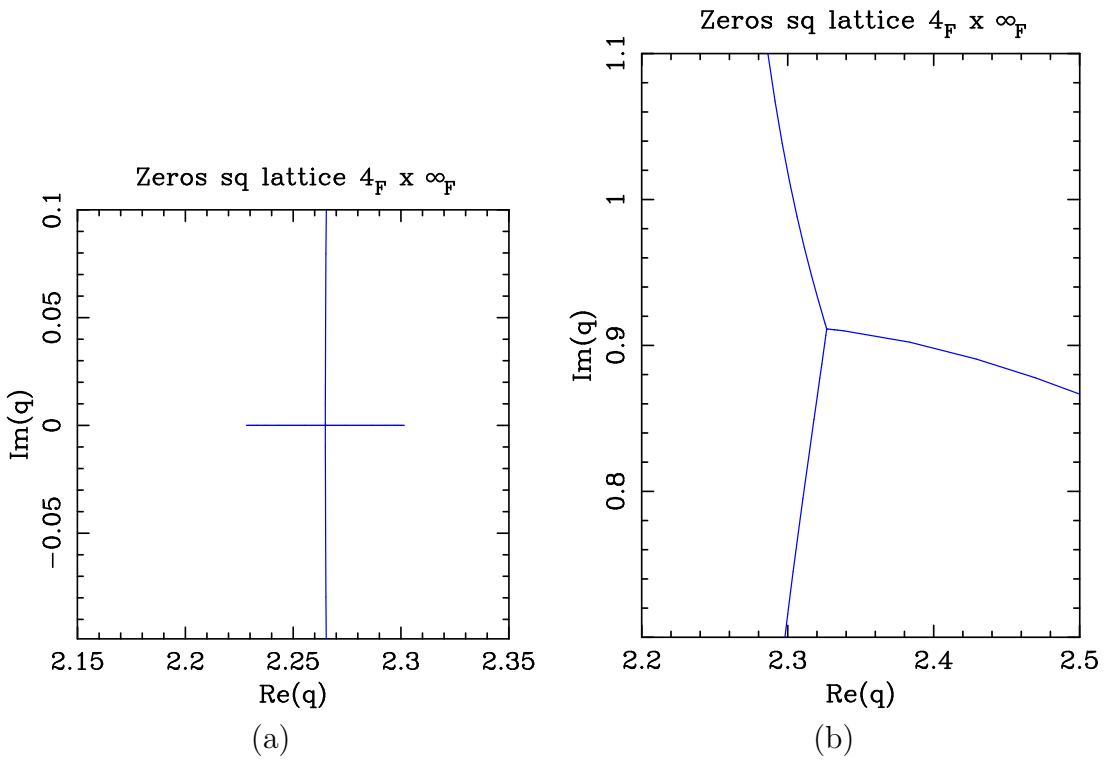

Figure 4: Detail of the limiting curves $\mathcal{B}$ for the q-state Potts antiferromagnet on a square lattice $4_F \times \infty_F$. (a) Region near the double point $q \approx 2.2649418565$. The value of t is continuous around the double point, with $t \approx 0.0621$. (b) Region near the T point $q \approx 2.327 + 0.9113\,i$. At this T point we have $t \approx (1.818, 12.962, 0.655)$ and hence $\theta \approx (2.136, 2.988, 1.160)$, so that $\sum \theta = 2\pi$.

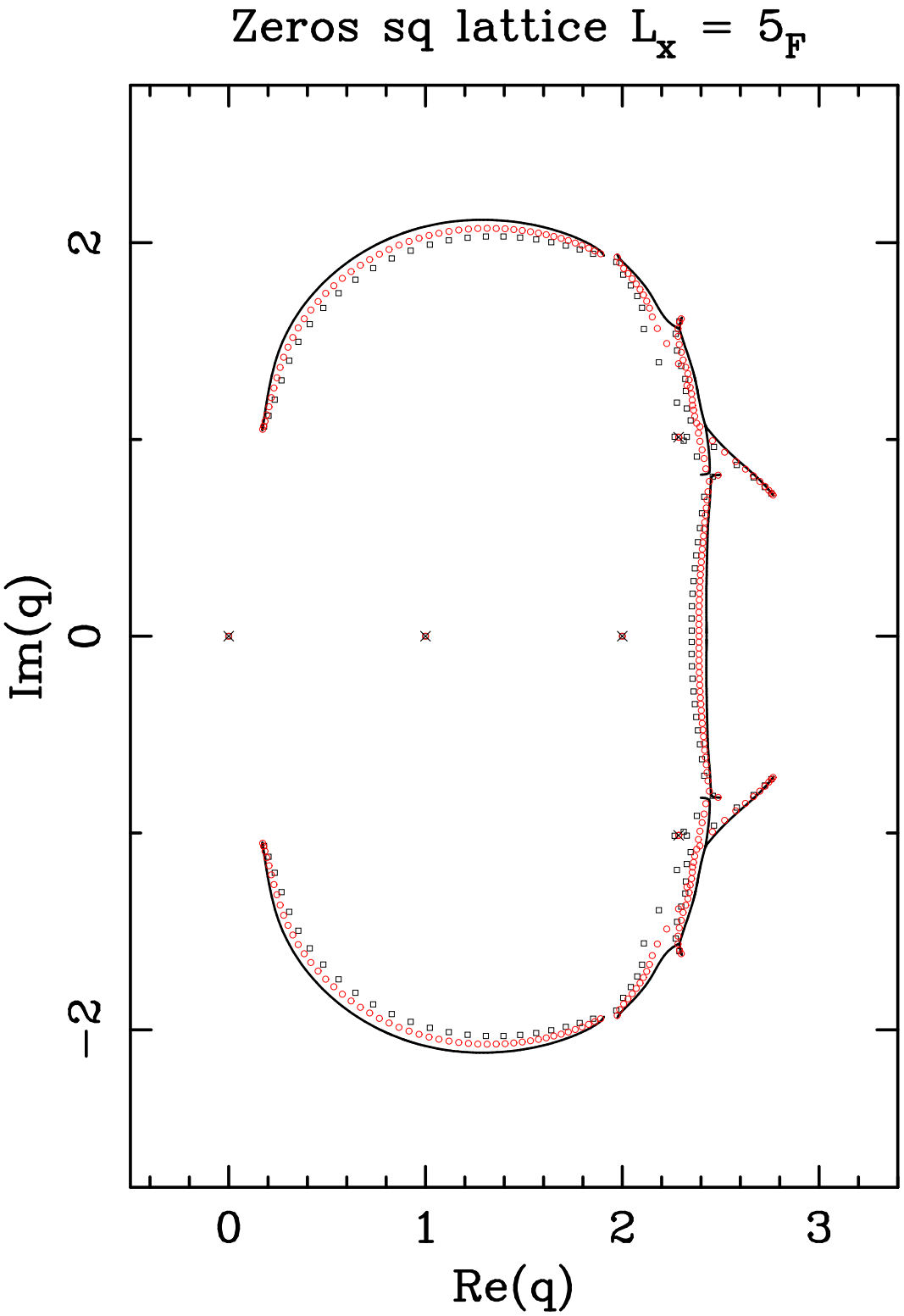

Figure 5: Zeros of the partition function of the q-state Potts antiferromagnet on a square lattices $5_F \times 25_F$ (squares), $5_F \times 50_F$ (circles) and $5_F \times \infty_F$ (solid line). The isolated limiting zeros are depicted by a $\times$. The limiting curve was computed using the resultant method.

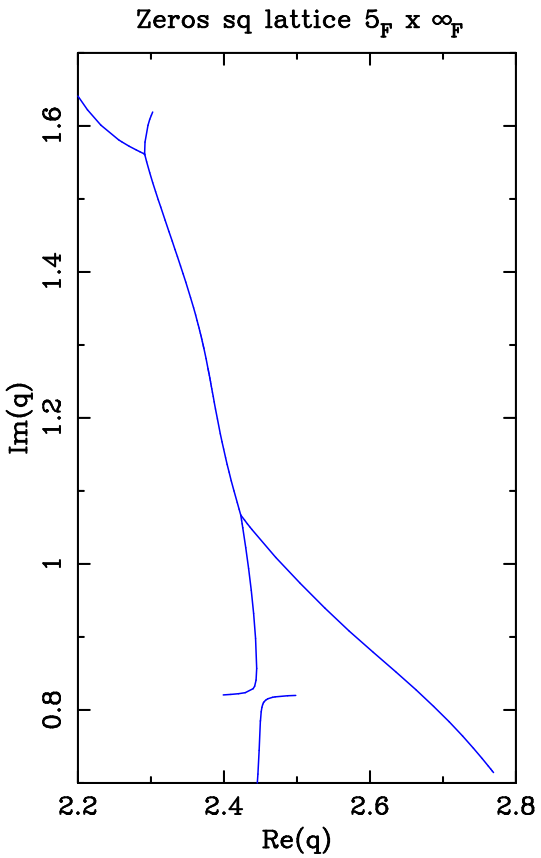

Figure 6: Detail of the limiting curves $\mathcal{B}$ for the q-state Potts antiferromagnet on a square lattice $5_F \times \infty_F$. Region near the T points of the limiting curve. On the upper T point $q \approx 2.291 + 1.561\,i$, we have $t \approx (0.999, 0.179, 1.434)$, corresponding to $\theta \approx (1.569, 0.354, 1.924)$. On the lower T point $q \approx 2.423 + 0.1067\,i$, we have $t \approx (1.823, 0.434, 0.774)$ with $\theta \approx (2.138, 0.820, 1.318)$.

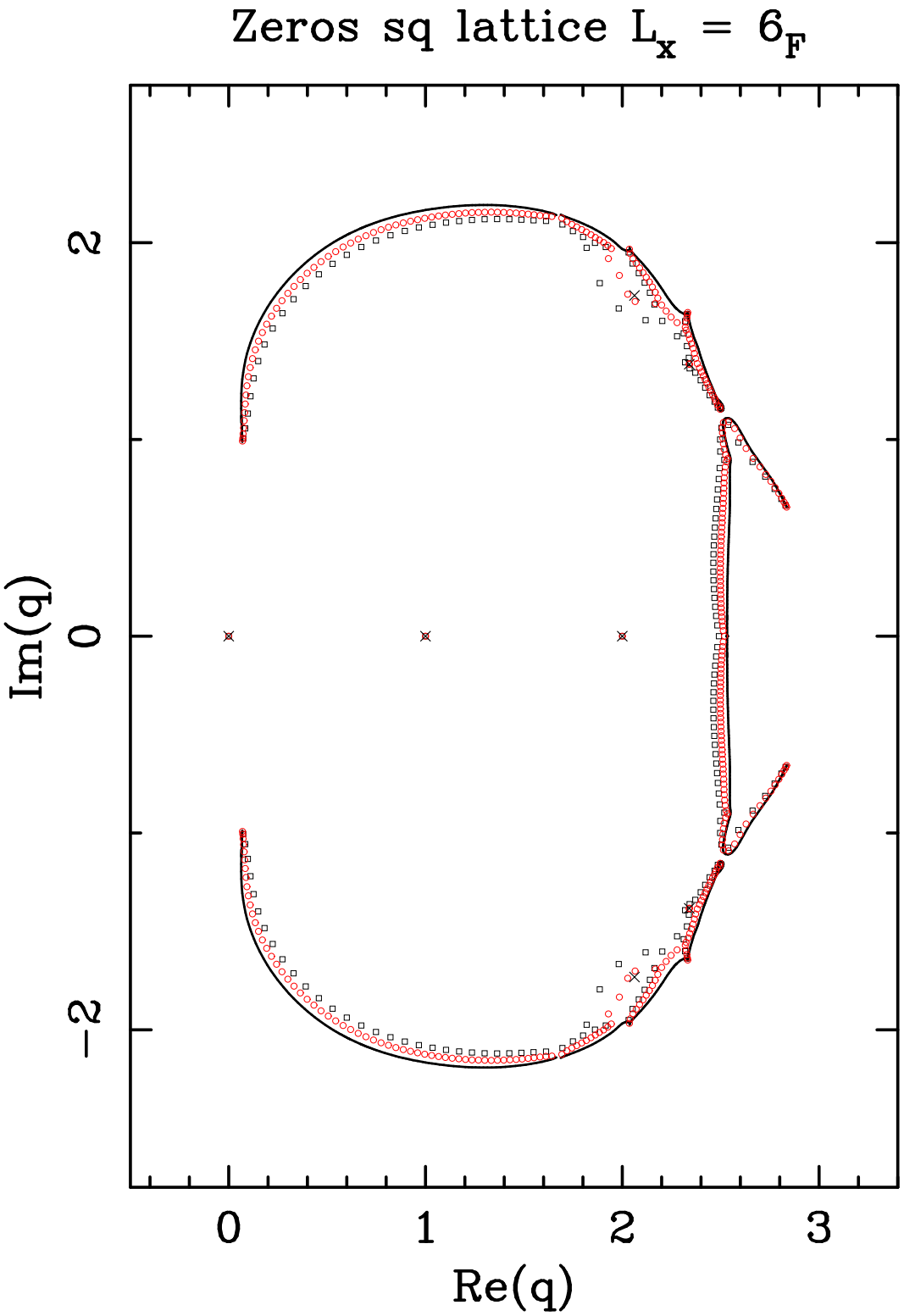

Figure 7: Zeros of the partition function of the q-state Potts antiferromagnet on a square lattices $6_F \times 30_F$ (squares), $6_F \times 60_F$ (circles) and $6_F \times \infty_F$ (solid line). The isolated limiting zeros are depicted by a $\times$. The limiting curve was computed using the resultant method.

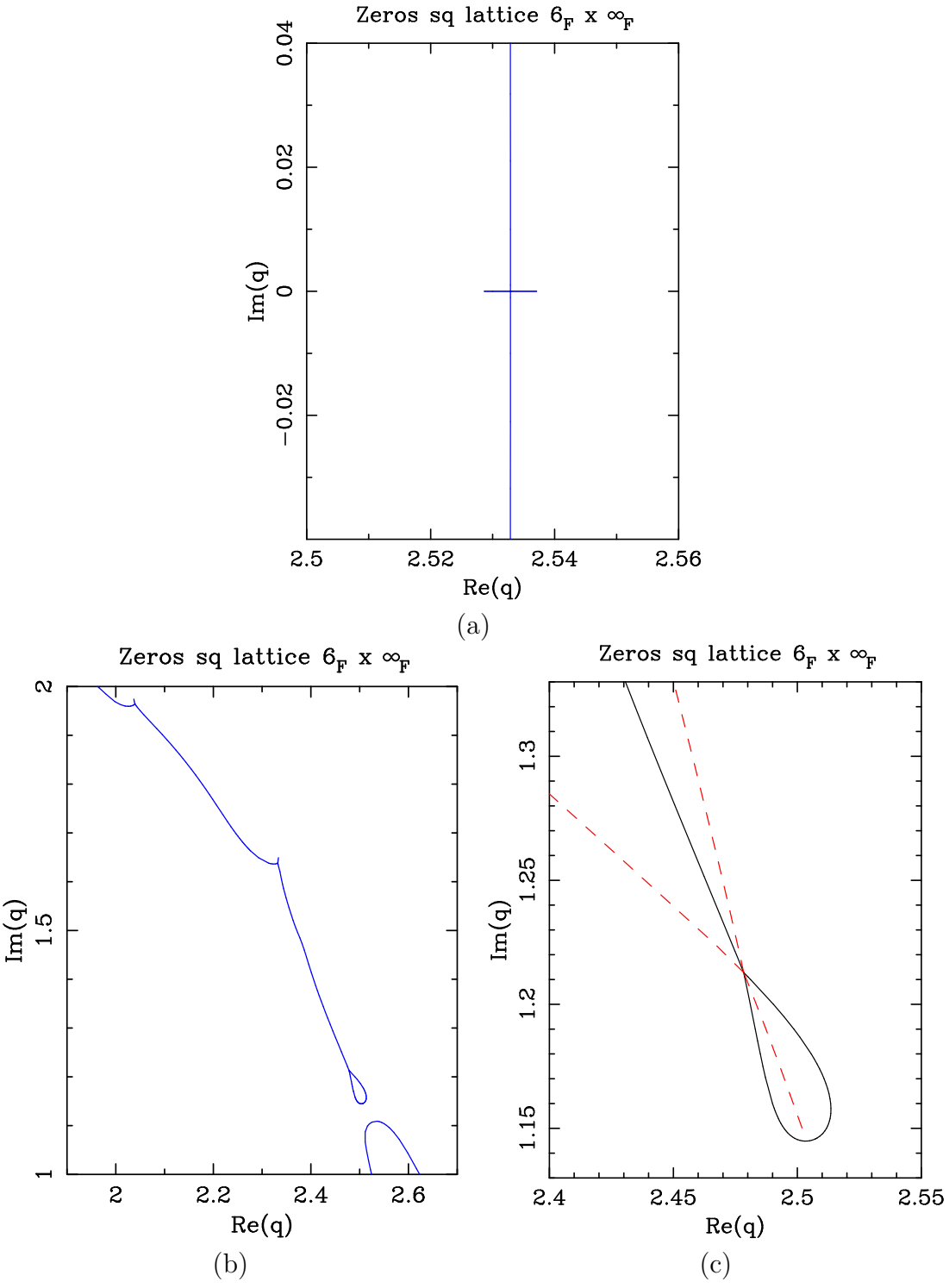

Figure 8: Detail of the limiting curves $\mathcal{B}$ for the q-state Potts antiferromagnet on a square lattice $6_F \times \infty_F$. (a) Region around the double point at $q \approx 2.53287$. The value of t is continuous around this double point, with $t \approx 0.00985$. (b) Region containing the three T points. On the upper T point $q \approx 2.039 + 1.964\,i$, we have $t \approx (0.871, 0.0521, 0.970)$ with $\theta \approx (1.434, 0.104, 1.540)$; on the middle T point $q \approx 2.332 + 1.638\,i$, we have $t \approx (18.021, 0.0843, 7.119)$ and $\theta \approx (3.031, 0.168, 2.863)$; on the lower T point $q \approx 2.478 + 1.213\,i$, we have $t \approx (0.272, 0.618, 1.069)$ and $\theta \approx (0.532, 1.107, 1.638)$. (c) Detail of the bulb-like region around $q \approx 2.478 + 1.213\,i$. Dominant crossing curves are depicted in solid black lines, while subdominant crossing curves are shown with dashed red lines.

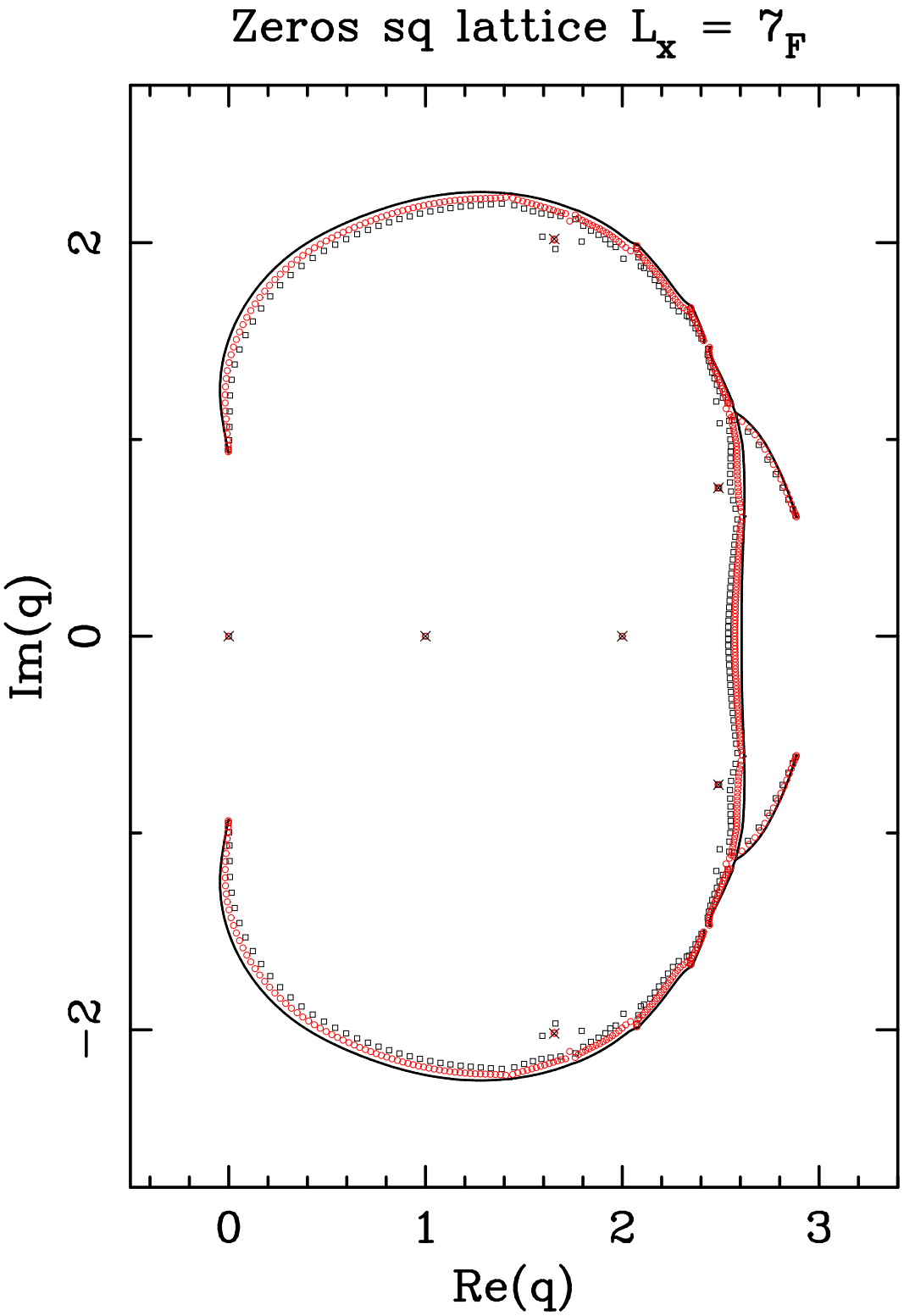

Figure 9: Zeros of the partition function of the q-state Potts antiferromagnet on a square lattices $7_F \times 35_F$ (squares), $7_F \times 70_F$ (circles) and $7_F \times \infty_F$ (solid line). The isolated limiting zeros are depicted by a $\times$. The limiting curve was computed using the direct-search method.

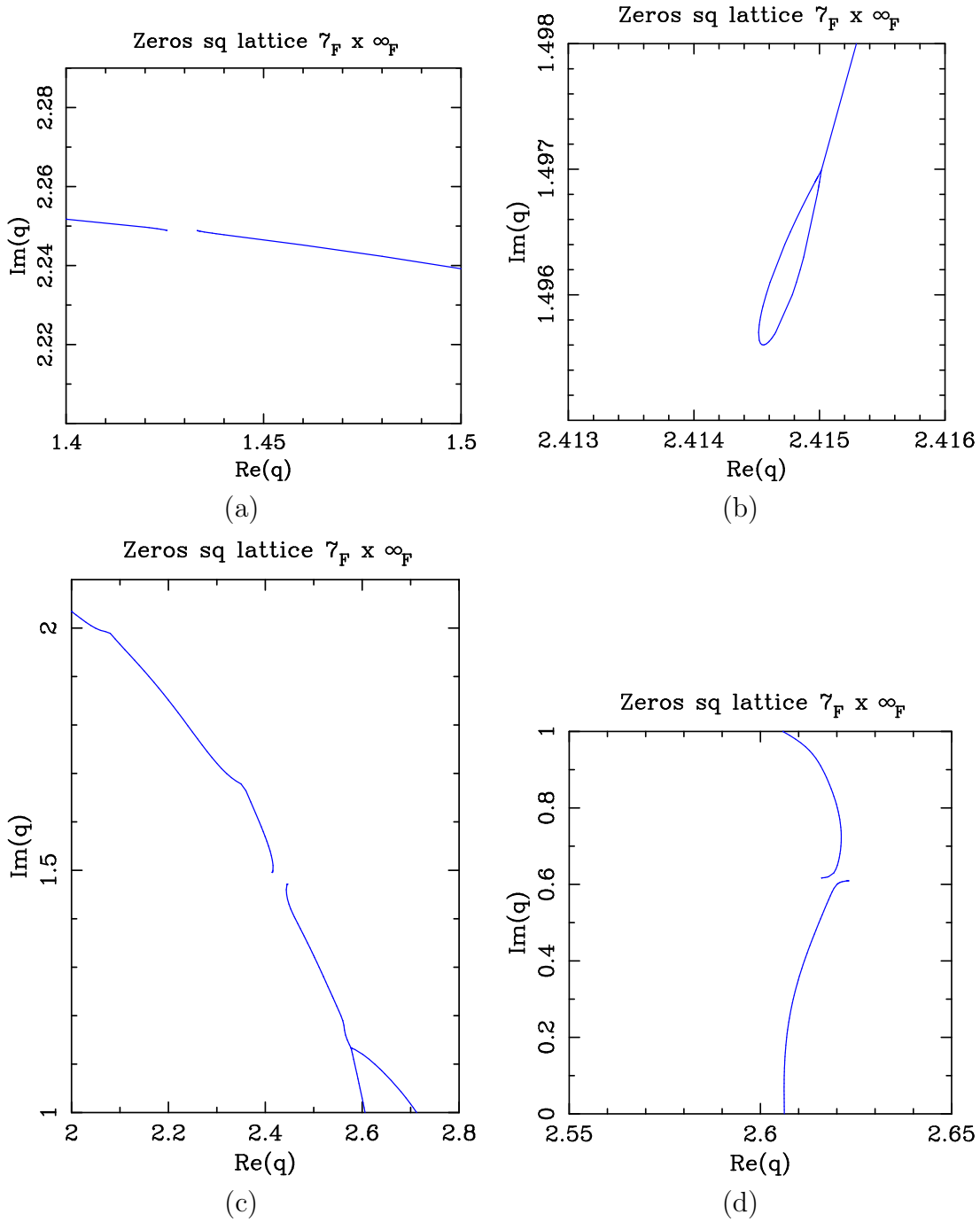

Figure 10: Detail of the limiting curves $\mathcal{B}$ for the q-state Potts antiferromagnet on a square lattice $7_F \times \infty_F$. (a) Region around the gap between $q \approx 1.425603 + 2.248902\,i$ and $q \approx 1.433184 + 2.248834\,i$. (b) Bulb-like region around the T point $q \approx 2.415 + 1.497\,i$. At this point we have $t \approx (0.023, 1.248, 1.310)$ and $\theta \approx (0.047, 1.791, 1.838)$. (c) Region around the gap between the bulb-like region at $q \approx 2.415 + 1.497\,i$ and the endpoint at $q \approx 2.445207 \pm 1.471332\,i$. There is also a T point at $q \approx 2.577 + 1.133\,i$, where $t \approx (2.108, 2.737, 1.016)$ and $\theta \approx (2.257, 2.441, 1.586)$. (d) Region around the gap between $q \approx 2.616006 + 0.616910\,i$ and $q \approx 2.622974 + 0.609548\,i$.

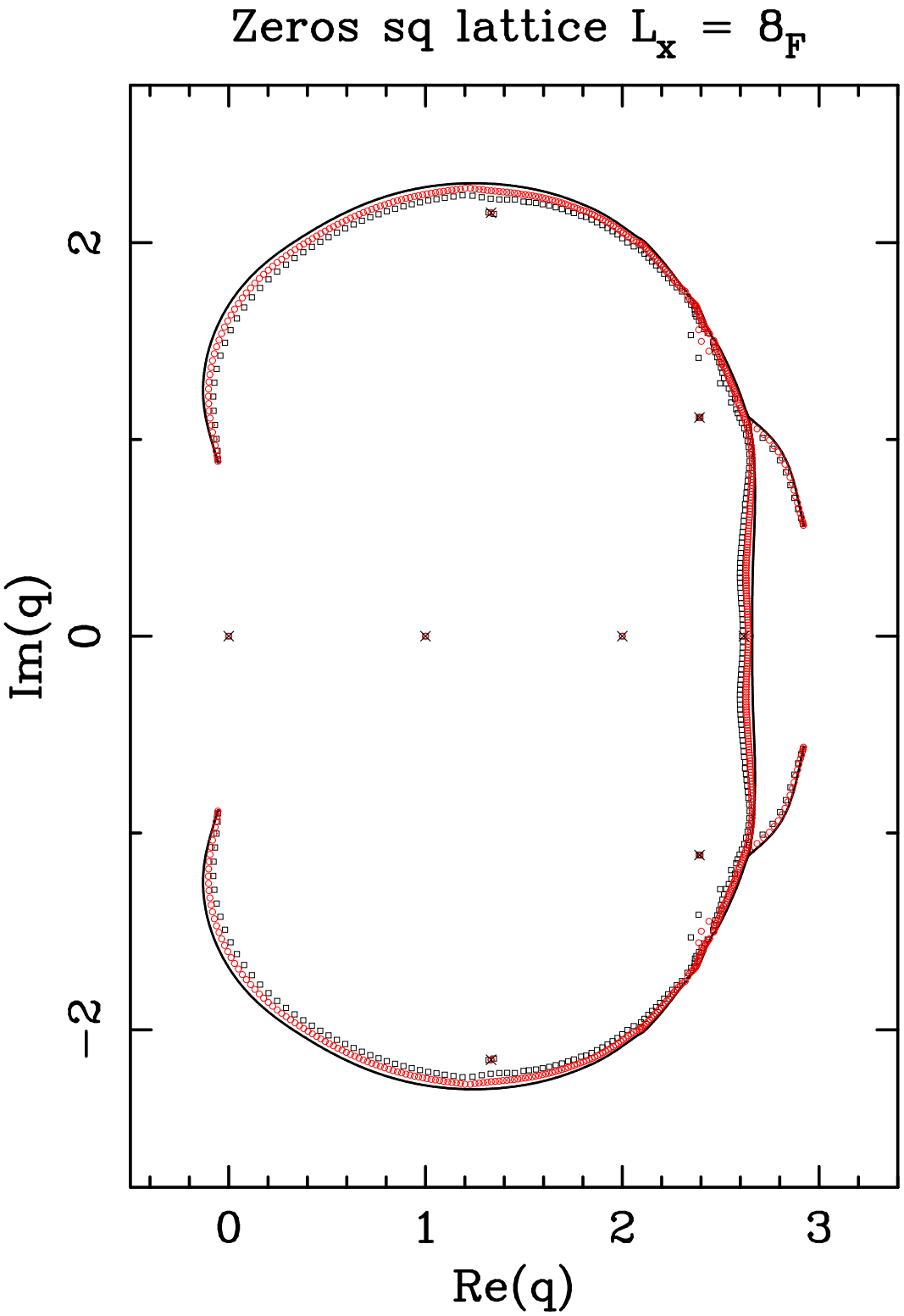

Figure 11: Zeros of the partition function of the q-state Potts antiferromagnet on a square lattices $8_F \times 40_F$ (squares), $8_F \times 80_F$ (circles) and $8_F \times \infty_F$ (solid line). The isolated limiting zeros are depicted by a $\times$. The limiting curve was computed using the direct-search method.

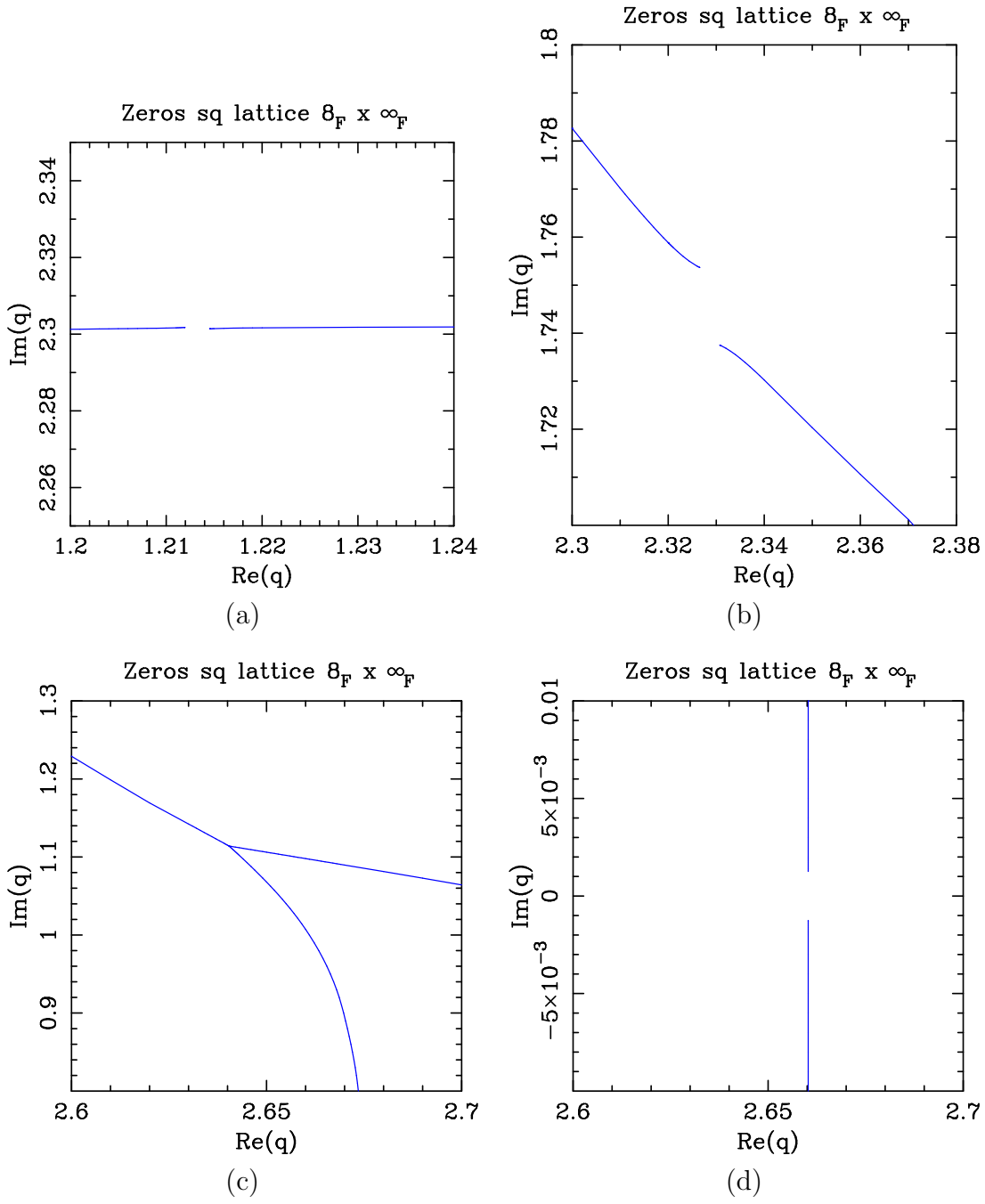

Figure 12: Detail of the limiting curves $\mathcal{B}$ for the q-state Potts antiferromagnet on a square lattice $8_F \times \infty_F$. (a) Region around the small gap at $q \approx 1.21 + 2.30\,i$. (b) Region around the gap at $q \approx 2.32 + 1.75\,i$. (c) Region around the T point at $q \approx 2.640 + 1.114\,i$. At this point we have $t \approx (0.993, 1.013, 0.0113)$ and $\theta \approx (1.563, 1.584, 0.023)$. (d) Region around the tiny gap at $q \approx 2.660260$.

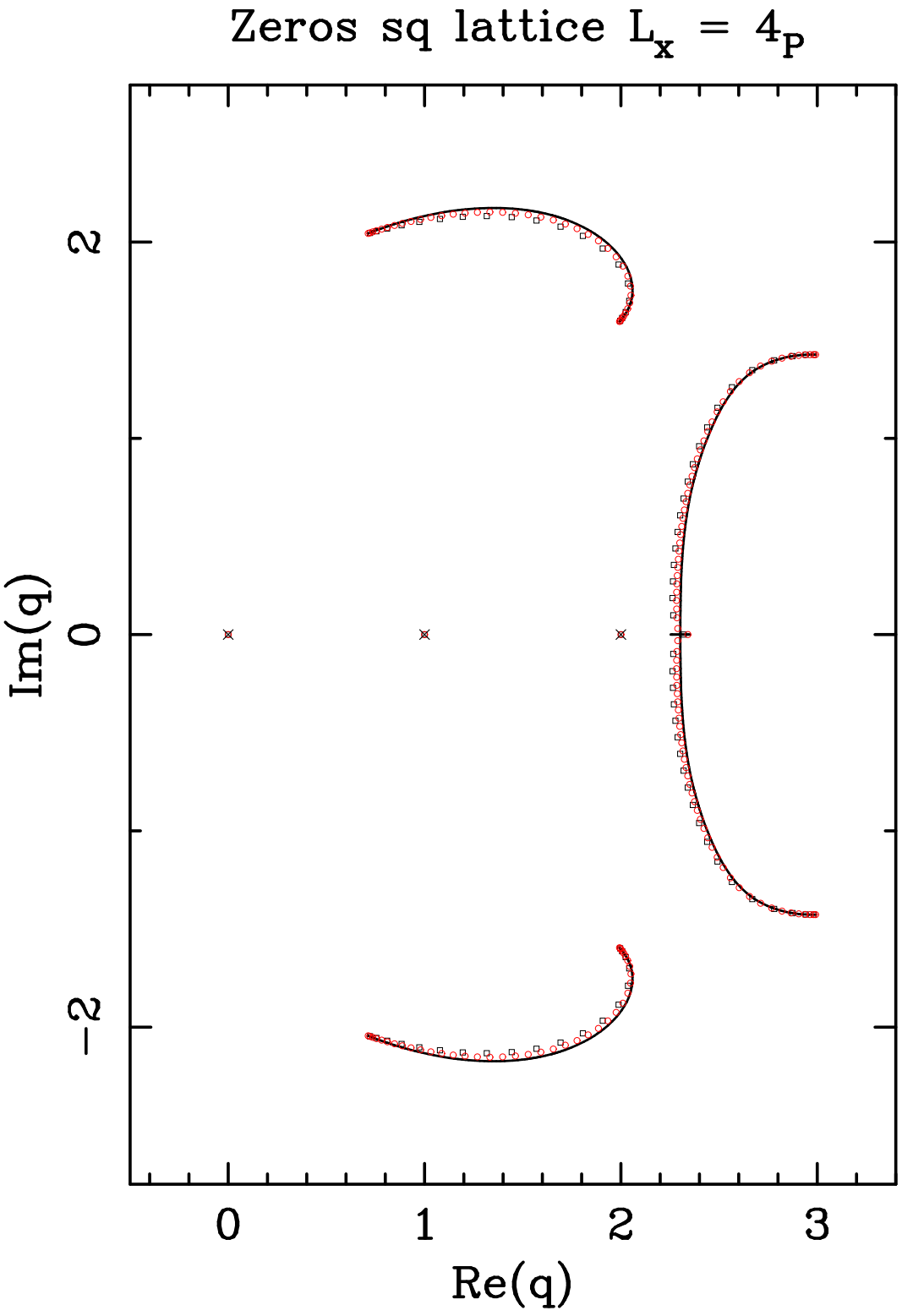

Figure 13: Zeros of the partition function of the q-state Potts antiferromagnet on a square lattices $4_P \times 20_F$ (squares), $4_P \times 40_F$ (circles) and $4_P \times \infty_F$ (solid line). The isolated limiting zeros are depicted by a $\times$. The limiting curve was computed using the resultant method.

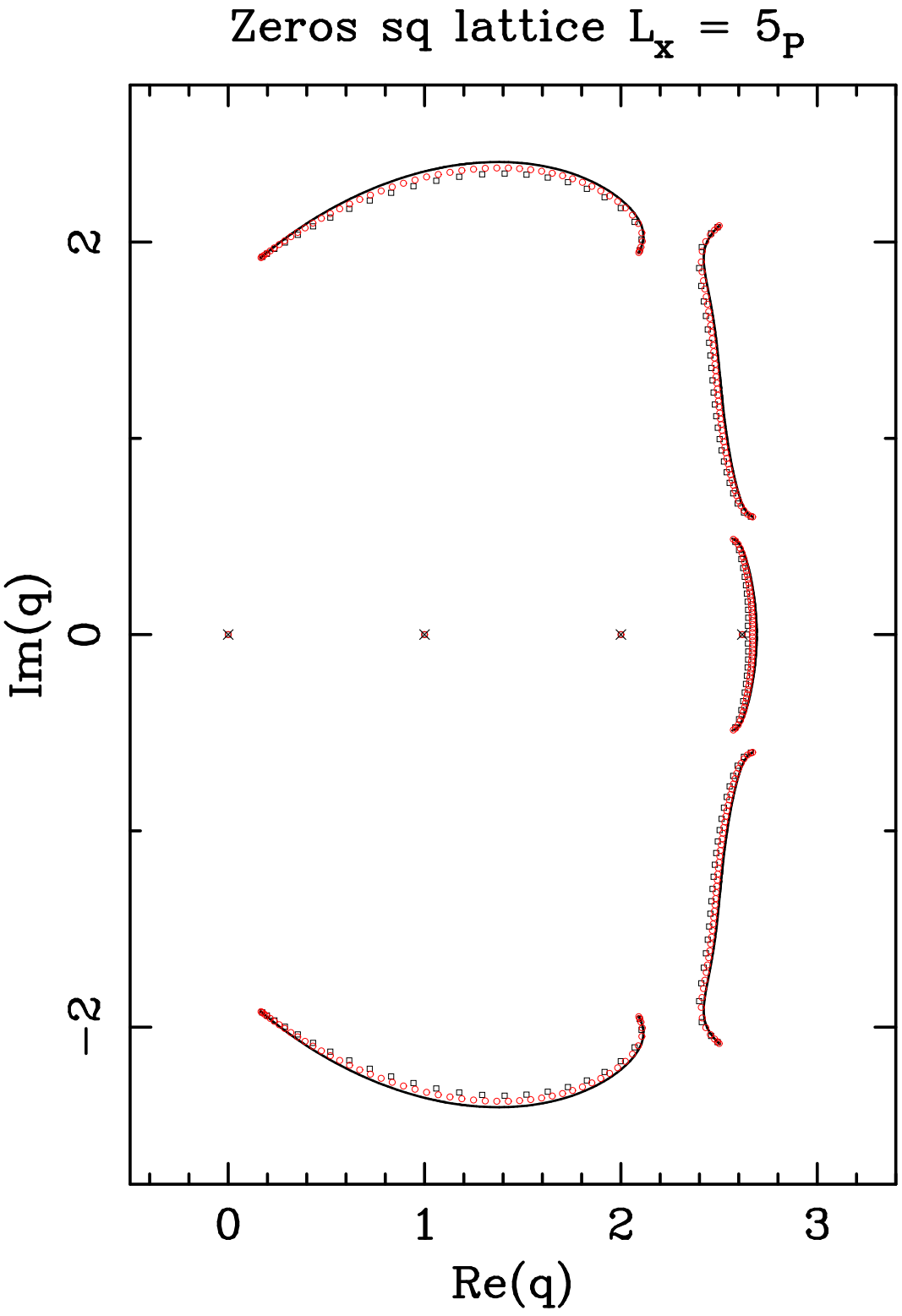

Figure 14: Zeros of the partition function of the q-state Potts antiferromagnet on a square lattices $5_P \times 25_F$ (squares), $5_P \times 50_F$ (circles) and $5_P \times \infty_F$ (solid line). The isolated limiting zeros are depicted by a $\times$. The limiting curve was computed using the resultant method.

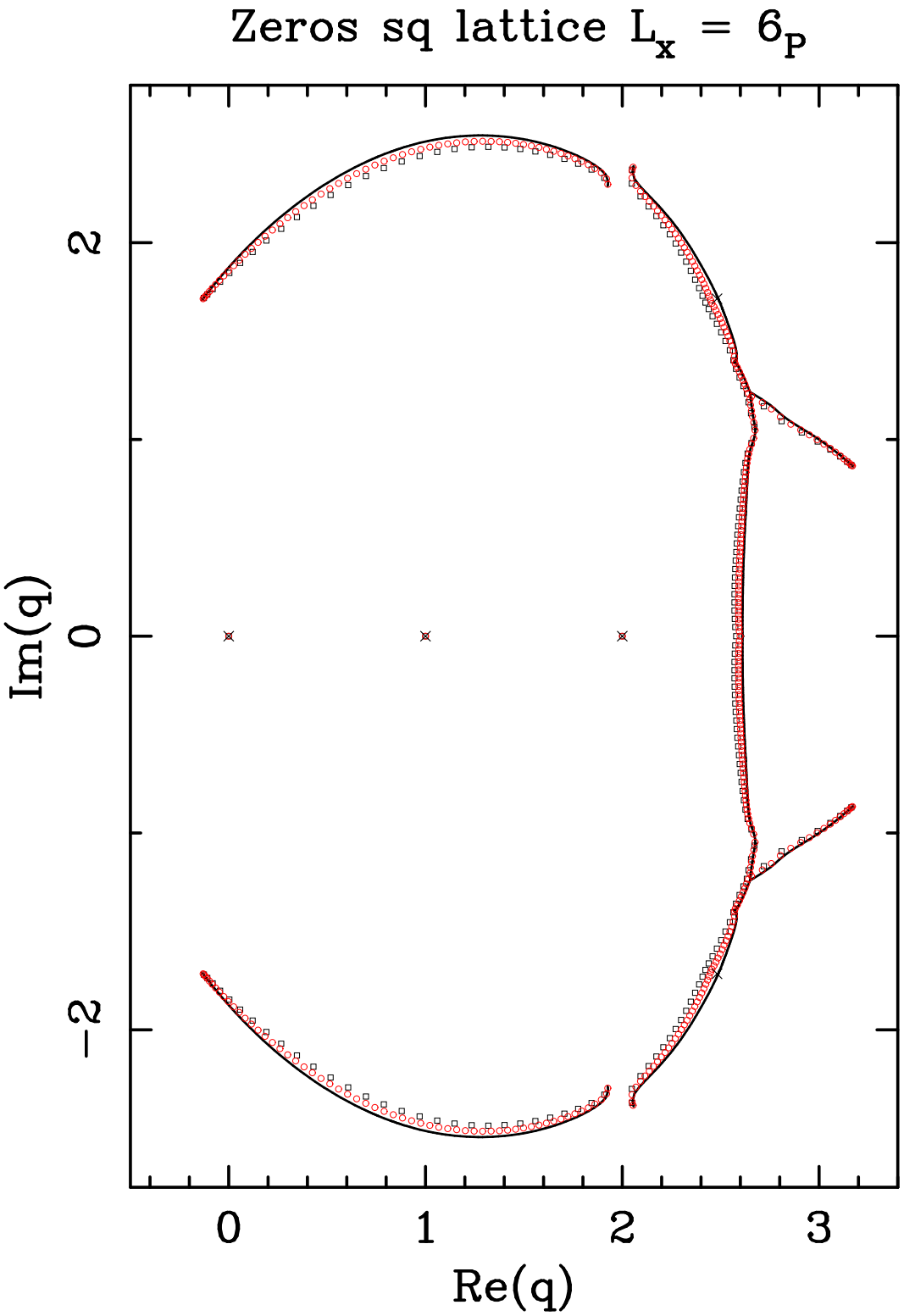

Figure 15: Zeros of the partition function of the q-state Potts antiferromagnet on a square lattices $6_P \times 30_F$ (squares), $6_P \times 60_F$ (circles) and $6_P \times \infty_F$ (solid line). The isolated limiting zeros are depicted by a $\times$. The limiting curve was computed using the resultant method.

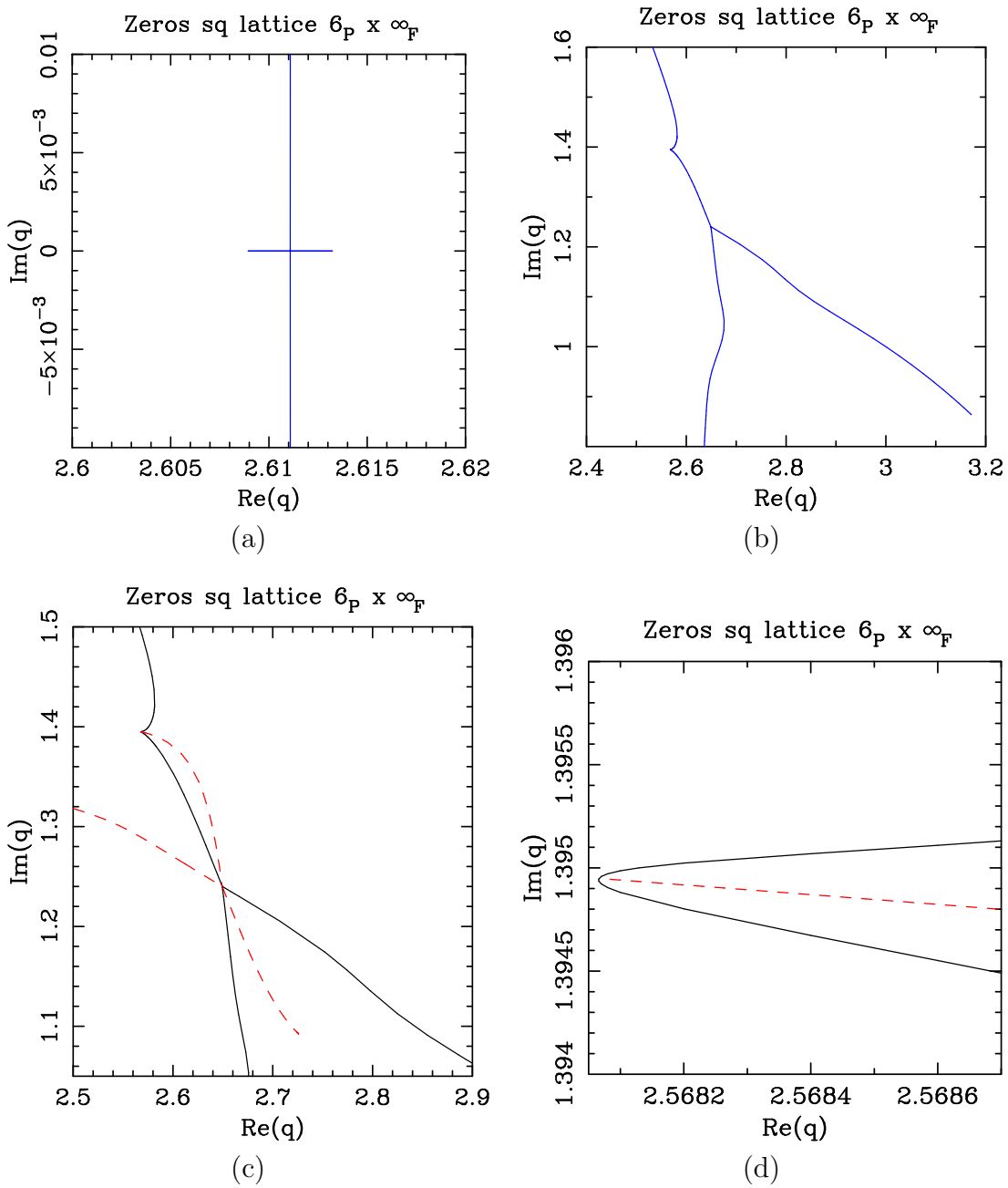

Figure 16: Detail of the limiting curves $\mathcal{B}$ for the q-state Potts antiferromagnet on a square lattice $6_P \times \infty_F$. (a) Region around the double point $q \approx 2.6110857$. At this double point we have $t \approx 0.0053$. (b) Region around the T point at $q \approx 2.650 + 1.240\,i$. At this T point we have $t \approx (0.392, 1.224, 0.562)$ and $\theta \approx (0.748, 1.771, 1.024)$. (c) The same as in (b), but we show the dominant (solid black line) and subdominant (dashed red line) crossing curves. (d) Blow-up of region around the quasi-cusp at $q \approx 2.568 + 1.398\,i$.

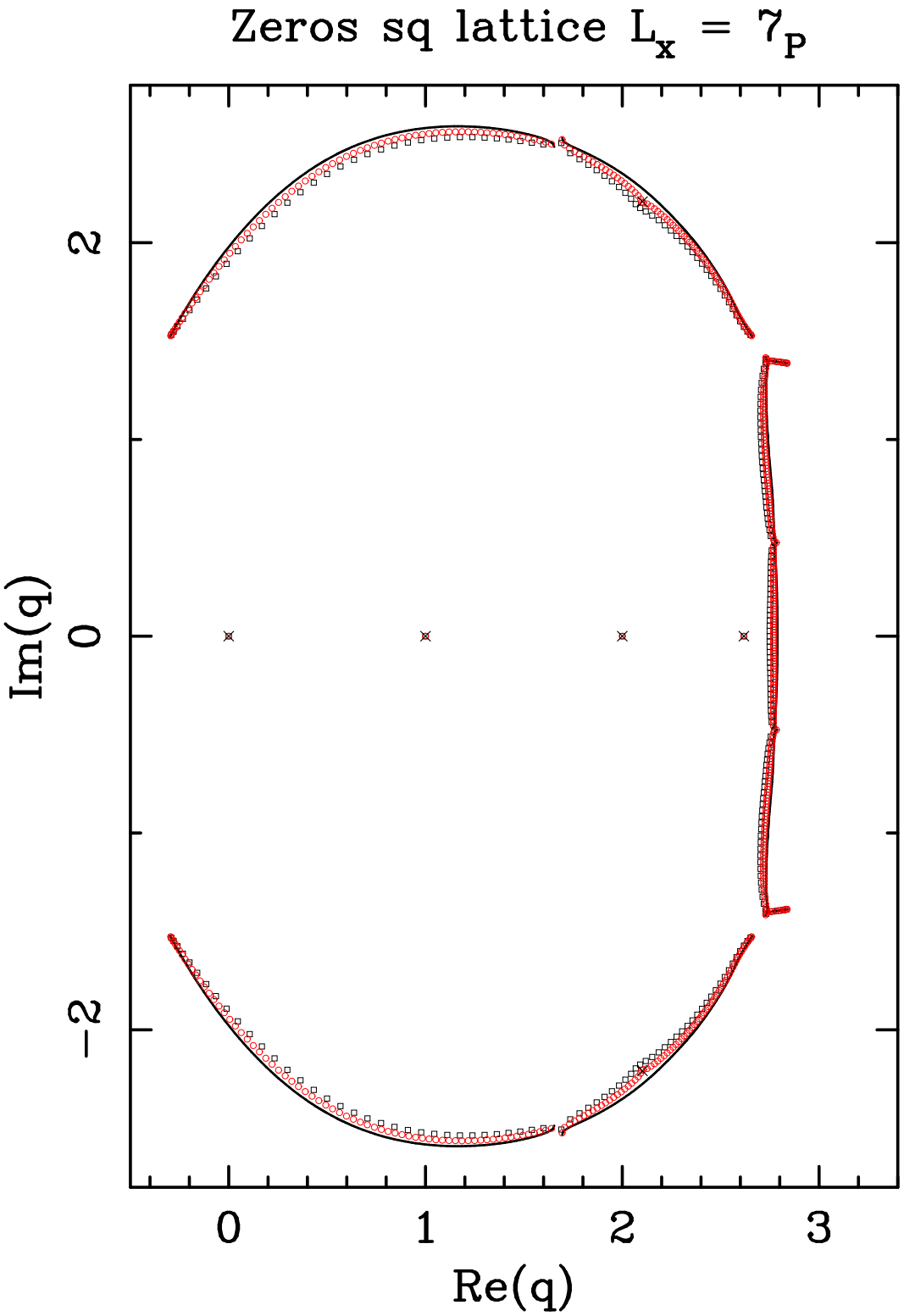

Figure 17: Zeros of the partition function of the q-state Potts antiferromagnet on a square lattices $7_P \times 35_F$ (squares), $7_P \times 70_F$ (circles) and $7_P \times \infty_F$ (solid line). The isolated limiting zeros are depicted by a $\times$. The limiting curve was computed using the resultant method.

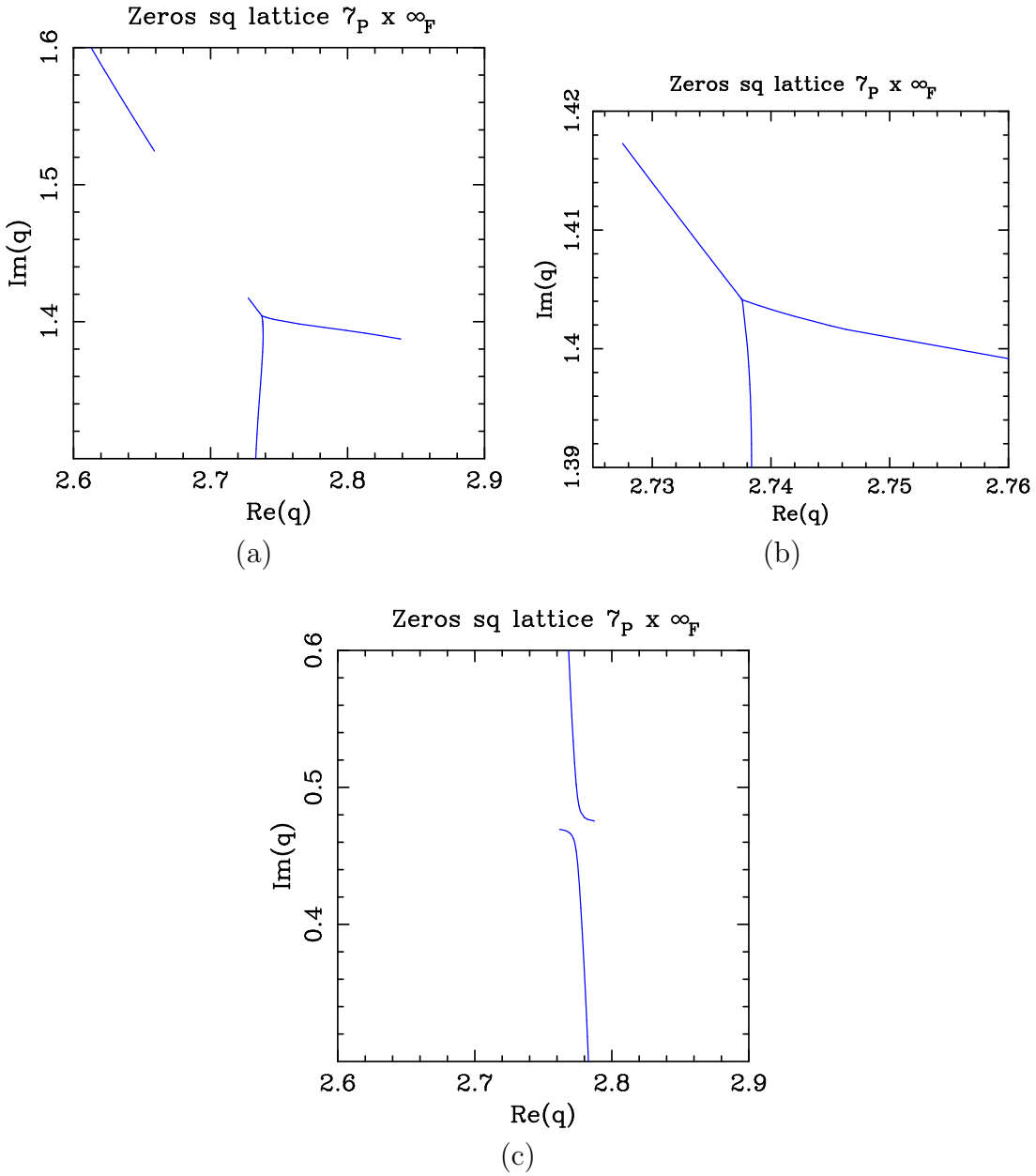

Figure 18: Detail of the limiting curves $\mathcal{B}$ for the q-state Potts antiferromagnet on a square lattice $7_P \times \infty_F$. (a) Region around the T point at $q \approx 2.737 + 1.405\,i$ and the gap between $q \approx 2.6590 + 1.525\,i$ and $q \approx 2.7275 + 1.4173\,i$. (b) Detail of the region around the T point. At this point we have $t \approx (0.125, 0.581, 0.425)$ and $\theta \approx (0.248, 1.053, 0.804)$. (c) Region around the gap between the points $q \approx 2.7619 + 0.46936\,i$ and $q \approx 2.7873 + 0.47546\,i$.

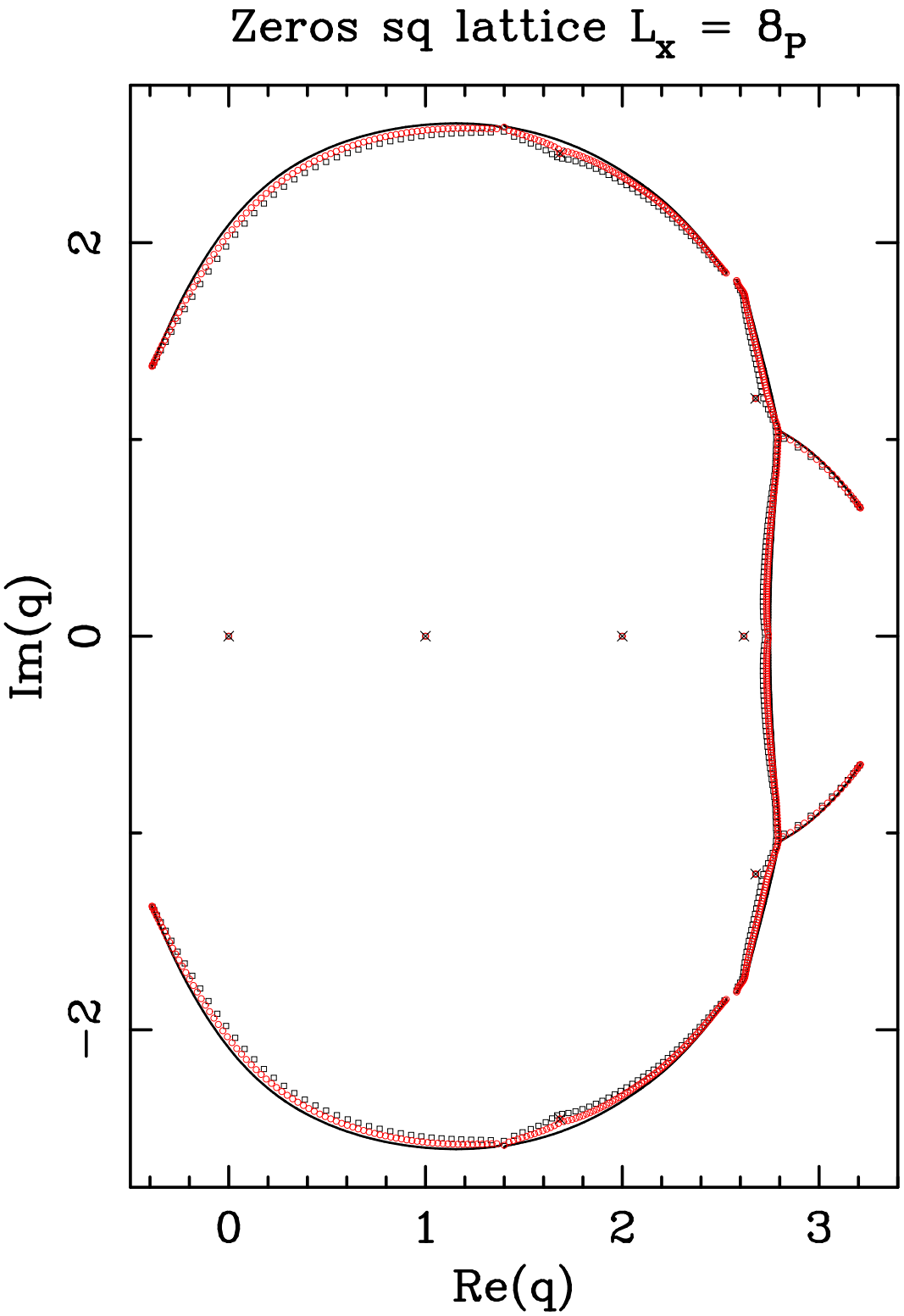

Figure 19: Zeros of the partition function of the q-state Potts antiferromagnet on a square lattices $8_P \times 40_F$ (squares), $8_P \times 80_F$ (circles) and $8_P \times \infty_F$ (solid line). The isolated limiting zeros are depicted by a $\times$. The limiting curve was computed using the resultant method.

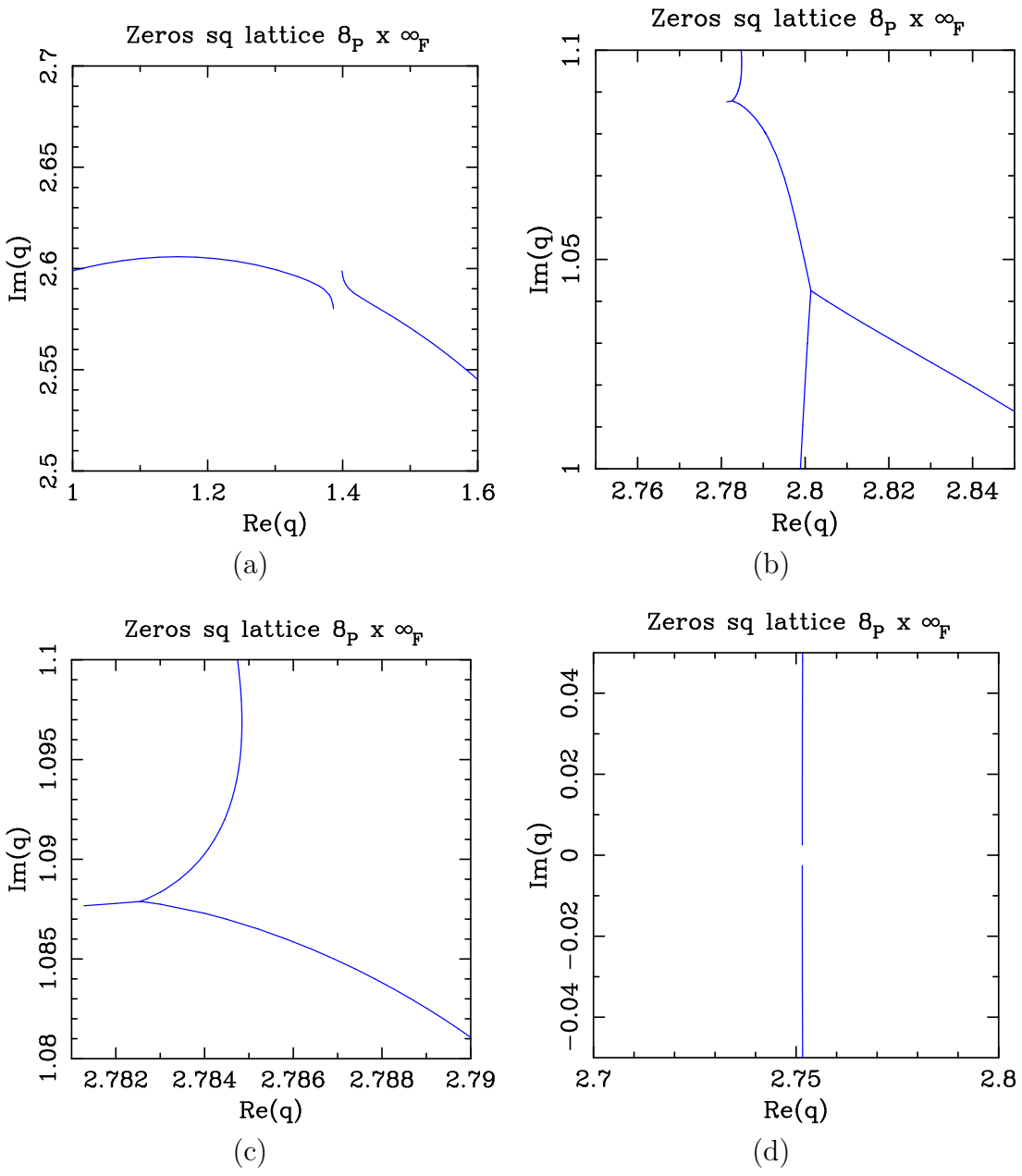

Figure 20: Detail of the limiting curves $\mathcal{B}$ for the q-state Potts antiferromagnet on a square lattice $8_P \times \infty_F$. (a) Region around the gap at $q \approx 1.39 + 2.59\,i$. (b) Region around the T points $q \approx 2.783 + 1.088\,i$ and $q \approx 2.801 + 1.043\,i$. At the former T point we have $t \approx (1.074, 0.0184, 1.115)$ and $\theta \approx (1.642, 0.037, 1.679)$; at the latter we have $t \approx (0.119, 0.813, 1.031)$ and $\theta \approx (0.237, 1.365, 1.601)$. (c) Detail of the T point at $q \approx 2.783 + 1.088\,i$. (d) Region around the tiny gap at $q \approx 2.7515$.

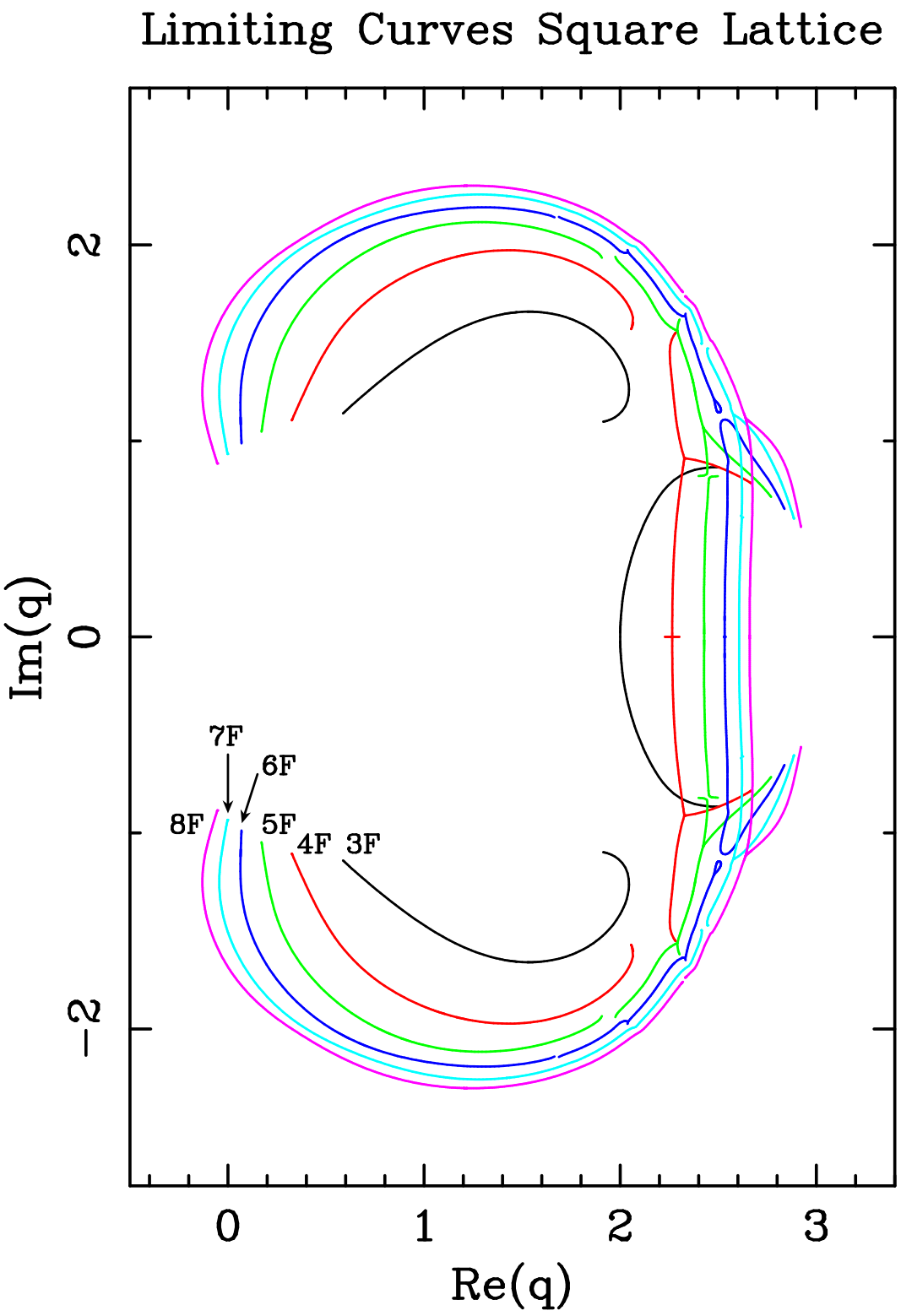

Figure 21: Limiting curves for the square-lattice strips $L_{\rm F} \times \infty_{\rm F}$ with $3 \le L \le 8$.

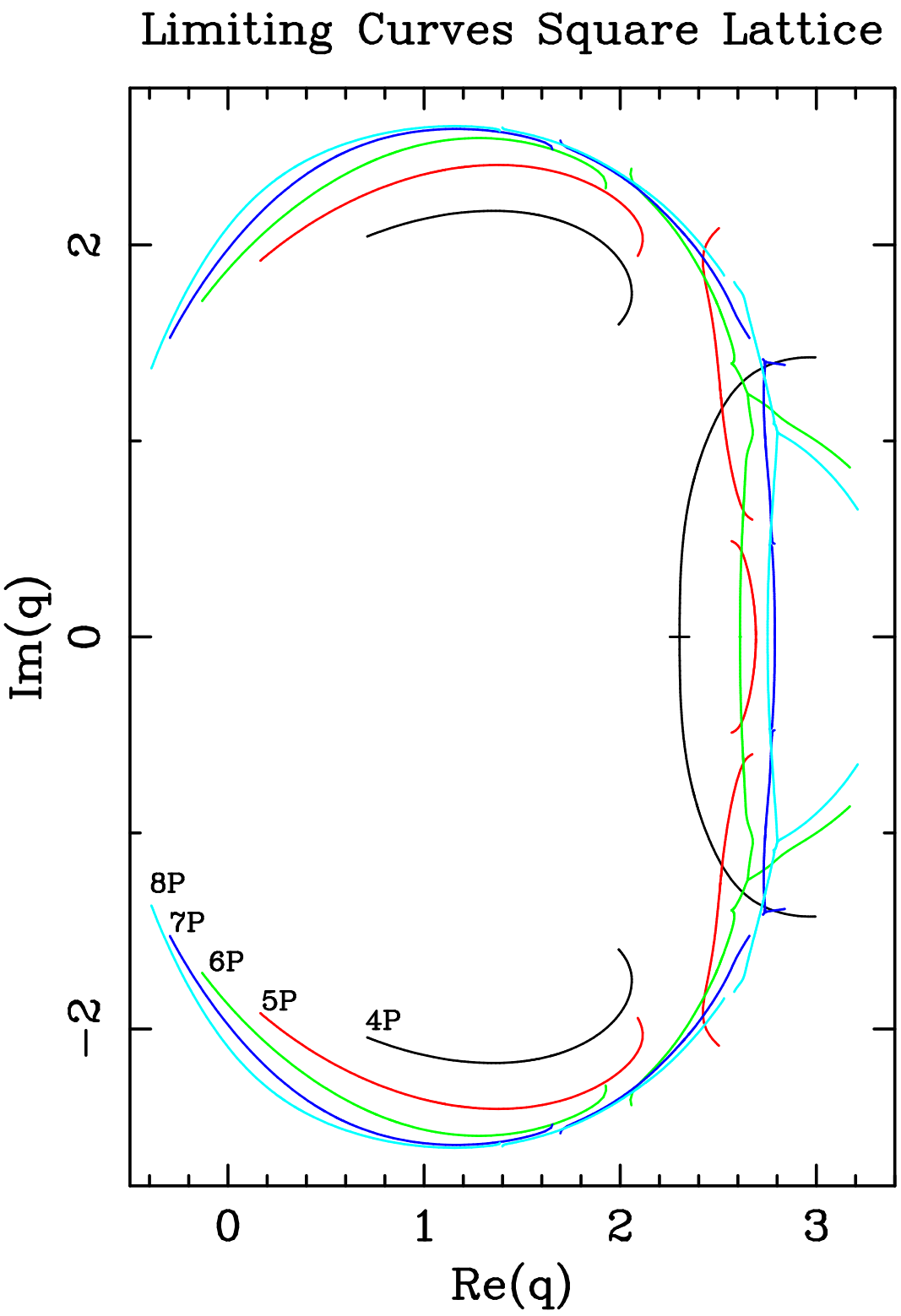

Figure 22: Limiting curves for the square-lattice strips $L_{\rm P} \times \infty_{\rm F}$ with $4 \le L \le 8$.